

**THE CATALYSED DECARBOXYLATION**

**OF**

**OXALOACETIC ACID**

**by**

**Robert W. Hay, B.Sc.**

**A thesis presented in accordance with the regulations for  
the degree of Doctor of Philosophy.**

**University of Glasgow**

**September 1959.**

ProQuest Number: 13850399

All rights reserved

INFORMATION TO ALL USERS

The quality of this reproduction is dependent upon the quality of the copy submitted.

In the unlikely event that the author did not send a complete manuscript and there are missing pages, these will be noted. Also, if material had to be removed, a note will indicate the deletion.



ProQuest 13850399

Published by ProQuest LLC (2019). Copyright of the Dissertation is held by the Author.

All rights reserved.

This work is protected against unauthorized copying under Title 17, United States Code  
Microform Edition © ProQuest LLC.

ProQuest LLC.  
789 East Eisenhower Parkway  
P.O. Box 1346  
Ann Arbor, MI 48106 – 1346

### Acknowledgements.

The author wishes to express his thanks to Dr. E. Gelles for his help and guidance with this work, and to acknowledge the receipt of a grant from the Department of Scientific and Industrial Research.

The measurements given on pages 45-46 and on pages 99-100 were carried out by Messrs. J.F.Reid and A.Groden respectively in this laboratory.

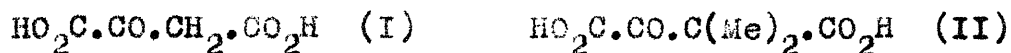
Microanalyses were carried out by Mr. J.M.L. Cameron in this department.

R.W. Hay

### Summary

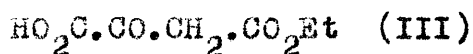
The nature of the chelate compounds formed by transition metal ions with oxaloacetic acid in aqueous solution, has been investigated spectrophotometrically and potentiometrically. The mechanism of the catalysed reaction has been clarified.

Thermodynamic information on the ketonic chelate compounds, which are the catalytically active species in decarboxylation, has been obtained by measuring association constants for dimethyloxaloacetic acid (II) (which cannot enolise), and comparing these with the known association constants for oxaloacetic acid (I).

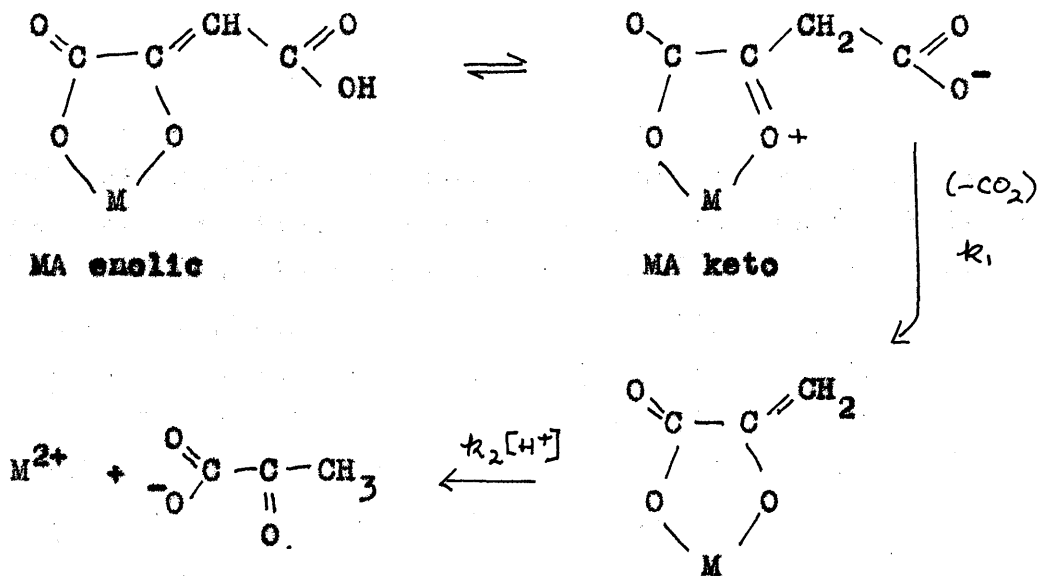


Spectrophotometric studies have demonstrated the presence of enolic chelate compounds which are not decarboxylated. Approximate values for the proportion of enolic complex for oxaloacetate chelates of  $\text{Ca}^{2+}$ ,  $\text{Mn}^{2+}$ ,  $\text{Zn}^{2+}$ ,  $\text{Co}^{2+}$ ,  $\text{Ni}^{2+}$  and  $\text{Cu}^{2+}$  have been obtained.

Spectrophotometric measurements on the chelate compounds of oxaloacetic acid (I) and its ethyl ester (III),



which cannot decarboxylate, have shown that oxaloacetate chelate compounds are formed very rapidly. The rise of optical density (270  $\text{m}\mu$ ) with time to a maximum; produced by addition of some metal ions to aqueous solutions of oxaloacetic acid, is due to the production of an enolic pyruvate intermediate. The mechanism of decarboxylation, may be represented by,



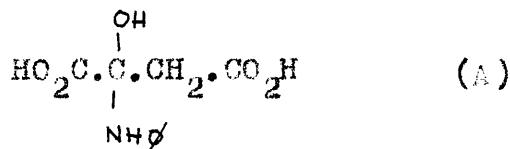
The changes of optical density with time are consistent with the above reaction scheme.

Inhibition of decarboxylation at high copper ion concentrations has been found to occur, and the results are related to previous potentiometric studies of the copper chelates. Inhibition at high pH ( $>6$ ) is due to the production of kinetically inactive enolic complexes.

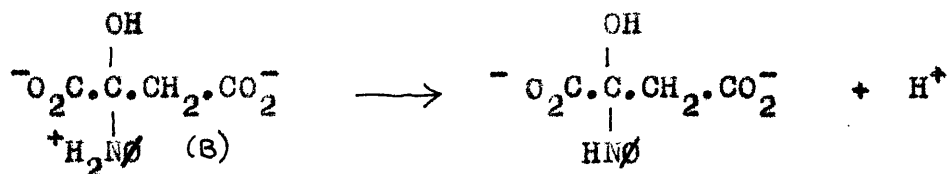
-ooOoo-

The aniline catalysed decarboxylation of oxaloacetic acid has been studied by manometric, spectrophotometric, and potentiometric methods.

Experiments with the half ester of oxaloacetic acid (III), have shown that in aqueous solution, the intermediate is the ketimine hydrate (A).

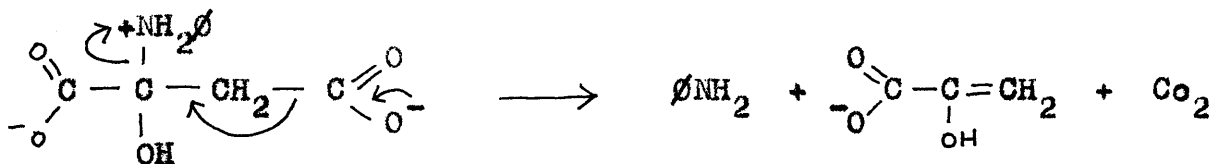


Kinetic measurements have demonstrated that the rate of the aniline catalysed decarboxylation passes through a maximum at around pH 4. The pH-Rate profile is consistent with a catalytically active species (B), the fall in rate at pH greater than 4, being attributed to ionisation according to the equation

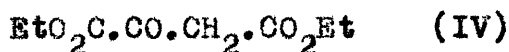


Kinetic measurements have shown that the ketimine hydrate is present only in small amounts, under the experimental conditions used, and that it loses  $\text{CO}_2$  in the rate-determining step.

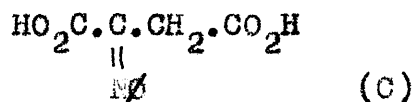
In aqueous solution the mechanism is of the type,



In ethanol, experiments with esters (III) and (IV)



have shown that the catalytically active species is the ketimine (C). This compound is formed in quantitative yield.



The aniline salt of compound (A), and the diethyl ester derivative of (C) have been isolated.

The formation of the ketimine has been studied spectrophotometrically and shown to be kinetically second order. The rate of formation of the ketimine is equal to

the rate of decarboxylation, indicating that in ethanol, the formation of the ketimine is the rate-controlling step in decarboxylation.

Metal ion and amine catalysis have been compared with the metal ion activated enzymatic decarboxylation of some biologically important keto acids.



## Contents.

Summary	pages
General Introduction .....	1-11
References .....	12

-ooOoo-

<b>Part 1. <u>Metal ion catalysed decarboxylation</u></b>	pages
<u>Introduction and nature of the work undertaken</u> ..	14-16
<u>Experimental</u> a) Materials .....	17-28
b) Methods .....	29-31
c) Infra-red Assignments .....	32-37
<u>Results and Discussion</u> .....	38-68
Association Constants .....	39-47
Nature of the chelate compounds of oxaloacetate..	47-49
Speed of formation of the chelates .....	49-50
Keto-enol equilibria .....	50-54
The enolic pyruvate intermediate .....	55-63
Inhibition .....	64-67
References .....	68

-ooOoo-

<b>Part 2 <u>Amine catalysed decarboxylation</u></b>	pages
<u>Introduction and nature of the work undertaken</u> ..	70-73
<u>Experimental</u> a) Materials .....	74-78
b) Methods .....	79-83
<u>Results and Discussion</u> .....	84-109
Nature of the intermediates .....	84-91
The ketimine equilibria in alcohol .....	91-93
Comparison of the rate of formation of the ketimine (K*), and the rate of decarboxylation of oxaloacetic acid in alcohol .....	93-97

Part 2. (continued)	pages
Decarboxylation in aqueous solution at 25°.....	97-103
Potentiometric measurements .....	103-107
Correction of the pH-Rate profile .....	107-109
References .....	110

-ooOoo-

Part 3. The mechanism of enzyme catalysed decarboxylation with special reference to amines and metal ions.	111-118
References .....	119

-ooOoo-

## Figures.

<u>Part 1. Experimental</u>	Between pages
Fig.1. Apparatus used for sodium triphenylmethide condensations.....	24-25
Fig.2. Infra-red spectra of derivatives of oxaloacetic acid.....	32
Fig.3. Correlation of Infra-red spectra of metal chelates with Stability Constants.....	36-37
Fig.4. Infra-red spectrum of the copper enolate of diethyloxaloacetate.....	36-37
 <u>Part 1. Results and Discussion</u>	
Fig.1. Ultra-violet spectra of pyruvic acid.....	44-45
Fig.2. Ultra-violet spectra of ethyl $\alpha$ -dimethyl oxaloacetate and its copper chelate.....	47-48
Fig.3. Ultra-violet spectra of oxaloacetic and $\alpha$ -dimethyloxaloacetic acids.....	
Fig.4. Ultra-violet spectra of oxaloacetic acid in ether and light petroleum, and of ethyl oxaloacetate in ether.....	48-49
Fig.5. Ultra-violet spectrum of the copper enolate of diethyl-oxaloacetate in $\text{CHCl}_3$ .	
Fig.6. Ultra-violet spectra of ethyl oxaloacetate in the presence of various metal ions.....	
Fig.7. Variation of O.D. with time for oxaloacetic acid in the presence of zinc ions at various pH's.....	49-50
Fig.8. Decarboxylation of $\alpha$ -dimethyloxaloacetic acid at pH 13.....	50-51

<u>Part 1. Results and Discussion (continued)</u>	Between pages
Fig.9. Variation of O.D. with time for oxaloacetic acid in the presence of various metal ions..	53-54
Fig.10 Variation of O.D. with time for the decarboxylation of oxaloacetic acid at pH 2.0 and 6.1.....	55-56
Fig.11 Enolic intermediate in the decarboxylation of $\alpha$ -dimethyloxaloacetic acid.....	56-57
Fig.12 Plots of optical density-time curves for the enolic pyruvate intermediate.....	61-62

Part 2. Experimental

Fig.1. Apparatus used for storing dry ethanol...	
Fig.2. Apparatus used for agitation of manometric tubes.....	79-80
Fig.3. Manometric decarboxylation tube.....	

Part 2. Results and Discussion

Fig.1. Ultra-violet spectra of $\text{NH}_3^+ \text{O}_2\text{C.C}(\text{NH}\emptyset, \text{OH})\text{CO}_2\text{Et}$ and $\text{O}_2\text{C.CO.CH}_2\text{CO}_2\text{Et}$ in water.....	84-85
Fig.2. Ultra-violet spectra of $\text{NH}_3^+ \text{O}_2\text{C.C}(\text{NH}\emptyset, \text{OH})\text{CH}_2\text{CO}_2\text{Et}$ and $\text{EtO}_2\text{C.C}(\text{:N}\emptyset)\text{CH}_2\text{CO}_2\text{Et}$ in absolute ethanol.....	84-85
Fig.3. Ultra-violet spectra of aniline and the anilinium ion.....	85-86
Fig.4. Ultra-violet spectra of $\text{MeO}_2\text{C.C}(\text{NH}\emptyset, \text{OH}).\text{CO}_2\text{Me}$ and $\text{MeO}_2\text{C.C}(\text{NH}\emptyset)_2.\text{CO}_2\text{Me}$ in absolute alcohol..	87-88
Fig.5. a) Ultra-violet spectra of $\text{NH}_3^+ \text{O}_2\text{C.C}(\text{NH}\emptyset, \text{OH}).\text{CH}_2\text{CO}_2\text{Et}$ in acetate buffers b) Ultra-violet spectrum of $\text{MeO}_2\text{C.C}(\text{NH}\emptyset, \text{OH}).\text{CO}_2\text{Me}$ in absolute alcohol.....	89-90

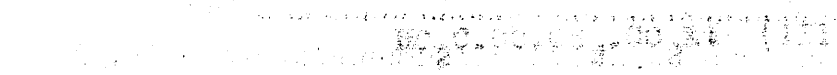
<u>Part 2. Results and Discussion (continued)</u>	Between pages
Fig.6. Ultra-violet spectra of $\phi\text{NH}_3^+\text{O}_2\text{C.C}(\text{NH}\phi,\text{OH})\text{CH}_2\text{CO}_2\text{Et}$ in alkaline solution showing the production of a new band at 273 m $\mu$ .....	90-91
Fig.7. Rate of ketimine formation at various aniline concentrations.....	93-94
Fig.8. Ultra-violet spectrum of ethyl oxaloacetate in absolute ethanol showing only partial enolisation.....	93-94
Fig.9. First order manometric plots for the aniline catalysed decarboxylation of oxaloacetic acid in absolute ethanol.....	93-94
Fig.10 Rate of decarboxylation of oxaloacetic acid in absolute ethanol at various aniline concentrations.....	93-94
Fig.11 Comparison of the rate of decarboxylation of oxaloacetic acid, and the rate of formation of the ketimine of $\text{EtO}_2\text{C.CO.CH}_2\text{CO}_2\text{Et}$ .....	93-94
Fig.12 Typical kinetic run in acetate buffers, for the decarboxylation of oxaloacetic acid.....	97-98
Fig.13 Rate of decarboxylation of oxaloacetic acid at various pH's and aniline concentrations.....	98-99
Fig. 14 pH-Rate profile.....	99-100
Fig.15 Aniline catalysed decarboxylation after Pedersen .....	99-100
Fig.16 Potentiometric titration of $\phi\text{NH}_3^+\text{O}_2\text{C.C}(\text{NH}\phi,\text{OH}).\text{CH}_2\text{CO}_2\text{Et}$ with N/5 sodium hydroxide.....	108-109

Part 2. Results and Discussion (continued)

Fig.17. Potentiometric titration of $\text{C}_6\text{H}_5\text{NH}_3^+\text{O}_2\text{C}(\text{C}_6\text{H}_5, \text{OH})\text{CH}_2\text{CO}_2\text{Et}$ with N/5 hydrochloric acid.....	Between pages 108-109
Fig.18. Correction of the pH-Rate profile.....	108-109

Spectrophotometric studies have been made of the reaction of the diester with various metal ions. The rate constants for the formation of the metal chelates of  $\text{Co}^{2+}$ ,  $\text{Cu}^{2+}$ ,  $\text{Zn}^{2+}$ , etc. have been obtained.

Spectrophotometric measurements of the absorption of the diester (I) and its

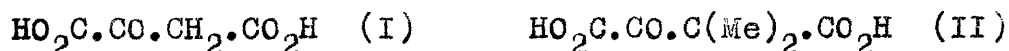


... cannot dissociate, have shown that the diester is formed very rapidly. The diester (I) with time to a

## Summary

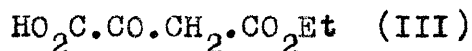
The nature of the chelate compounds formed by transition metal ions with oxaloacetic acid in aqueous solution, has been investigated spectrophotometrically and potentiometrically. The mechanism of the catalysed reaction has been clarified.

Thermodynamic information on the ketonic chelate compounds, which are the catalytically active species in decarboxylation, has been obtained by measuring association constants for dimethyloxaloacetic acid (II) (which cannot enolise), and comparing these with the known association constants for oxaloacetic acid (I).

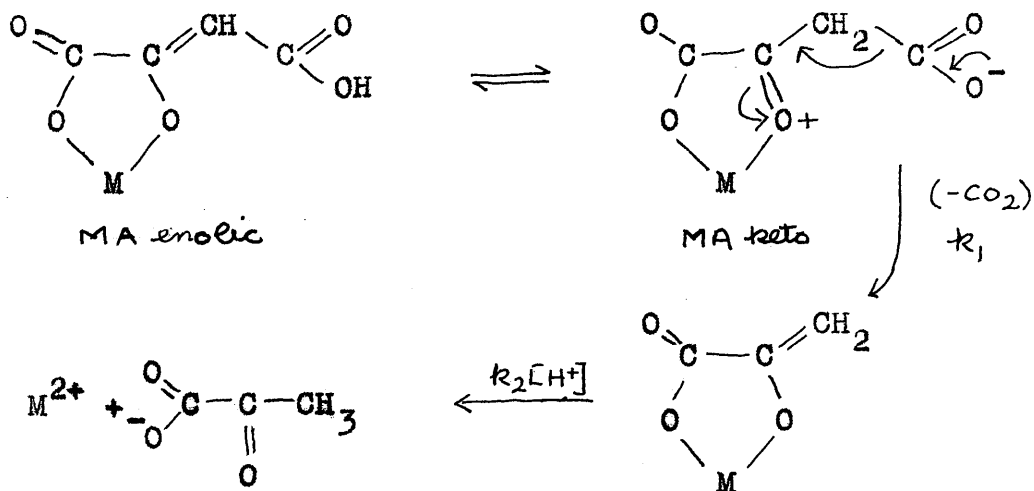


Spectrophotometric studies have demonstrated the presence of enolic chelate compounds which are not decarboxylated. Approximate values for the proportion of enolic complex for oxaloacetate chelates of  $\text{Ca}^{2+}$ ,  $\text{Mn}^{2+}$ ,  $\text{Zn}^{2+}$ ,  $\text{Co}^{2+}$ ,  $\text{Ni}^{2+}$  and  $\text{Cu}^{2+}$  have been obtained.

Spectrophotometric measurements on the chelate compounds of oxaloacetic acid (I) and its ethyl ester (III),



which cannot decarboxylate, have shown that oxaloacetate chelate compounds are formed very rapidly. The rise of optical density ( $270 \text{ m}\mu$ ) with time to a maximum; produced by addition of some metal ions to aqueous solutions of oxaloacetic acid, is due to the production of an enolic pyruvate intermediate. The mechanism of decarboxylation, may be represented by,



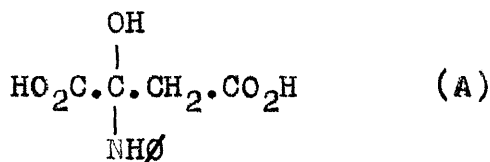
The changes of optical density with time are consistent with the above reaction scheme.

Inhibition of decarboxylation at high copper ion concentrations has been found to occur, and the results are related to previous potentiometric studies of the copper chelates. Inhibition at high pH (> 6) is due to the production of kinetically inactive enolic complexes.

- ooOoo-

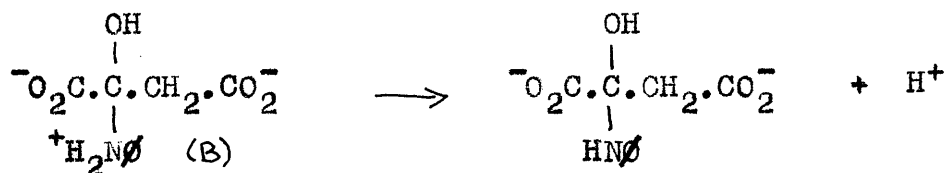
The aniline catalysed decarboxylation of oxaloacetic acid has been studied by manometric, spectrophotometric, and potentiometric methods.

Experiments with the half ester of oxaloacetic acid (III), have shown that in aqueous solution, the intermediate is the ketimine hydrate (A).



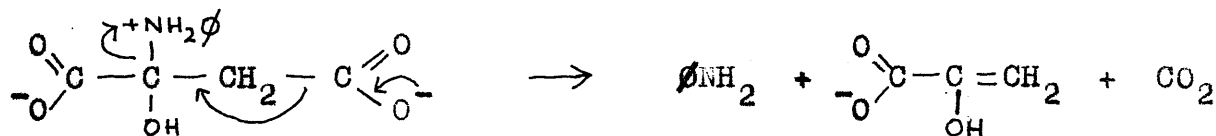


Kinetic measurements have demonstrated that the rate of the aniline catalysed decarboxylation passes through a maximum at around pH 4. The pH-Rate profile is consistent with a catalytically active species (B), the fall in rate at pH greater than 4, being attributed to ionisation according to the equation

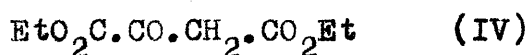


Kinetic measurements have shown that the ketimine hydrate is present only in small amounts, under the experimental conditions used, and that it loses  $\text{CO}_2$  in the rate-determining step.

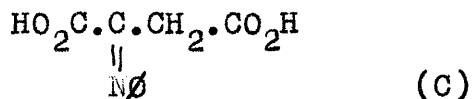
In aqueous solution the mechanism is of the type,



In ethanol, experiments with esters (III) and (IV)



have shown that the catalytically active species is the ketimine (C). This compound is formed in quantitative yield.



The aniline salt of compound (A), and the diethyl ester derivative of (C) have been isolated.

The formation of the ketimine has been studied spectrophotometrically and shown to be kinetically second order. The rate of formation of the ketimine is equal to the rate of decarboxylation, indicating that in ethanol,

the formation of the ketimine is the rate-controlling step in decarboxylation.

Metal ion and amine catalysis have been compared with the metal ion activated enzymatic decarboxylation of some biologically important keto acids.

General Introduction

In order to obtain a deeper understanding of the mechanism of a chemical reaction, it is necessary to have information on both the structure of the various species involved and on their concentration as a function of time. Kinetic studies must thus be supplemented by thermodynamic studies on the reactive species. Thermodynamic studies, however, give no indication as to the structure of the intermediates; information of this type can often be obtained from spectroscopy and from other physical methods.

The study of mechanism involves a number of different approaches, each aimed at discovering some aspect of the reaction. Thus much of the early kinetic work on the decarboxylation of organic acids in solution, such as that carried out by WIIG<sup>1</sup> on acetonedicarboxylic acid, is of little value. The first order rate constants obtained are apparent constants for a system involving the simultaneous decomposition of the undissociated acid and its anions. An analysis of the kinetic data could not be made until the dissociation constants of the acids were measured. The concentration of the various species under different conditions could then be calculated and it was found that the kinetics could be quantitatively explained by an equation of the type:<sup>2</sup>

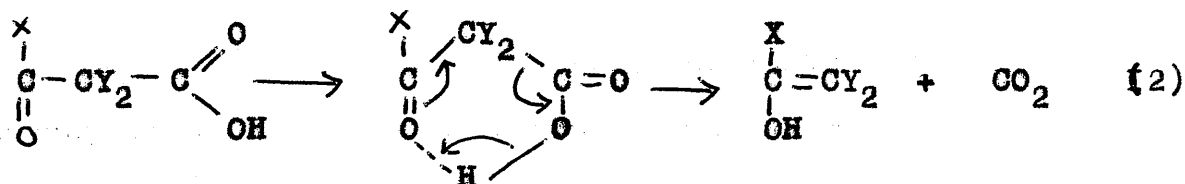
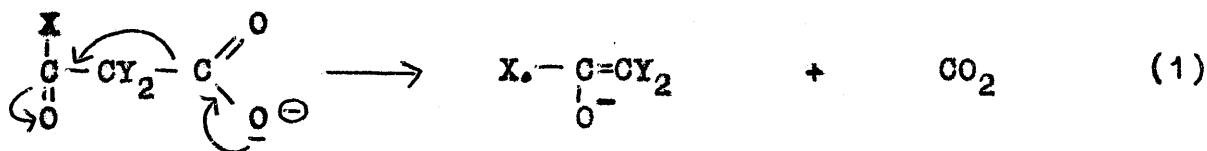
$$k_{\text{obs}} = k_1[\text{H}_2\text{A}] + k_2[\text{HA}^-] + k_3[\text{A}^{2-}]$$

where  $k_1$ ,  $k_2$  and  $k_3$  are the specific first order rate constants for the undissociated acid and its mono- and dianions.

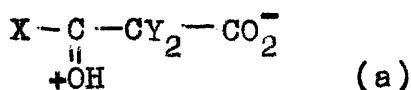
The necessity of having thermodynamic and structural information on the various reacting species is possibly of even greater importance in the study of catalysed reactions. A homogeneous catalysed reaction in solution involves interaction of the catalyst with the substrate to form some type of 'complex'. Since a number of different complexes can often be formed, usually having considerable differences in reactivity, it is difficult to analyse the kinetics of the reaction without some information as to the concentration of the various species under different conditions, and also as to their structure. Thus although kinetic measurements of the amine catalysed decarboxylation of  $\beta$ -keto acids have been made over a period of more than 50 years, it has proved impossible to elucidate the mechanism of the reaction using these experiments alone.

The mechanism by which  $\beta$ -keto acids decarboxylate is now reasonably well understood. The subject has been reviewed by BROWN.<sup>3</sup> It has been shown both spectroscopically<sup>5</sup> and by bromine titration<sup>4</sup> that decarboxylation leads directly to an enolic intermediate. Since both  $\alpha\alpha$ -dimethyl acetoacetic acid<sup>4</sup> and  $\alpha\alpha$ -dimethyl oxaloacetic acid,<sup>5</sup> which cannot enolise, decarboxylate readily, it is concluded that the keto forms of these acids are unstable.

It has also been shown by WESTHEIMER<sup>6</sup> that the rate of decarboxylation of  $\alpha$ -dimethyl acetoacetic acid is virtually independent of the dielectric constant of the solvent. If the  $\beta$ -keto acid is represented by  $X.CO.CY_2.COOH$  the decarboxylation of the acid and anion can be represented by the equations (1) and (2) respectively.



The undissociated acid is regarded as decomposing through a hydrogen-bonded form rather than as a zwitter-ion (a) as originally suggested by PEDERSEN.<sup>4</sup>



The differences in reactivity of  $\beta$ -keto acids have been discussed by GELLES.<sup>7</sup> These differences are most easily interpreted in terms of the substituent groups X and Y. When a  $\beta$ -keto acid decarboxylates the rest of the molecule must absorb the pair of electrons initially bonding the

carboxyl group. Electrophilic groups in the molecule will facilitate this transfer, while electron-donating groups will hinder it.

The decarboxylation of a number of  $\beta$ -keto acids is catalysed by metal ions. Part 1 of this thesis deals with the transition metal ion catalysed decarboxylation of oxaloacetic acid. Kinetic information has been obtained directly from manometric decarboxylation experiments. Thermodynamic and structural information on the various chelates involved has been obtained from potentiometric work and from spectrophotometry. A combination of these data has elucidated the mechanism of the reaction.

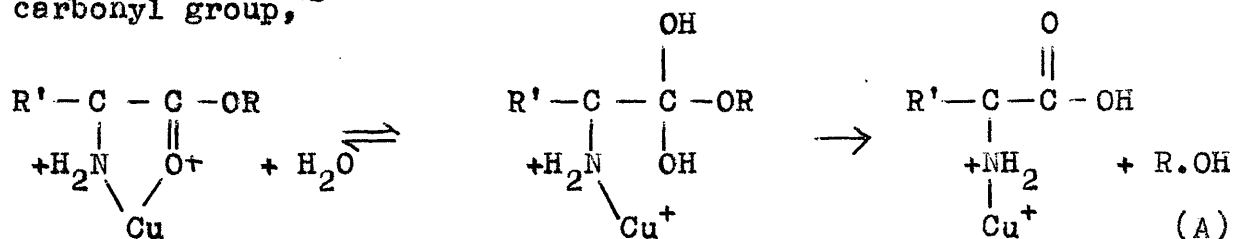
Homogeneous metal ion catalysed reactions in solution fall naturally into two classes. The metal ion can act as an oxidation-reduction catalyst, this involves a change in its valency state; or it can also act as a generalised acid in the Lewis sense. The metal ion catalysed decarboxylation of  $\beta$ -keto acids is of the second type.

When a metal ion combines with an electron donor the resulting structure is a metal complex. However, if the ligand contains two or more donor groups, the resulting structure is a metal chelate. Since the ligand is an electron donor, it can be considered as a generalised base in the Lewis sense, while the metal ion acts as a generalised acid.

Specific acid catalysis can take place in a number

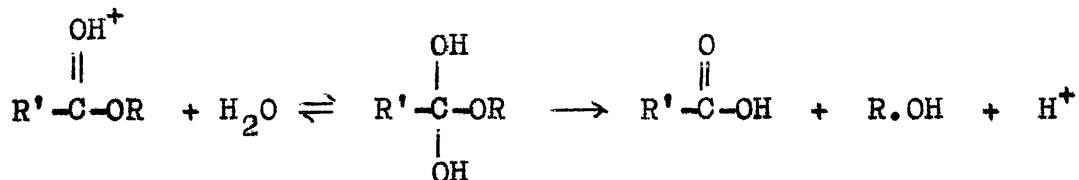
of different ways. The major effect, however, may be considered to be that of the proton coupling itself to the substrate in such a way as to drain electrons towards the site of attachment. This then facilitates reaction at some other part of the molecule. Metal ions act in a similar manner and it is to be expected that metal ions will catalyse reactions which are acid catalysed provided chelation of some kind is possible. In such cases metal ions will be much more effective than hydrogen ions, provided that they can drain electrons from the reactive group, and may be regarded as 'super acid' catalysts. If only a single point of attachment is possible (simple esters and amides) then hydrogen ion catalysis will be more important. Hydrogen ion usually has the greatest affinity of all cations for basic monodentate ligands.

Recently it has been found that metal ions catalyse the hydrolysis of the esters and amides of  $\alpha$ -amino acids.<sup>11-12</sup> From tracer studies using oxygen 18, it appears that a chelate is formed which leads to addition of water to the carbonyl group,<sup>13</sup>

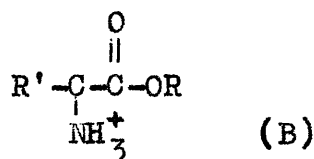


(6)

This is to be compared to the ordinary acid catalysed hydrolysis of esters,

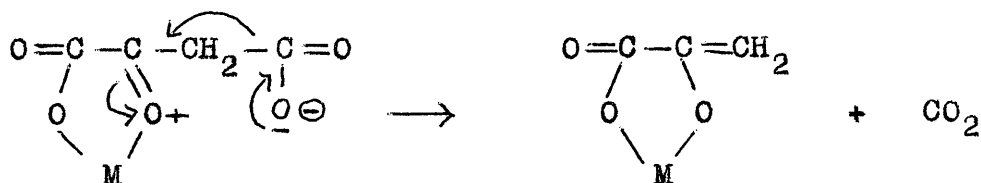


The effect of cupric ion in reaction A is much greater than that of an equivalent amount of hydrogen ion. Thus, at 0.01M  $\text{Cu}^{2+}$ , the half life is 10-30 minutes for several samples, whereas the acid catalysed reaction is extremely slow. The reason for this superiority is clearly the fact that the metal ion has a greater coordination number than hydrogen ion. Thus in (B),



the proton cannot interact with the carbonyl group except by the less efficient electrostatic induction. In general it is found that two or more points of attachment for a metal ion are required for it to display catalytic activity.

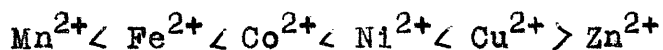
The method by which a metal ion catalyses the decarboxylation of a  $\beta$ -keto acid is illustrated for oxaloacetic acid,





The metal ion forms an  $\alpha$ -keto carboxylate chelate<sup>5</sup> with the oxaloacetate dianion. The charge produced on the oxygen atom assists the transfer of electrons from the carboxyl group to the rest of the molecule and so accelerates the reaction. Both oxalosuccinic and acetone dicarboxylic<sup>10</sup> acids show similar behavior. It is interesting to note that metal ions do not catalyse the decarboxylation of acetoacetic acid  $\text{CH}_3 \cdot \text{CO} \cdot \text{CH}_2 \cdot \text{CO}_2\text{H}$ .<sup>9</sup> In this case a six-membered ring chelate involving the unstable carboxyl group is formed; this tends to stabilise the molecule rather than accelerate its decomposition.

A large body of experimental evidence suggests that in transition metal ion chelates, the order of stability of the chelates is practically independent of the nature of the ligand and is a function solely of the metal ion; thus for many chelates the order of stability is,<sup>14</sup>



The primary role of the metal ion in chelates undergoing chemical change is to withdraw electrons from the reaction centre. Many examples of this type of reaction are known; the catalysed hydrolysis of simple peptides<sup>15</sup> and organic esters,<sup>11-12</sup> the halogenation of keto esters<sup>16</sup> and the decarboxylation of  $\beta$ -keto acids<sup>10,17,18</sup> are specific examples.

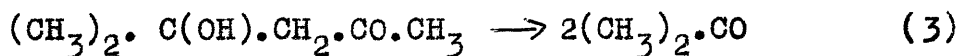
Since the stability constants between the substrate and various metal ions are a measure of the strength of

binding between the substrate and the metal ion, it would be expected that a relationship would exist between the catalytic power of the metal ion and its degree of interaction with the substrate. Qualitative ~~EXPERIMENTAL~~ agreement of this type has been found in a number of cases. Quantitative experimental data has been very scarce. However PRUE<sup>10</sup> has shown that the catalytic power of transition metal ions in the decomposition of acetone dicarboxylic acid follows the thermodynamic stability of the corresponding malonates. A similar correlation has been established between the catalytic effect of rare earth ions in the decarboxylation of oxaloacetic acid and the stability of the rare earth oxaloacetates.<sup>18</sup>

Recently GELLES and SALAMA<sup>19</sup> have made a thorough study of the transition metal ion catalysed decarboxylation of oxaloacetic acid and have shown that the catalytic effect of the ions does not follow the stability of the oxaloacetates but follows that of the oxalates. It thus appears that interaction in the transition state (the enolic intermediate closely resembles the oxalates and is a contributing structure to the activated complex) is more important in determining the catalytic effect than interaction in the initial state. It will be interesting to discover if similar behavior is found in other metal ion catalysed systems.

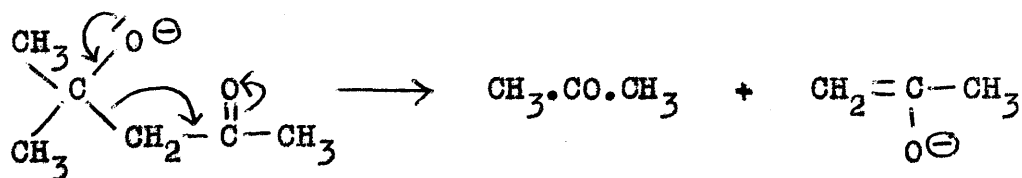
The decarboxylation of all  $\beta$ -keto acids is catalysed by primary and secondary amines, but not by tertiary amines.<sup>1,20</sup> Aniline is usually by far the most efficient catalyst. Part 2 of this thesis is a comprehensive study of the aniline catalysed decarboxylation of oxaloacetic acid. Kinetic measurements of the rate of decarboxylation have been made, these have been coupled with spectrophotometric and potentiometric measurements on model compounds closely resembling reaction intermediates. From these data it has been possible to postulate a mechanism for the aniline catalysed decarboxylation, which can be extended to other primary and secondary amines.

Many reactions in solution are subject to general base catalysis; a certain amount of evidence, however, has now accumulated to show that some reactions are specifically catalysed by amines. The decarboxylation of  $\beta$ -keto acids, mentioned above, and the dealdolization of diacetone alcohol (3) are examples of such catalysis.<sup>6,20-23</sup>

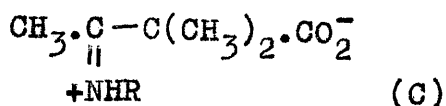


The dealdolisation of diacetone alcohol is strictly first order with respect to the concentration of diacetone alcohol and the rate varies linearly with hydroxide ion concentration. The reaction is not subject to general base catalysis. The most probable mechanism involves the unimolecular decomposition of the diacetone alcoholate ion. Since the alcohol is

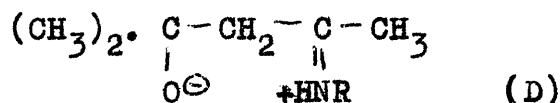
undoubtedly a very weak acid, the concentration of this ion will be strictly proportional to the hydroxide ion concentration.



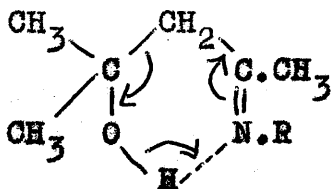
The enolate ion subsequently reacts with water to give acetone and hydroxide ion. Primary and secondary amines are effective catalysts, but tertiary amines are not. Further, the rate constants for the various amines investigated by MILLAR and KILPATRICK<sup>21</sup> in the dealdolization of diacetone alcohol bear no relation to the base strengths of the amines. This is in agreement with the observation of FRENCH<sup>23</sup> that the reaction is not catalysed by phenolate ion, a base in the BRONSTED sense. In the absence of general base catalysis it seems logical to assume that the amine is effective because it reacts with the carbonyl group of the keto acid or alcohol to form a Schiff base or ketimine. This suggestion was first put forward by PEDERSEN<sup>20</sup> to account for the amine catalysed decarboxylation of acetoacetic acid, the reactive intermediate being the zwitterion (C),



WESTHEIMER<sup>22</sup> has applied a similar idea to diacetone alcohol, the intermediate being (D),



However WESTHEIMER and JONES<sup>6</sup> have since shown that the rate of the amine catalysed dealdolization in water-dioxane, water-alcohol mixtures is independent of the solvent, it thus seems unlikely that a dipolar ion (D) is involved in the reaction. However, the rate controlling step could for example, be the rate of formation of the ketimine, or the rate of decomposition of a hydrogen bonded intermediate (E).



(E)

## References

1. Wiig, J. Physical Chem. 32, 961, 1928.
2. Franke and Brathuhn, Ann. 487, 1, 1931.
3. Brown, Quarterly Reviews, 5, 131, 1951.
4. Pedersen, J. Phys. Chem. 38, 559, 1934.
5. Steinberger and Westheimer, J.A.C.S. 71, 4158, 1949.
6. Westheimer and Jones, J.A.C.S. 63 3283, 1941.
7. Gelles, J.C.S. 4736, 1956.
8. Krebs, Biochem. J. 36 303, 1942.
9. Kornberg, Ochoa and Mehler, J.Biol. Chem. 174, 159, 1948.
10. Prue, J.C.S. 2331, 1952.
11. Kroll, J.A.C.S. 74, 2036, 1952.
12. Meriwether and Westheimer, J.A.C.S. 78, 5119, 1956.
13. Bender and Turnquist, J.A.C.S. 79, 1889, 1957.
14. Irving and Williams, Nature, 162, 746, 1948.
15. Rabin, Biochemical Society Symposia, 15 "Metals and Enzyme Activity"
16. Pedersen, Acta Chem. Scand. 2, 252, 385, 1948.
17. Pedersen, Acta Chem. Scand. 3 676, 1949.
18. Gelles and Clayton T.F.S. 52, 353, 1956.
19. Gelles and Salama J.C.S. 3684, 1958.
20. Pedersen J.A.C.S. 51, 2098, 1929. 58, 240, 1936. 60, 595, 1938  
J.Phys. Chem. 38, 559, 1934.
21. Miller and Kilpatrick, J.A.C.S. 53, 3217, 1931.
22. Westheimer, Ann. N.Y.Acad. Sci. 299, 1940.
23. French, J.A.C.S. 51, 3215, 1929.

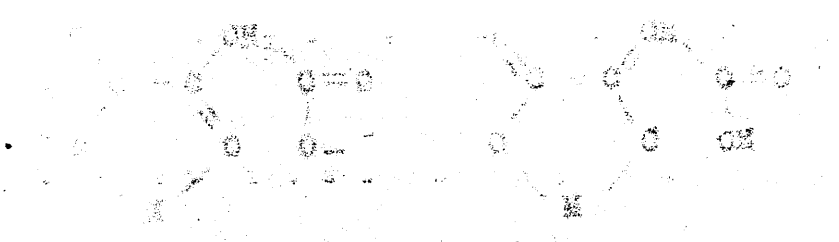
oxaloacetic acid

...the reaction of ... with ...  
...of oxaloacetic acid was ...  
...and ... and ...  
...  
...  
...  
...  
...

**Part I**

**The Metal Ion Catalysed Decarboxylation  
of Oxaloacetic Acid.**

...  
...  
...  
...  
...  
...

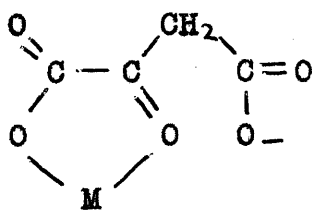


Part 1. The Metal Ion Catalysed Decarboxylation of Oxaloacetic Acid

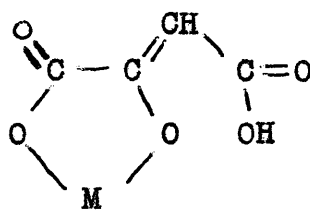
Introduction

The fact that various bi and ter-valent metal ions catalyse the decarboxylation of oxaloacetic acid was first discovered by KREBS<sup>1</sup> and KRAMPITZ and WERKMAN.<sup>2</sup> KORNBERG, OCHOA and MEHLER<sup>3</sup> observed the appearance and decline of a strong absorption band in the region of 260-300 m $\mu$  on adding metal ions under certain conditions to oxaloacetic acid. They attributed this to the slow formation of an enolic complex B, followed by its rapid decay on decarboxylation.

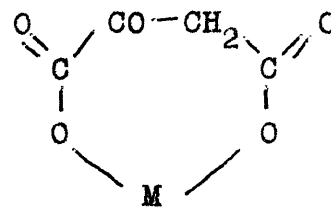
STEINBERGER and WESTHEIMER<sup>4</sup> showed that the decarboxylation of  $\alpha$ -dimethylethoxaloacetic acid  $\text{EtO}_2\text{C}\cdot\text{CO}\cdot\text{C}(\text{Me})_2\cdot\text{CO}_2\text{H}$  was not catalysed by metal ions, indicating that the catalytically active species formed by  $\alpha$ -dimethyl-oxaloacetic acid was a five membered ring  $\alpha$ -oxo-carboxylate chelate compound.



(A)



(B)



(C)

Dimethyl-oxaloacetic acid cannot form an enolic complex of type B, and so by analogy a ketonic complex (A) seemed to be the catalytically active species in the decarboxylation



of oxaloacetic acid. PEDERSEN<sup>5</sup> interpreted the kinetics of the copper and zinc ion catalysed decomposition at low pH and metal ion concentration in terms of the first order decomposition of the acid, its two anions and a species MA, where  $M^{2+}$  is the metal ion and  $A^{2-}$  the oxaloacetate dianion. WILLIAMS<sup>6</sup> suggested that in addition to  $\alpha$ -oxo carboxylate complexes a dicarboxylate complex C might also be formed, and that this could retard decarboxylation under certain conditions.

Inadequate explanations have been advanced for the observed retardation of the reaction at high pH and metal ion concentration.<sup>6-7</sup> Previous work has established that at low pH and low concentration of metal ion the catalytically active species must be the complex A, but it has produced no clear evidence, (1) on whether a catalytically inactive complex B is also formed, (2) if this is formed slowly enough to account for the spectrophotometric observations,<sup>3,8</sup> (3) whether these observations in fact provide evidence for a strongly absorbing enolic pyruvate intermediate, (4) on what the thermodynamic stabilities of the ketonic and enolic complexes, A and B are, (5) how the proportion of these two complexes changes with pH, and whether increasing concentrations of the enolic complex at high pH might account for the observed retardation in the rate of decarboxylation (6) whether other complexes such as the dicarboxylate complex C, are also present under certain

conditions, and (7) whether there is any correlation between the thermodynamic stability of the complexes and the catalytic power of the metal ion.

Experimental Part 11) Materialsa) Oxaloacetic acid HOOC.CO.CH<sub>2</sub>.COOH

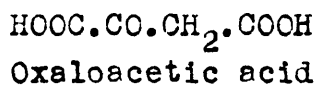
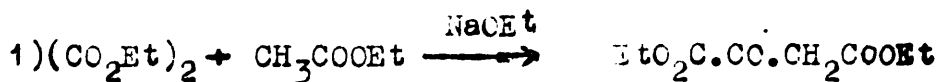
was obtained from Messrs. Light and Co. m.p. 152° (decomp.). Found for a dicarboxylic acid by titration against alkali M; 132.6. Calculated for C<sub>4</sub>H<sub>4</sub>O<sub>5</sub>, M; 132.1.

b) Diethyloxaloacetate EtO<sub>2</sub>C.CO.CH<sub>2</sub>.CO<sub>2</sub>Et

was prepared essentially as described by ~~XXXXXXXXXXXX~~ ROSSI and SCHINZ.<sup>9</sup> 34.5 gms. of clean sodium was atomised in 75 ml. of purified xylene. The washed sodium (by dry ether) was placed in a 3-litre Quickfit flask fitted with a water condenser, silica gel guard tube and bunsen valve. 600 ml. of sodium-dried ether, followed by 87.6 ml. of absolute alcohol, was then added and the mixture refluxed until all the sodium had dissolved (overnight). On dissolution of the sodium, 201 ml. of diethyl oxalate (dried over sodium sulphate) was added through the condenser followed by 145.5 ml. of ethyl acetate (dried with sodium sulphate) in small portions. The mixture was then refluxed until the solid yellow reaction product formed (1/2 hr.). A theoretical yield of the sodium enolate of diethyl oxaloacetate was obtained.

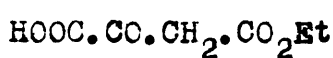
Water was poured over the sodium enolate in a 3-litre beaker and the mixture cooled in ice and rapidly stirred. 40 ml. (calculated amount) of concentrated sulphuric

Synthesis of Derivatives of Oxaloacetic and Dimethyl-oxaloacetic acids

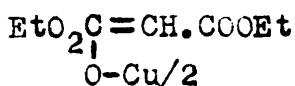


HCl

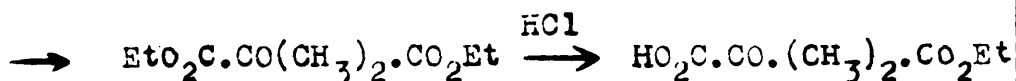
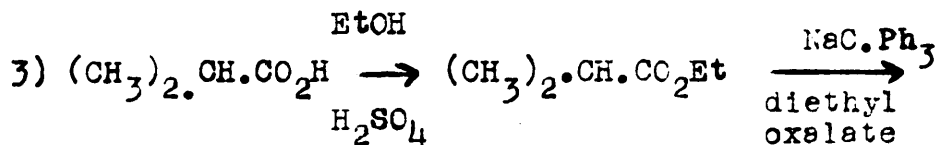
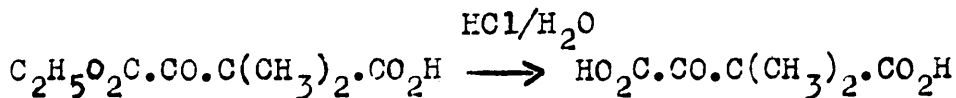
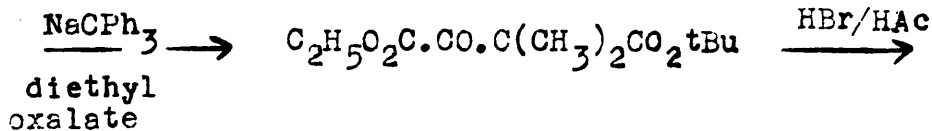
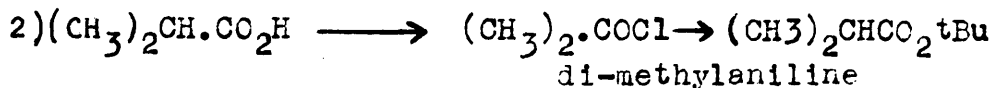
CuAc



NaOMe



t-butenol



acid diluted to about a litre was then slowly added. An oily ester separated and was extracted with ether (The ether layer should not be dried with potassium carbonate as this leads to decomposition of the ester on distillation). The ether was removed on the pump and the residue carefully vacuum distilled in small portions at about 4 mm; much tarry residue remained. The pure material vacuum distilled readily without pyrolysis. B.p. 116/16 mm., 131-3/24mm. Yield 65 % Found for  $C_8H_{12}O_5$ , C, 50.83; H, 6.18. Calc. C, 51.06; H, 6.32 %.

c) Ethyl oxaloacetate  $HO_2C.CO.CH_2.CO_2Et$

was prepared by the alkaline hydrolysis of the copper enolate of ethyl oxaloacetate  $Cu[EtO_2C.CO.CH.CO_2Et]_2^{10}$ .

Hydrated ( $2H_2O$ ) copper acetate (7 gms.) dissolved in the minimum amount of warm water (100 ml.) was added slowly to pure ethyl oxaloacetate (10 ml.) in ethanol (25 ml.). The bright green precipitate was filtered off after one hour, dried at  $100^\circ$  and recrystallised from absolute alcohol. This gave the unhydrated form (m.p.  $163^\circ-164^\circ$ ) as green microcrystalline needles. Recrystallisation from water-ethanol gave the hydrated form  $Cu[EtO_2C.CO.CH.CO_2Et]_2 \cdot H_2O$

as bright green needles of m.p.  $156^\circ-157^\circ$ , Calculated for  $(C_8H_{11}O_5)_2Cu.H_2O$ , C, 42.15; H, 5.27; Cu, 13.96;  $H_2O$ , 3.95 %. Found C, 42.44; H, 5.27; Cu, 14.55;  $H_2O$ , 4.02 %. In this preparation pure ethyl oxaloacetate must be used. Yield 80 %.

10 gms. of the copper enolate were dissolved in warm 50 % aqueous methanol and hydrolysed with sodium (1 gm.) dissolved in methanol (water must be present). A brown precipitate formed immediately, the solution was heated and the precipitate recrystallised. It was then allowed to stand undisturbed overnight. This gave easily filterable material. The brown precipitate was filtered off, dried at  $100^{\circ}$ , suspended in water and acidified in an ice bath with dilute sulphuric acid. The solution was then filtered and extracted with ether. The ether layer was dried with magnesium sulphate and the ether removed at the pump. An oil remained, which crystallised on cooling. Recrystallisation from benzene gave ethyl oxaloacetate (2 gms.) m.p.  $98^{\circ}$ . (Found for a monocarboxylic acid by titration against alkali, M, 161.6, Calculated for  $C_6H_8O_5$ : 160.1.). Found: C, 44.8; H, 5.1 %. Calculated for  $C_6H_8O_5$ : C, 45.0; H, 5.0%.

Ethyl  $\alpha$ -dimethylethoxaloacetate<sup>11</sup> and t-butyl  $\alpha$ -dimethyl ethoxaloacetate<sup>12</sup> were prepared by condensation of diethyl oxalate with ethyl isobutyrate and t-butyl isobutyrate respectively using sodium triphenylmethide. This is the synthetic method developed by HAUSER.<sup>13</sup>

d) Triphenylchloromethane  $(\text{Ph})_3\text{C.Cl}$ 

600 gms. (684 ml.) of sodium-dried A.R. benzene and 240 gms. (141 ml.) of pure dried carbon tetrachloride (water azeotroped off) were placed in a 3-litre Quickfit three necked flask fitted with a reflux condenser attached to a trap for the absorption of hydrogen chloride, a mercury-sealed mechanical stirrer and a device for the addition of a solid. The last named was charged with 180 gms. of finely powdered anhydrous aluminium chloride. The flask was cooled in an ice bath and the aluminium chloride added in small amounts to the contents of the flask, at such a rate that the reaction mixture did not reflux during the addition (about 1.5 hours). The ice bath was removed 15 minutes after all the solid had been introduced, and the reaction was allowed to proceed without further cooling. When heat was no longer evolved, the mixture was refluxed until evolution of hydrogen chloride subsided (2 hrs.), then allowed to cool to room temperature. The cold reaction product was poured in a thin stream on to a mixture of 900 gms. of crushed ice and 900 ml. of concentrated hydrochloric acid. The mixture was stirred vigorously. The benzene layer was separated, the aqueous layer extracted with a little benzene, and the combined extracts washed once with 600 ml. of cold concentrated hydrochloric acid. The benzene layer was dried by leaving for at least two hours over 75 gms. of anhydrous calcium

chloride or magnesium sulphate. The benzene was distilled from a Claisen flask until the temperature rose to about 200°. The warm residue was transferred with the aid of a little dry benzene to a 1-litre conical flask, cooled to about 40°, 9-12 ml. of acetyl chloride added and the mixture heated nearly to boiling point. The solution was shaken vigorously whilst cooling rapidly to room temperature, then left in a refrigerator overnight. The solid triphenylchloromethane was filtered on a large Buchner funnel and washed with three 90 ml. portions of light petrol (b.p. 60°-80°), then dried in a vacuum desiccator over paraffin wax shavings or silica gel to remove solvent. Pale greenish yellow crystals m.p. 110°-111°. Yield 270 gms. Stored in a screw-topped bottle sealed with paraffin wax and kept in a desiccator to prevent hydrolysis by atmospheric moisture. The partially hydrolysed product may be purified by recrystallisation from 1/3 of its weight of pure dry benzene containing 10-20 % acetyl chloride.

Ethyl isobutyrate  $(\text{CH}_3)_2\text{CH.COO}_2\text{Et}$

A mixture of 184 ml. of isobutyric acid, 58 ml. of absolute alcohol and 10 ml. of concentrated sulphuric acid were refluxed for 20 hrs. The reaction mixture was poured into water and stirred, then washed several times with water, followed by saturated bicarbonate, until all the acid was removed, and finally with water. A little ether was added to increase the mobility of the solution which was then



dried with magnesium sulphate. The ether was removed on a 30 cm. Widmer column, the ester being distilled on the same column.

Yield 100 gms. B.p. 110/760 mm. d. 0.869.

Sodium triphenylmethide  $(Ph)_3C.Na$

a) Preparation of 1.5 % sodium amalgam

14 gms. of cut sodium was placed in a 500 ml. round-bottomed three necked flask fitted with nitrogen inlet and outlet tubes in the side openings and a dropping-funnel in the centre opening. The flask was flushed out with nitrogen and the funnel charged with 935 gms. (69.6 ml.) of mercury. About 20 ml. of mercury were added rapidly to start the reaction and the rest at such a rate as to prevent the amalgam hardening. Once all the mercury had been added the flask was shaken several times and the amalgam poured into a mortar. To aid solidification and prevent attack from the air, the amalgam was covered with sodium-dried ether, this quickly evaporated leaving the solid, which was used immediately as follows.

b) A mixture of 950 gms. of amalgam (total prepared above) and 70 gms. (0.25 mole) of triphenylchloromethane was placed in a 2.5-litre Pyrex glass stoppered bottle and 1.5 litres of absolute ether added (dried with sodium wire and refluxed for six hours over sodium). The glass stopper was greased and taped down with 'Elastoplast'.

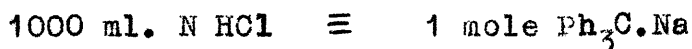
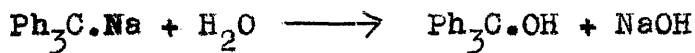
The bottle was then shaken in a mechanical shaker

for six hours. The reaction is exothermic and shaking was stopped when necessary and the bottle cooled with wet towels. Red colours appeared quickly (10 minutes), but the characteristic blood-red of sodium triphenylmethide does not appear for about 1-1½ hours.

After shaking for six hours the bottle was cooled to room temperature, removed from the shaker and the stopper wired down. The mixture was then allowed to stand undisturbed overnight. Sodium chloride and particles of mercury settle to the bottom.

Ethyl  $\alpha$ -dimethylethoxalacetate  $\text{EtO}_2\text{C.C}(\text{CH}_3)_2.\text{CO}_2\text{Et}$

25 ml. of the ether solution of sodium triphenylmethide were withdrawn and run into 25 ml. of water contained in a small separating-funnel and the mixture shaken. The aqueous layer was run off into a 250 ml. conical flask and the ether layer extracted with two additional 25 ml. portions of water. The combined aqueous extracts were titrated with 0.2 N HCl using methyl red as indicator.



Titre is 18 ml. of 0.2 N HCl

Wt. per 25 ml. =  $18 \times 0.2 / 1000$  moles. Vol. of ether 1300ml

Amount  $\text{Ph}_3\text{C.Na} = 1300 \times 3.6 / 25 \times 1000 = 0.187$  moles

The apparatus illustrated in Fig 1 was set up. The ethereal solution of sodium triphenylmethide was siphoned from the sludge under a slight pressure head of pure dry oxygen-free nitrogen into a calibrated 3-litre conical flask.

Ethyl isobutyrate (23.8 gms., 27.4 ml., 0.205 mole) was added with shaking to a solution of 0.19 mole of sodium triphenylmethide in 1.3-1.4 litres of ether. After 5 minutes at room temperature (colour red to reddish orange), 30 gms. (28 ml., 0.205 mole) of dry diethyl oxalate were added with shaking. The mixture became warm. After 10 minutes, 15 ml. of glacial acetic acid were added and the mixture extracted with 100 ml. of water. The ether solution was washed with saturated sodium bicarbonate solution, dried with sodium sulphate and the solvent distilled. The residue was distilled in vacuo (up to 150° at 20 mm.)

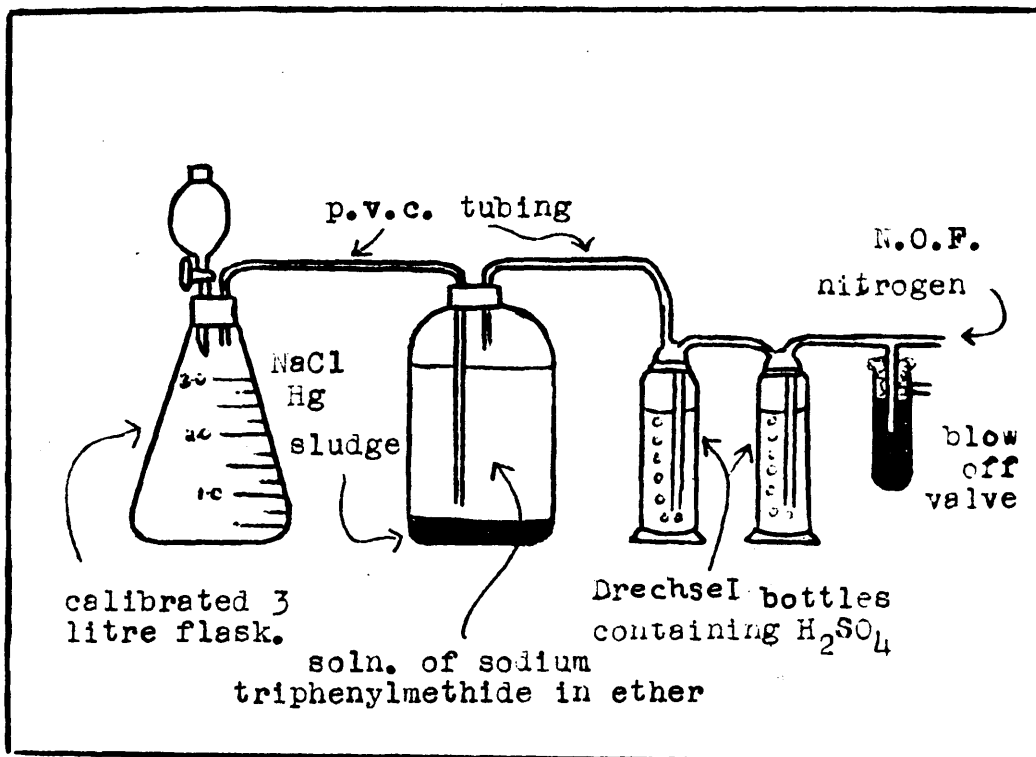
The distillate was fractionated using a Claisen flask with fractionating side-arm. Yield 27.2 gms. (61 %) of ethyl  $\alpha$ -dimethylethoxaloacetate. B.p. 122°-123° at 15 mm. 115°-120° at 11mm. Semicarbazone m.p. 97°-98°. Found C, 55.80; H, 7.10. Calculated for  $C_{10}H_{16}O_5$ , C, 55.60; H, 7.40 %.

Ethyl  $\alpha$ -dimethyloxaloacetate  $HO_2C.CO.C(Me)_2.CO_2Et$

was prepared by hydrolysis of the diester  $EtO_2C.CO.C(Me)_2.CO_2Et$  (10 ml.) with concentrated hydrochloric acid (87 ml.) for 2-3 days. The solution was diluted, extracted with ether and the ether layer dried with sodium sulphate. The ether

FIG 1

Apparatus used for sodium triphenylmethide condensations



was removed at the pump; an oil remained. This was purified by four micro-distillations in a sublimation tube under a pressure of 0.3 mm. and a temperature of 80°-100° produced by a sublimation furnace.

Found C, 51.00; H, 6.50. Calc. for  $C_8H_{12}O_5$  C, 51.00; H, 6.40 %.

This acid cannot be further hydrolysed, probably due to steric hindrance by the two methyl groups.

Tert-butyl isobutyrate  $(CH_3)_2C.COOt.Bu$

was prepared by a general method of synthesis of sterically hindered t-butyl esters reported by HAUSER.<sup>15</sup>

65 ml. of t-butanol(dried over calcium sulphate and distilled to azeotrope off water.), 88 ml. of dimethylaniline (redistilled) in 140 ml. of sodium dried ether and 73 ml. of iso-butyryl chloride in 35 ml. of sodium-dried ether were stood for 15 hours at room temperature. The ether was distilled and the residue heated for 5 hours on a water bath. The solution was acidified with cold 10 % sulphuric acid and then extracted with ether. The ether layer was separated and extracted with 50 ml. portions of 10 % sulphuric acid (to remove all dimethylaniline) until the extract did not become cloudy when made alkaline with sodium hydroxide. After a final washing with 25 ml. of saturated sodium bicarbonate solution, the ether solution was dried by shaking with 10 gms. of anhydrous sodium sulphate. The solution was filtered, the ether removed by

distillation through a 30 cm. Widmer column and the ester distilled through the same column.

Yield, 65 % b.p. 127.5°-128.5°.

Found C, 66.40; H, 11.00. Calc.  $C_8H_{16}O_2$  C, 66.67; H, 11.10 %.

Tert-butyl  $\alpha\alpha$ -dimethylethoxaloacetate  $EtO_2C.CO.C(Me)_2.CO_2tBu$

was prepared by condensing diethyl oxalate and tert-butyl isobutyrate using sodium triphenylmethide, as described for ethyl $\alpha\alpha$ -dimethylethoxaloacetate. Tert-butyl isobutyrate (28 gms., 0.19 mole) was added with shaking to sodium triphenylmethide (0.19 mole) in ether (1300 ml.). After 25 minutes at room temperature diethyl oxalate (28 ml. 0.19 mole) was added with shaking. After standing 15 minutes, glacial acetic acid (15 ml.) was added and the mixture extracted with water (100ml). The ether solution was washed with saturated sodium bicarbonate, dried with sodium sulphate and the solvent distilled. The residue was fractionated in vacuo. Tert-butyl  $\alpha\alpha$ -dimethylethoxaloacetate (23 gms. 43 %) had a b.p. 104°-105°/4mm.  $n_{20} = 1.4252$ .

Found C, 58.8; H, 7.9. Calc. for  $C_{10}H_{20}O_5$ , C, 59.0; H, 8.2 %.

WESTHEIMER<sup>4</sup> gives, Yield 40 %,  $n_{20} = 1.4257$ , b.p. 107°-111/7mm.

#### Note

The times given must be strictly adhered to; if exceeded, starting material is obtained.

#### Hydrolysis of tert-butyl $\alpha\alpha$ -dimethylethoxaloacetate

In order to hydrolyse the ethyl-tert-butyl ester to the

mono-ethyl ester,  $\text{EtO}_2\text{C.COC}(\text{Me})_2.\text{CO}_2\text{H}$ ,<sup>12</sup> 10 gms. of the former were mixed with an equal volume of a saturated solution of hydrobromic acid in glacial acetic acid. After 5 minutes at room temperature, the mixture was placed in a vacuum desiccator. The acetic acid, hydrogen bromide and t-butyl bromide were removed by pumping off the gases (mechanical pump, Drikold and liquid oxygen traps) for several hours and then allowing the mixture to stand in vacuum with soda-lime overnight. Yield of crude liquid monoester 55 %. The synthesis outlined above were adopted because hydrolysis of the diethyl ester of dimethyloxaloacetic acid leads to the undesirable monoethyl ester  $\text{HO}_2\text{C.CO.C}(\text{Me})_2.\text{CO}_2\text{Et}$ . No means could be found to complete this hydrolysis to give the diacid. Presumably the carboxyl group adjacent to the quaternary carbon atom is sterically protected. The synthetic method here adopted takes advantage of the fact that t-butyl esters can be cleaved by a mechanism (presumably through a solvated carbonium ion) unavailable to the corresponding ethyl ester.

ΔΔ-dimethyloxaloacetic acid  $\text{HO}_2\text{C.CO.C}(\text{Me})_2.\text{CO}_2\text{H}$

5 gms. of the crude monoester  $\text{EtO}_2\text{C.CO.C}(\text{Me})_2.\text{CO}_2\text{H}$  were hydrolysed to the diacid by adding it to 50 ml. of concentrated hydrochloric acid and allowing the mixture to stand 2-3 days. The solution was then placed in a stream of dry air, in order to remove as much hydrochloric acid

and ethyl alcohol as possible. The residue was diluted with water and extracted four times with ether. The ether layer was dried with sodium sulphate and the ether removed in a stream of dry air. The acid was recrystallised twice from sodium-dried benzene. Yield 3 gms., m.p.  $104^{\circ}$ - $105^{\circ}$  (decomp.). Found C, 44.8; H, 4.8; M (by titration against alkali) 162.4. Calculated for  $C_6H_8O_5$ , C, 45.0; H, 5.0 % M. 160.1. The overall yield from t-butyl  $\alpha$ -dimethyl-ethoxaloacetate was 35 %.

Pyruvic acid  $CH_3.CO.CO_2H$

was obtained from B.D.H. and was vacuum distilled twice, then frozen. (m.p.  $13^{\circ}$ ). Found (by titration against alkali) M. 88.2. Calculated for  $C_3H_4O_3$ , M. 88.1. Only freshly prepared aqueous solutions were used, since it was found during potentiometric measurements that aqueous pyruvic acid solutions were definitely unstable if kept for some days.

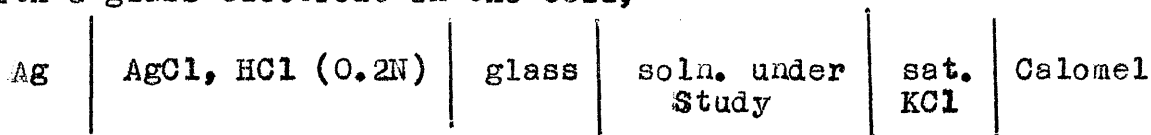


## 2) Measurements

Spectrophotometric measurements were carried out using a Hilger Uvispek spectrophotometer fitted with a standard quartz prism. Spectra, unless otherwise stated, were measured at room temperature ( $20^{\circ}$ ) in a pair of standard 1 cm. quartz cells capable of holding 3 ml. of solution. Kinetic runs were carried out in similar cells at room temperature ( $20^{\circ}$ ). In all cases the metal-ion solution was used as blank. 2 ml. of oxaloacetic acid were pipetted into the cell, followed by 1 ml. of the metal ion solution. Timing was begun when half the pipette had drained. The solution was then rapidly shaken for 30 seconds and readings begun at 45 seconds, on the initially checked instrument. Readings were taken at 15 second intervals. Distilled water and A.R. spectroscopic solvents were used in all cases. Ether was first dried with sodium wire, then refluxed over sodium for six hours and distilled. It was then kept in a dark sealed bottle protected by a silica gel guard tube. In all cases where accurate temperature control was required, a Hilger water jacket was used in conjunction with a 'Circotherm' unit.

Potentiometric measurements were made by means of a Cambridge bench-type pH-meter and a commercial glass electrode. The dissociation constants of dimethyloxaloacetic acid and its association constant with  $\text{Cu}^{2+}$  ions were obtained from the ~~measured~~ pH's of solutions measured

with a glass electrode in the cell,<sup>16</sup>



The glass electrode was made from Corning 015 glass and had a resistance of 20 megohms. Potentials were measured on a Tinsley potentiometer reading to 0.05 mv., a valve voltmeter being used as null-point indicator. The electrode system, as for the Cambridge meter, was standardised using B.D.H. tabloid phthalate buffer pH 4.01 at 25° and B.D.H. tabloid phosphate buffer pH 6.99 at 25°. The factor for converting e.m.f. into pH was constant over the whole buffer range. The calomel electrode and a beaker containing the glass electrode and fitted with a stirrer were mounted in a water bath kept at 25° ± 0.1°.

0.0700 gm. of  $\alpha$ -dimethyloxaloacetic acid were dissolved in 75 ml. of distilled water and the requisite amount of 0.2N HCl or NaOH added (usually 1-2 ml.). 20 ml. of this solution was used to rinse out the cell. 50 ml. of the solution was then pipetted into the cell and allowed to equilibrate. While stirring, the requisite amount of 0.1M  $\text{CuCl}_2$  was pipetted in (1-2 ml.), when the pipette was half drained timing was begun. E.M.F. readings were taken at approximately 2 minute intervals, values were then extrapolated to the time of mixing, this was necessary since a slow drift in E.M.F. occurred due to decarboxylation.

The dissociation constant of pyruvic acid and its association constant with  $\text{Cu}^{2+}$  ions were measured in a similar manner; in this case no drift in E.M.F. with time occurred.

Manometric measurements were carried out using the apparatus described in detail in Part 2.

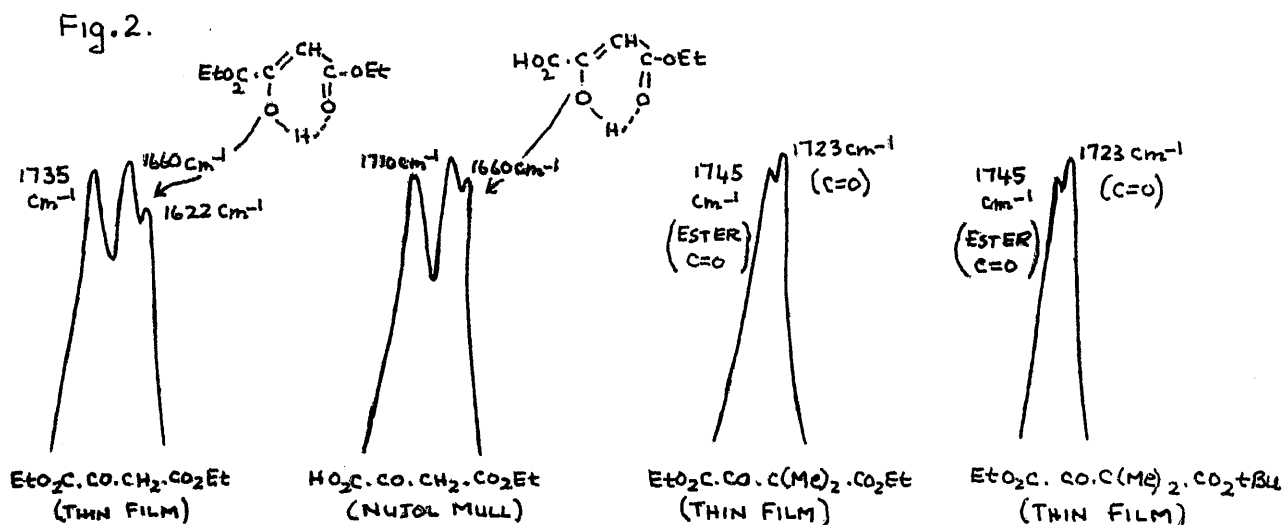
Grade 'A' volumetric apparatus and 'A.R.' reagents were used throughout.



These observations agree with those of [illegible] and [illegible] who have shown that [illegible] in dilute solution, it is [illegible] and [illegible] and [illegible] are [illegible] these are ascribed to the [illegible]

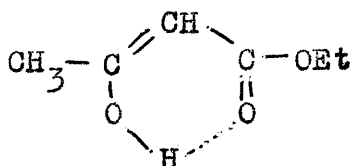
Infra-red Assignments

It was found that those compounds capable of enolisation such as  $\text{EtO}_2\text{C}\cdot\text{CO}\cdot\text{CH}_2\cdot\text{CO}_2\text{Et}$  and  $\text{HO}_2\text{C}\cdot\text{CO}\cdot\text{CH}_2\cdot\text{CO}_2\text{Et}$  gave two bands in the carbonyl region of the infra-red, while  $\text{EtO}_2\text{C}\cdot\text{CO}\cdot\text{C}(\text{Me})_2\cdot\text{CO}_2\text{Et}$  and  $\text{EtO}_2\text{C}\cdot\text{CO}\cdot\text{C}(\text{Me})_2\cdot\text{CO}_2\text{tBu}$  gave single bands. (Fig 2).



These observations agree with those made by RASMUSSEN.<sup>17</sup>

Ethyl  $\alpha$ -dimethyl acetoacetate shows a single band at  $1727\text{ cm}^{-1}$ , examined in dilute solution, it is seen that there is a strong component at  $1718\text{ cm}^{-1}$  and a weaker one appearing as a shoulder at  $1742\text{ cm}^{-1}$ , these are ascribed to the ketone and ester carbonyl groups respectively. Ethyl  $\alpha$ -methylacetoacetate and ethyl acetoacetate each exhibit an additional band near  $1650\text{ cm}^{-1}$  ascribable to the conjugated chelate ring,

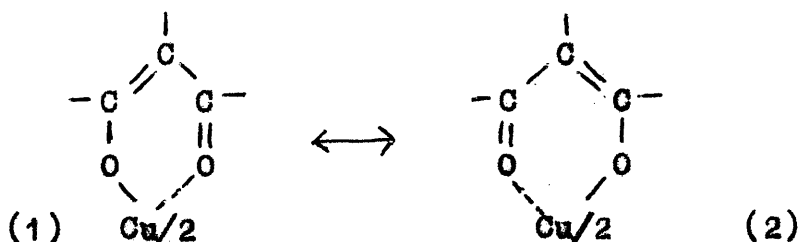


of the enol lowering the carbonyl frequency. That enolisation is only partial is seen from the persistence of a strong  $1730 \text{ cm.}^{-1}$  band.

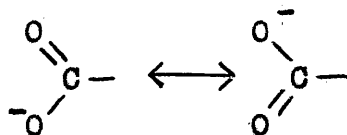
### Infra-red spectra of metal chelates

Practically no work on the infra-red spectra of metal chelates has been carried out; in fact only five papers (all on  $\beta$ -diketone derivatives) have been published up to 1957.<sup>18-22</sup>

It has been shown that in acetylacetonate complexes, the complete resonance between the forms (1) and (2) leads to modification of the character of both C=O and C-O links. As a result both take double bond character.



Two bands of approximately equal intensity are shown in the spectra and by analogy to the ionised carboxyl group,



these have been assigned by LECOMPTE<sup>23-24</sup> to the asymmetric and symmetric vibrations of these two groups. Salicylaldehyde is an exception as only one strong band is shown, presumably indicating that owing to the weaker double bond involved the resonance is less complete.

Table 1 Assigned carbonyl frequencies

	<u>Frequency cm.<sup>-1</sup></u>	<u>Assignment</u>	<u>Structures</u>
acetylacetone	1724	keto	$\text{CH}_3\text{CO}\cdot\text{CH}_2\cdot\text{COCH}_3$
	1608	enol chelate	
benzoylacetone	1724	keto	$\text{C}_6\text{H}_5\cdot\text{CO}\cdot\text{CH}_2\cdot\text{COCH}_3$
	1600	enol chelate	
salicylaldehyde	1668	chelate	
acetoacetic ester	1733	ester CO	$\text{CH}_3\cdot\text{CO}\cdot\text{CH}_2\cdot\text{CO}_2\text{Et}$
	1709	keto CO	
	1645	enol chelate	

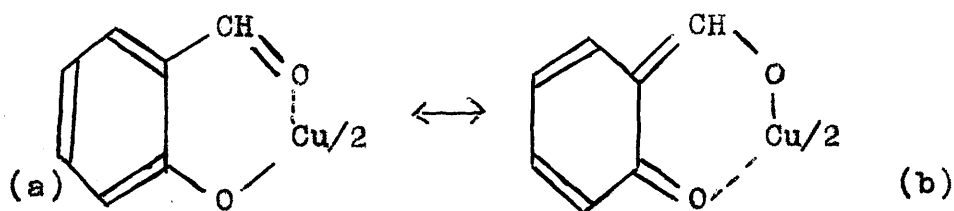
These values are compared with those of the metal chelates (Table 2).

Table 2 Carbonyl frequencies ( $\text{cm}^{-1}$ ) of metal chelate compounds

Salicylaldehyde (Nujol)		Acetylacetonone ( $\text{CHCl}_3$ )	
Cu	1608	1580	1390
Co	1656	1586	1373
Ni	1652	1605	1389
Mg	1681	1590	1397
Zn	1658	1577	1375
Fe	-	1575	1370
Cd	1650	-	-

Salicylaldehyde Chelates

do not show any second C-O absorption comparable in intensity with the first, and in some cases the carbonyl absorption is not far removed from that of salicylaldehyde itself. The carbonyl group thus retains at least a proportion of its original character. There appears to be little resonance between structures (a) and (b).



MELLOR and MALEY<sup>25</sup> give stability constants for the salicylaldehyde chelates. Cadmium, iron and manganese are omitted as there appears to be some doubt as to whether they are mono or di-salicylaldehyde complexes. It will be seen that the

carbonyl shift follows the order,  $\text{Cu} > \text{Ni} > \text{Co} > \text{Zn} > \text{Mg}$ , which is the usual order of stability of bivalent metal complexes. When the carbonyl frequencies are plotted against the stabilities ( $\log K_1 K_2$ ) given by MELLOR<sup>25</sup> a straight line relationship is found. Fig.3.

It should therefore be possible to utilise I.R. measurements to determine directly the stabilities of other chelate compounds of bivalent metals with salicylaldehyde. In addition a plot of atomic number against frequency (carbonyl) results in a curve which is similar in shape to that derived by IRVING and WILLIAMS.<sup>26</sup> Fig.3.

#### Acetylacetonate chelates

The frequencies of the first carbonyl absorption in metal acetylacetonates is essentially the same, and only Ni and Mg show any departure from the common value. Resonance effects are clearly operating sufficiently strongly to dwarf any variations in frequency which might be expected to follow alterations in the metal. The second carbonyl absorption near  $1400 \text{ cm.}^{-1}$  shows rather more variation, but there is no obvious relationship with stability.

#### Oxaloacetate chelates

Since the metal chelate (c) had been prepared, its infra-red spectrum was taken on a 'Unicam' instrument.



Fig. 3.

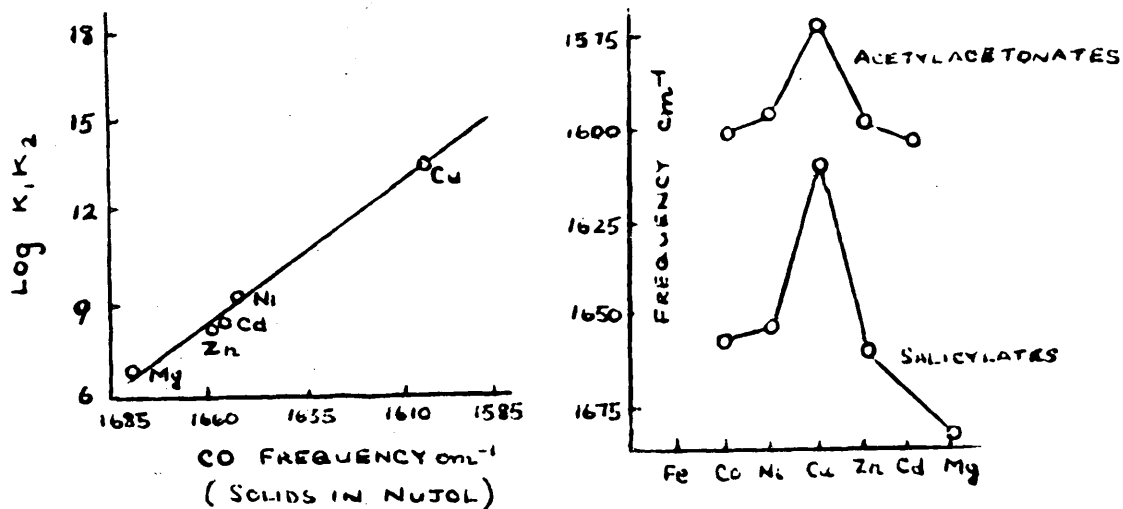
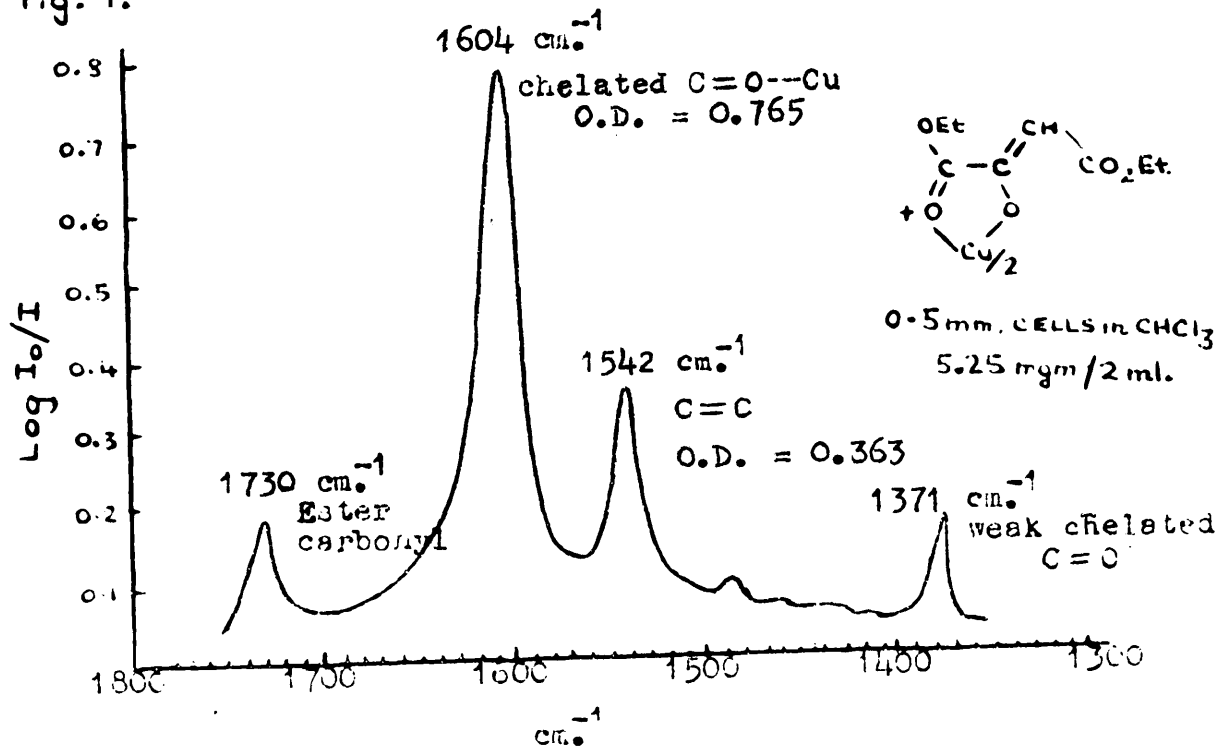
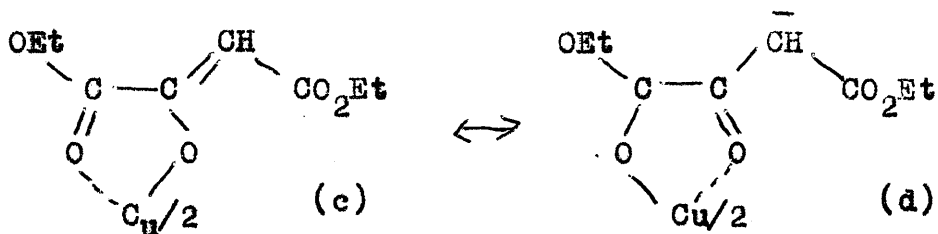


Fig. 4.





The assignments given for the ester, by comparison with its dimethyl derivative are  $1745 \text{ cm.}^{-1}$  (ester carbonyl),  $1723 \text{ cm.}^{-1}$  (ketone),  $1650 \text{ cm.}^{-1}$  (enol chelate). The copper chelate should resemble salicylaldehyde complexes, since little resonance will be involved between structures (c) and (d), and should show an intense  $\text{C}=\text{O} \cdots \text{M}$  band around  $1608 \text{ cm.}^{-1}$  with only a very weak band in the region of  $1380 \text{ cm.}^{-1}$  (resonating acetylacetonates). In the acetylacetonates there is a band around  $1515 \text{ cm.}^{-1}$ , attributed by LECOMPTE<sup>18</sup> to  $\text{C}=\text{C}$  in the enol structure. There should also be an ester carbonyl absorption around  $1735 \text{ cm.}^{-1}$ . All these bands are observed. Fig.4.

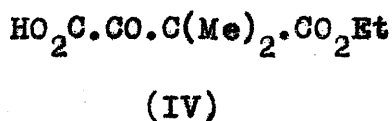
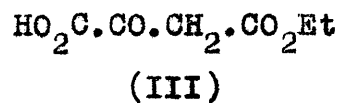
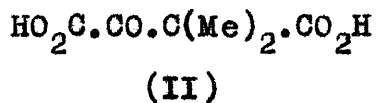
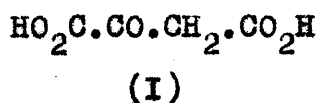
This spectrum gives further evidence that chelation of a metal ion by a ketone results in a very considerable carbonyl shift of over  $100 \text{ cm.}^{-1}$   $\left[ (1745 - 1605 \text{ cm.}^{-1}) = 141 \text{ cm.}^{-1} \right]$ , while in the acetylacetonates the shift is  $144 \text{ cm.}^{-1}$  for the copper ion.

The magnitude of these shifts is comparable with the shift produced by chelation with the enol; thus acetylacetone gives a shift of  $116 \text{ cm.}^{-1}$  (ketone to enol chelate), and benzoyl acetone a shift of  $124 \text{ cm.}^{-1}$ .

Part 1 Results and Discussion \*

The metal ion catalysed decomposition of oxaloacetic acid to pyruvic acid and carbon dioxide involves the interaction of metal ions with oxaloacetate in the initial state, and with pyruvate in the final state. These states can be studied directly by thermodynamic methods, while interaction in the transition state is indicated by kinetic measurements.

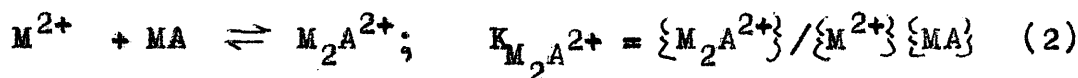
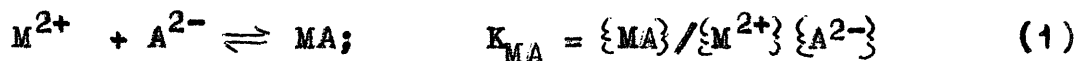
For the initial state, experiments were made with oxaloacetic acid (I),  $\alpha\alpha$ -dimethyloxaloacetic acid (II), which cannot enolise, ethyl oxaloacetate (III), which cannot decarboxylate or form a dicarboxylate complex, and ethyl  $\alpha\alpha$ -dimethyloxaloacetate (IV), which cannot enolise or be decarboxylated and can only form a ketonic  $\alpha$ -oxo carboxylate complex.



\* ( The results of the work on metal ion catalysed decarboxylation have already been published (GELLES and HAY, J.C.S., 3673 (1958)). )

Association Constants at 25°1) Oxaloacetic Acid (I)

A detailed study of the association equilibria has been made by GELLES.<sup>16</sup> In the pH range investigated the significant association equilibria are,



where  $M^{2+}$  represents a metal ion,  $A^{2-}$  the oxaloacetate anion, and  $K_{MA}$  and  $K_{M_2A^{2+}}$  are the thermodynamic association constants, (Table 1).

Table 1 Association constants of the oxaloacetates

	Ca <sup>2+</sup>	Mn <sup>2+</sup>	Co <sup>2+</sup>	Zn <sup>2+</sup>	Ni <sup>2+</sup>	Cu <sup>2+</sup>
10 <sup>-3</sup> K <sub>MA</sub>	0.4	0.7	1.4	1.7	3.2	75
10 <sup>-2</sup> K <sub>M<sub>2</sub>A<sup>2+</sup></sub>	1	1	2	2	1.5	-

2) α-dimethyloxaloacetic Acid (II)

The ionisation constants were calculated from the pH of mixtures of the acid with varying proportions of alkali.<sup>27</sup> The pH values were extrapolated to the time of addition of alkali.

If the total concentrations of the dicarboxylic acid and of sodium hydroxide are a and b respectively,

and

$$L = b + [H^+], \quad M = a - b - [H^+], \quad N = 2a - b - [H^+], \quad [OH^-] \ll [H^+]$$

$$\text{then } \left[ \frac{\{H^+\}^2 L f_2}{N} \right] = \left[ \frac{\{H^+\} M f_2}{N f_1} \right] K_1 + K_1 K_2 \quad (3)$$

$$\text{or } X = Y K_1 + K_1 K_2 \quad (4)$$

where  $K_1$  and  $K_2$  are the two thermodynamic ionisation constants

$$K_1 = \frac{\{H^+\} \{HA^-\}}{\{H_2A\}}; \quad K_2 = \frac{\{H^+\} \{A^{2-}\}}{\{HA^-\}}$$

Square brackets and braces are used to indicate concentrations and activities, respectively.  $f_1$  and  $f_2$  are ionic activity coefficients for univalent and bivalent ions, calculated from the Davies equation,

$$- \log f_z = 0.5 z^2 \left( I^{1/2} / 1 + I^{1/2} - 0.2 I \right) \quad (5)$$

The ionic strength  $I$  is calculated from successive approximations.  $f_0$ , the activity coefficient for an uncharged species is little different from unity at ionic strengths below 0.01. (The highest ionic strength used was 0.0125).  $K_1$  and  $K_2$  are obtained from the slope and intercept of the linear plot of  $X$  against  $Y$ . The results of some pH measurements and the quantities  $X$  and  $Y$  are given in Table 2

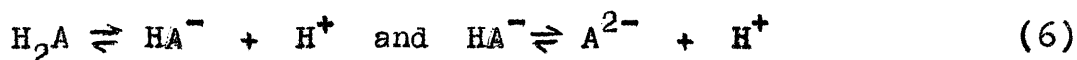
Table 2 Ionisation constants of *DL*-dimethyloxaloacetic acid

$10^3 a$	.....	5.76	5.67	5.76	5.59	5.52
$10^3 b$	.....	2.88	3.41	4.56	6.74	9.40
pH	.....	2.66	2.77	3.31 <sub>5</sub>	4.02 <sub>5</sub>	4.99
$10^8 X$	.....	298	185	136	0.98	0.062
$10^6 Y$	.....	142	93.8	40.8	-20.7	-28.4

$$K_1 = 1.7 \times 10^{-2}; \quad K_2 = 2.4 \times 10^{-5}.$$

The values obtained for the ionisation constants can be compared with approximate values of  $3 \times 10^{-2}$  and  $1.7 \times 10^{-5}$  obtained by an indicator method at  $I = 0.5$ , and corrected to zero ionic strength.<sup>4</sup>

In the presence of copper the pH changed with time due to decarboxylation of the copper chelate compound; measurements could be made only over a limited range of pH and metal ion concentration. The pH curve was extrapolated to the time of addition of metal ion. The two ionisation equilibria of the acid (II) are,



If the only significant association equilibrium is



we have for the concentration of the acid (II)

$$C_a = [H_2A] + [HA^-] + [A^{2-}] + [MA] \quad (8)$$

for the total copper ion concentration

$$C_m = [M^{2+}] + [MA] \quad (9)$$

and for electroneutrality ( $OH^- \ll H^+$ )

$$2[M^{2+}] + [Na^+] + [H^+] = [Cl^-] + [HA^-] + 2[A^{2-}] \quad (10)$$

The ionic strength and the ionic activity coefficients are obtained by successive approximations;

$$I = 0.5 \left( 4[M^{2+}] + [H^+] + [HA^-] + 4[A^{2-}] + [Na^+] - [Cl^-] \right) \quad (11)$$

from equations (6) - (10) we obtain,

$$[\text{H}_2\text{A}](2 + K_1/\{\text{H}^+\}f_1) = [\text{Cl}^-] + 2C_a - 2C_m - [\text{Na}^+] - [\text{H}^+] \quad (12)$$

The concentration of all other species, and hence the association constant  $K_{MA}$ , can be calculated.

Table 3 Association constant of copper  $\alpha$ -dimethyloxaloacetate

$10^3 C_a$	$10^3 C_m$	$10^3 \text{HCl}$	pH	I	$10^{-3} K_{MA}$
5.61	1.96	5.10	2.08	0.0141	55
5.38	3.85	7.40	1.99	0.0215	51
5.54	3.85	2.53	2.16 <sub>5</sub>	0.0169	45
5.26	7.41	7.12	2.00	0.0316	40

In view of errors due to rapid decarboxylation of the chelate compound the constancy of the values of  $K_{MA}$  given in Table 3 must be regarded as satisfactory, although the range of pH studied is too small to exclude the presence of other complexes. It is noted that the average value of  $K_{MA}$ ,  $48 \times 10^3$  is of the same order of magnitude as the association constant of copper oxaloacetate. (c.f. Table 1).

### Ethyl oxaloacetate (III)

The thermodynamic ionisation constant of this monobasic acid was determined in the usual way, by measurements with a glass electrode, to be  $1.9 \times 10^{-3}$  which is slightly smaller than the first ionisation constant of oxaloacetic acid ( $2.79 \times 10^{-3}$ ). Some measurements are illustrated in Table 5.

Table 5 Ionisation constant of ethyl oxaloacetate

$10^3[\text{III}]$	$10^3[\text{NaOH}]$	pH	$10^3K$
1.94	-	2.93	1.89
1.94	0.495	3.07 <sub>5</sub>	1.96
1.94	0.693	3.15	1.91
1.94	0.99	3.28	1.90
0.97	0.75	3.86	1.83

Measurements of the pH of solutions containing copper ions could not be interpreted in terms of the association equilibria;



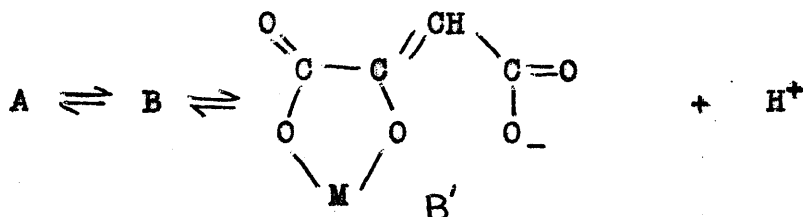
The data in Table 6 show that the hydrogen ion concentration can exceed the initial ester concentration when cupric chloride is added. This implies that in addition to equilibria (13) and (14) there is appreciable formation of an enolic complex with the displacement of a proton,

Table 6 Formation of an enolic copper complex from ethyl oxaloacetate.

$10^3[\text{III}]$	2.00	1.96	1.92	1.88	1.85	1.82	1.78
$10^3[\text{CuCl}_2]$	-	1.96	3.85	5.66	7.40	9.09	10.71
pH	2.90 <sub>5</sub>	2.84	2.80 <sub>5</sub>	2.78 <sub>5</sub>	2.77	2.75 <sub>5</sub>	2.74 <sub>5</sub>



In contrast to ethyl oxaloacetate, oxaloacetic acid can form an enolic complex B from which a further proton will only be displaced at a higher pH. Equation (1) represents the formation of A and B. Potentiometric measurements on oxaloacetates were made in a pH range in which the enolic complex B' is not significant.



### Pyruvic Acid

A value of  $3.24 \times 10^{-3}$  for the thermodynamic ionisation constant has been obtained by PEDERSEN<sup>5</sup> from potentiometric measurements. A spectrophotometric determination of this constant was carried out as a comparison. The extinction coefficient of the anion of pyruvic acid was obtained directly from its sodium salt. A rough value for the free acid was determined by measurements in strong hydrochloric acid. Equation (16) was used to calculate approximate values of  $[\text{A}^{\frac{3-}}}]$ ,  $[\text{HA}]$  and the thermodynamic dissociation constant  $K$ .

$$\epsilon_{\text{obs}} = (\epsilon_{\text{A}^{\frac{3-}}} [\text{A}^{\frac{3-}}] + \epsilon_{\text{HA}} [\text{HA}]) / [\text{A}^{\frac{3-}}] + [\text{HA}] \quad (16)$$

These were refined by successive approximations. Activity coefficients were calculated from the Davies equation. Table 7 shows a typical set of results calculated from

FIG 1

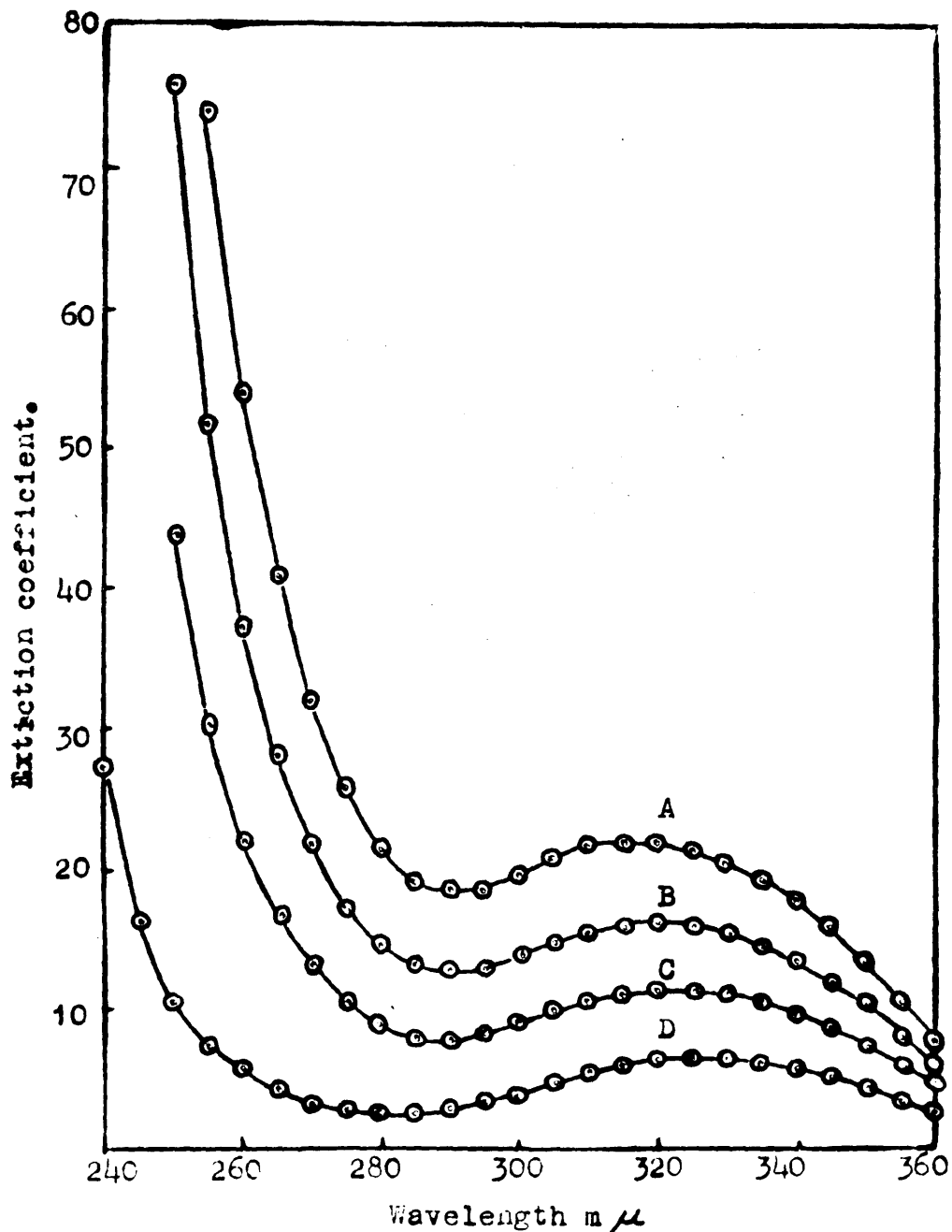
Ultra-violet absorption spectra of pyruvic acid, in the region of the  $\alpha$ -keto acid peak.

(A) 0.1156 M Pyruvic acid + 0.1156 M NaOH.

(B) 0.1156 M Pyruvic acid + 0.0578 M NaOH.

(C) 0.1156 M Pyruvic acid.

(D) 0.1156 M Pyruvic acid + 0.33 N HCl.

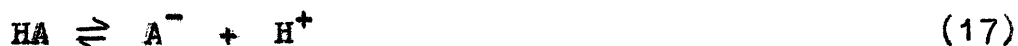


curve C, Fig 1. The average value of  $3.19 \times 10^{-3}$  agrees very well with the value of  $3.24 \times 10^{-3}$  obtained by FEDERSEN.<sup>5</sup>

Table 7 Spectrophotometric determination of the dissociation constant of pyruvic acid

Wavelength $m\mu$	$10^3[A^-]$	$10^3[H^+]$	$10^3[HA]$	$f_1$	$10^3K$
300	7.77	7.77	15.35	0.912	3.27
310	7.64	7.64	15.48	0.913	3.15
320	7.66	7.66	15.46	0.913	3.16
330	7.66	7.66	15.46	0.913	3.17

If the monobasic acid is represented by HA



and if the only association equilibrium is



we have for the total concentration of metal

$$C_m = [M^{2+}] + [MA^+] \quad (19)$$

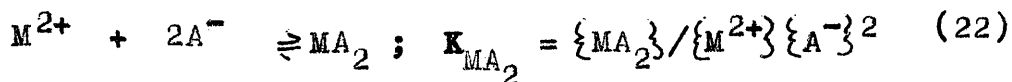
for the total concentration of acid

$$C_a = [HA] + [A^-] + [MA^+] \quad (20)$$

and for electroneutrality

$$[H^+] + 2[M^{2+}] + [Na^+] + [MA^+] = [Cl^-] + [A^-] \quad (21)$$

If on the other hand, the only significant association equilibrium is



Then equations (19)-(21) become

$$C_m = [M^{2+}] + [MA_2] \quad (23)$$

$$C_a = [HA^-] + [A^-] + 2[MA_2] \quad (24)$$

$$[H^+] + 2[M^{2+}] + [Na^+] = [Cl^-] + [A^-] \quad (25)$$

in either case

$$[HA] = [Cl^-] + [C_a] - 2C_m - [Na^+] - [H^+] \quad (26)$$

the ionic strength and activity coefficients are obtained as before, and the concentration of all other species can be calculated.

The results of some pH measurements on copper pyruvate are given in Table 8.

Table 8 Association constant of copper pyruvate

$10^3 C_a$	$10^3 C_m$	$10^4 [Cl^-]$	$10^4 [Na^+]$	pH	$\log_{10} K_{MA^+}$	$\log_{10} K_{MA_2}$
2.33	5.0	105	5.9	2.83	2.3	5.0
2.33	5.0	105	11.9	2.98	2.2	4.9
2.39	5.0	105	17.9	3.17	2.3	4.9
7.13	10.0	21	2.96	2.75	3.1	4.8
9.50	10.0	21	3.95	2.69	4.2	4.8

Association constants were calculated on the assumption of there being only one complex,  $MA^+$  or  $MA_2$ . It can be seen that the association constant for  $MA_2$  remains approximately constant, while that for  $MA$  changes as

the Pyruvate/Copper ratio is increased; the predominant species is clearly  $MA_2$ .

The monobasic acids, ethyl oxaloacetate and pyruvic acid, tend to form chelates of the type  $MA_2$  with no net charge. The compounds of ethyl oxaloacetate are more stable than those of pyruvic acid, which appear to be entirely ketonic. The dibasic acids, oxaloacetic and  $\alpha\alpha$ -dimethyl oxaloacetic acid tend to form chelate compounds of the type  $MA$  with no net charge, and these appear to have association constants of the same order of magnitude.

#### Chelate compounds from oxaloacetate

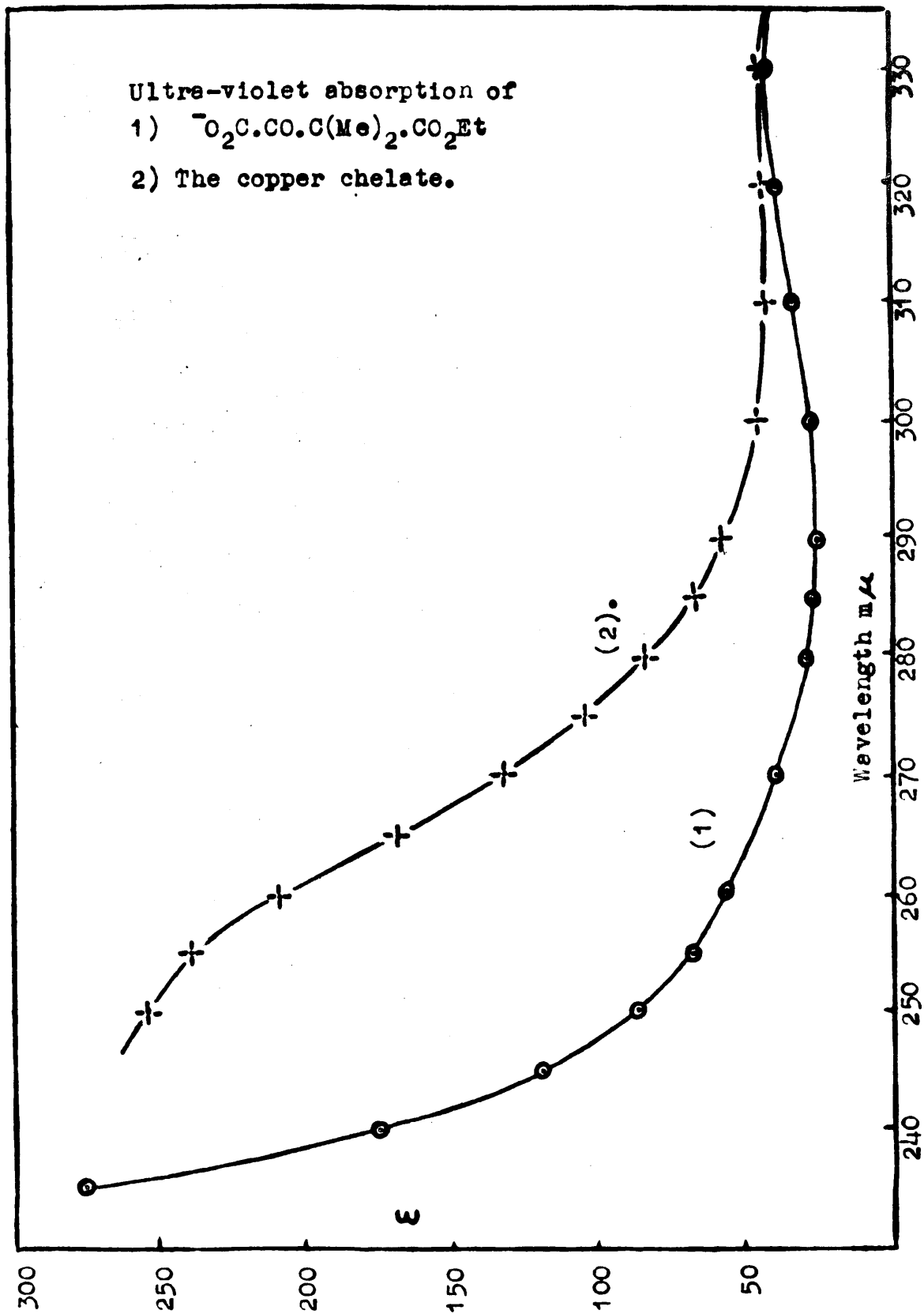
##### The ketonic chelate compound A.

Chelate compounds of oxaloacetic acid are not entirely ketonic. The ketonic compounds are decarboxylated to a strongly absorbing enolic pyruvate intermediate, as are those of  $\alpha\alpha$ -dimethyl oxaloacetic acid (II). The monoester (IV), however, forms only stable ketonic chelate compounds.

Fig. 2 shows the ultra-violet absorption spectra for the anion of ester (IV) and for its copper chelate compound.

Experiments were carried out with anion concentrations of  $1 \times 10^{-3}$  and  $3.37 \times 10^{-3}$  M. and with copper concentrations of  $1 \times 10^{-2}$  and  $3.33 \times 10^{-2}$  M. The association constants for the copper chelate compounds of esters (III) and (IV) are of the same order of magnitude. With the above concentrations the anion of ester (IV) should be completely

FIG 2



chelated, and this is borne out by the constancy of the extinction coefficient as the copper concentration is increased. The  $\alpha$ -oxo peak occurs at  $338 \text{ m}\mu$  ( $\epsilon = 43$ ). At  $295 \text{ m}\mu$  which is  $\lambda_{\text{max}}$  for the enolic chelate compounds,  $\epsilon$  is 27 for the anion of ester (IV), and 68 for the copper chelate. Ketonic chelates of  $\alpha$ -oxo carboxylates with other transition metal ions are also expected to have extinction coefficients of around 70 at  $295 \text{ m}\mu$ . This is borne out by further spectrophotometric measurements described below.

#### The enolic chelate compound B

Enols  $\text{HO.CR:CH.CO.R'}$  have absorption maxima at about  $260 \text{ m}\mu$ ; on chelation with transition metal ions the maximum absorption of the enolate ion is shifted to higher wavelengths, and the extinction coefficient is increased two or three fold. Studies of enolic chelate compounds in chloroform indicate that  $\lambda_{\text{max}}$  and  $\epsilon$  are not greatly affected by the nature of the bivalent metal ion.<sup>21</sup>

Fig. 3 shows that the peak at c.a.  $260 \text{ m}\mu$  is due to the enol of oxaloacetic acid. Fig. 4 shows the ultra-violet absorption spectra of oxaloacetates (I) and (II) in ether and light petroleum (b.p.  $40^\circ$ ). Both oxaloacetic acid and ethyl oxaloacetate appear to be completely enolised ( $\lambda_{\text{max}} = 295 \text{ m}\mu$ ,  $\epsilon = 8,800$ ). (Oxaloacetic acid is not decarboxylated in these solvents).

Fig 5 relates to the copper enolate of ethyl oxaloacetate,

FIG 3

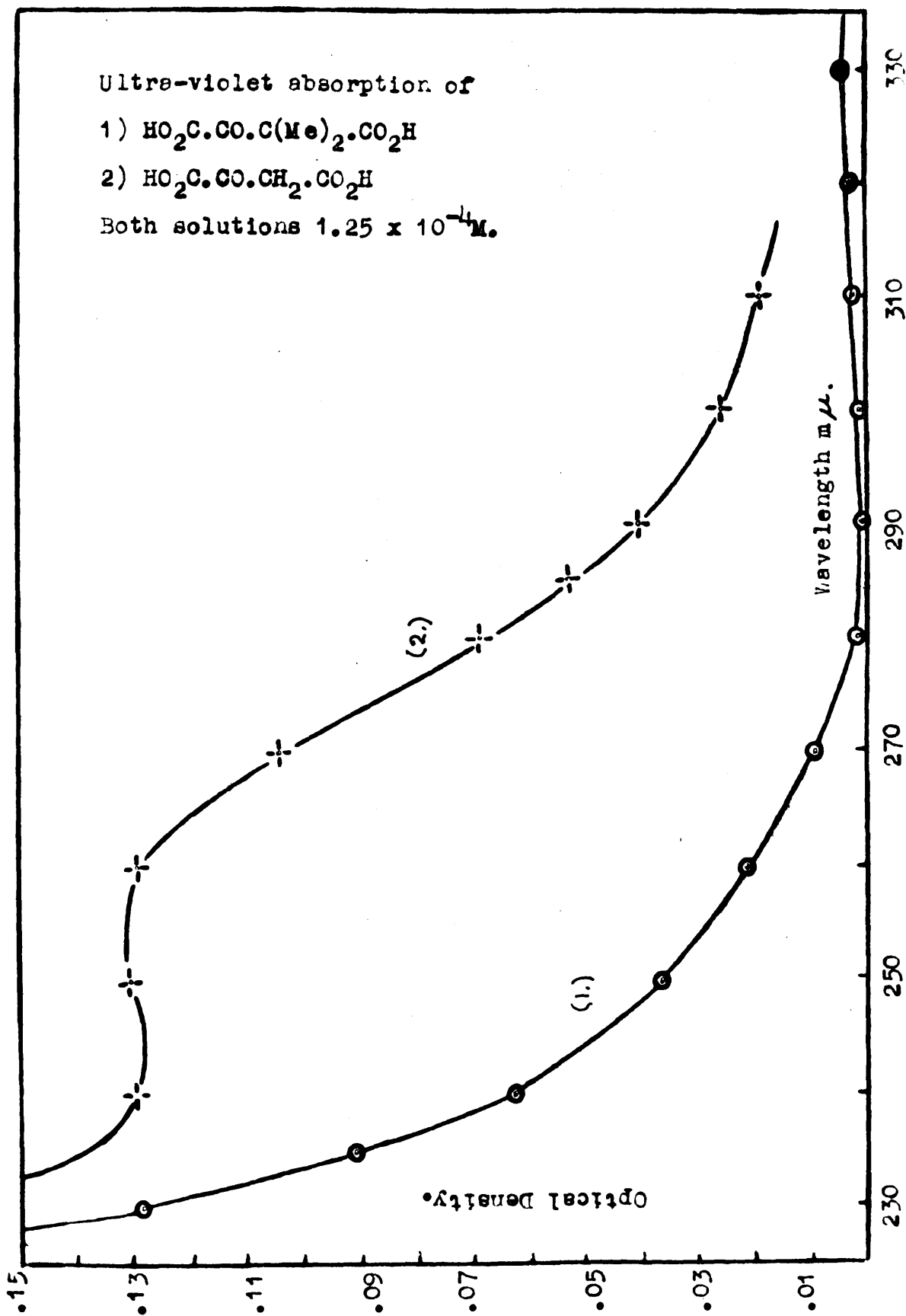




FIG 4

Ultra-violet absorption of  $\text{HO}_2\text{C}\cdot\text{CO}\cdot\text{CH}_2\cdot\text{CO}_2\text{H}$   
 in ether and light petroleum (b.p.  $40^\circ$ ) and  
 for  $\text{HO}_2\text{C}\cdot\text{CO}\cdot\text{CH}_2\cdot\text{CO}_2\text{Et}$ . in ether.

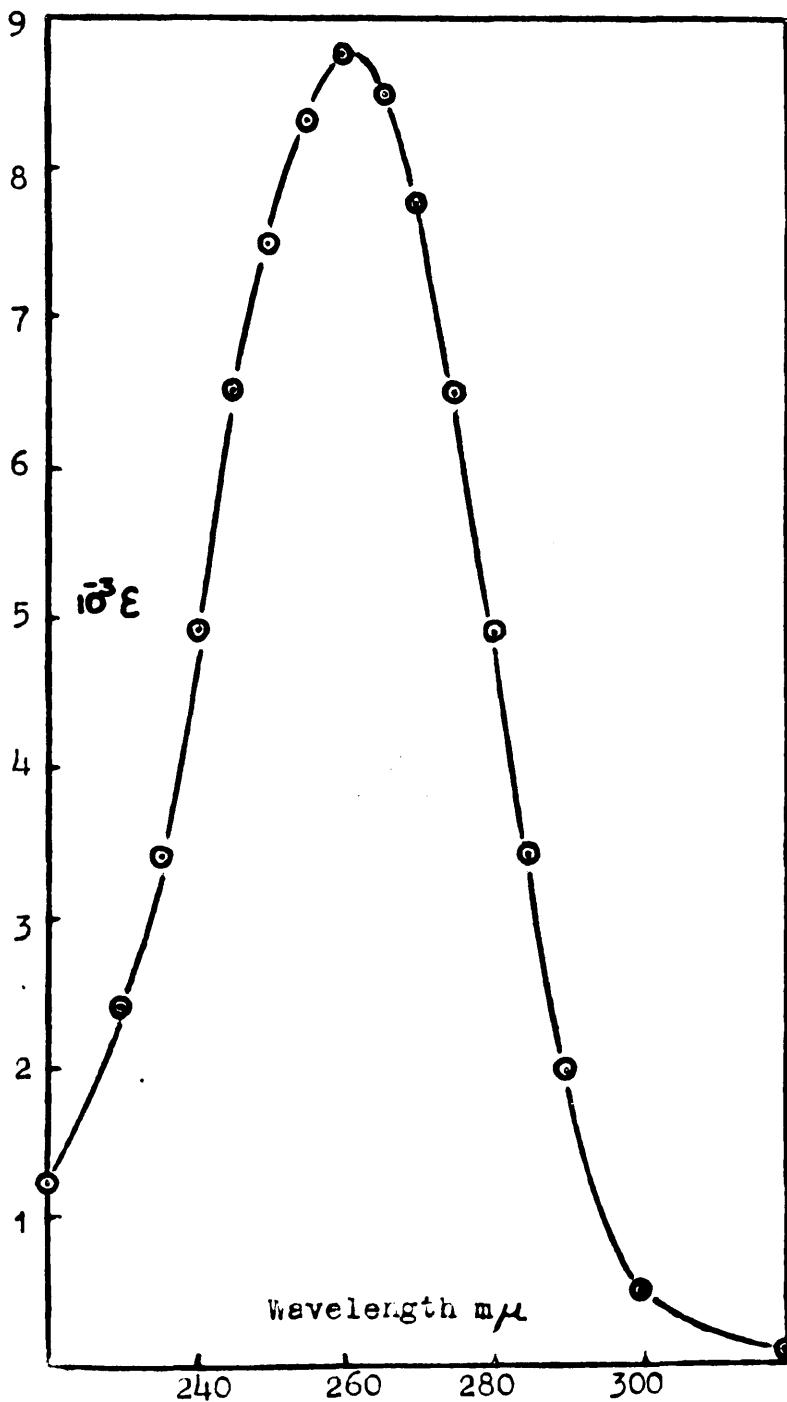
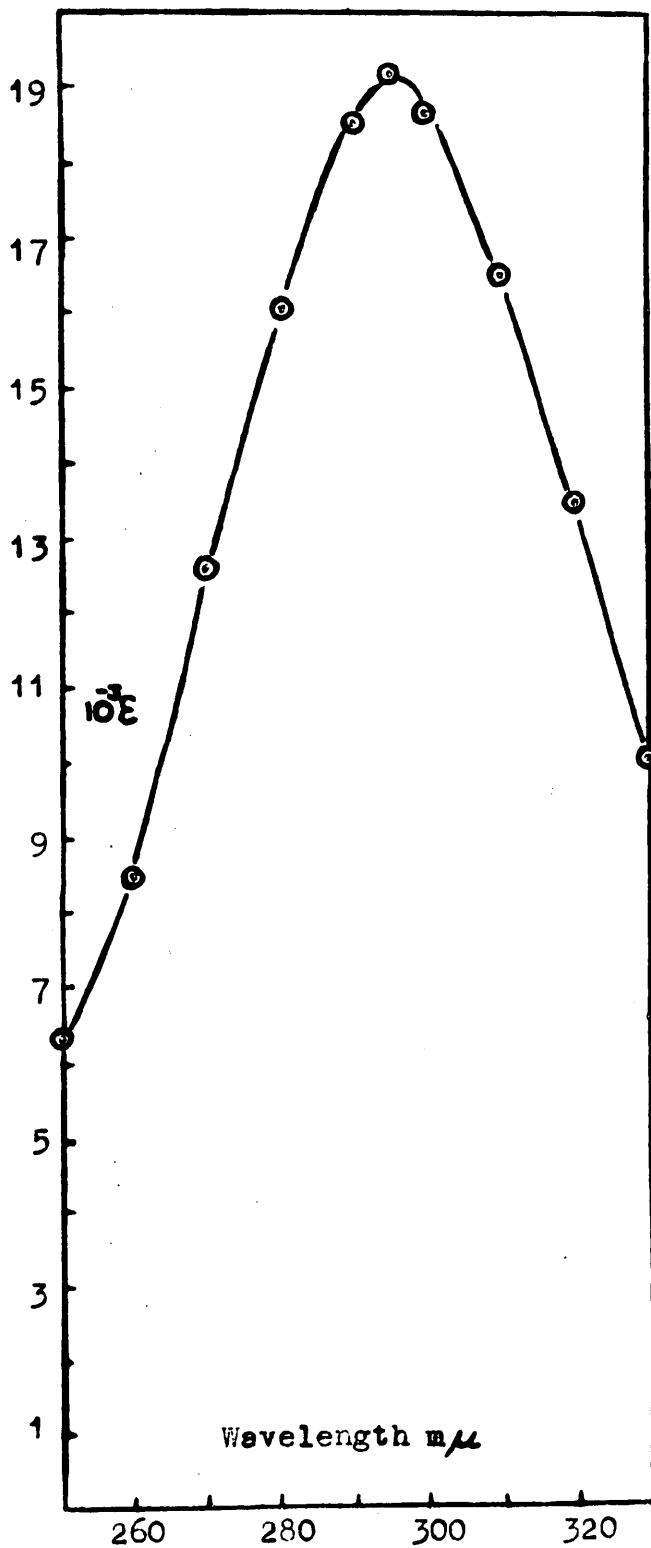
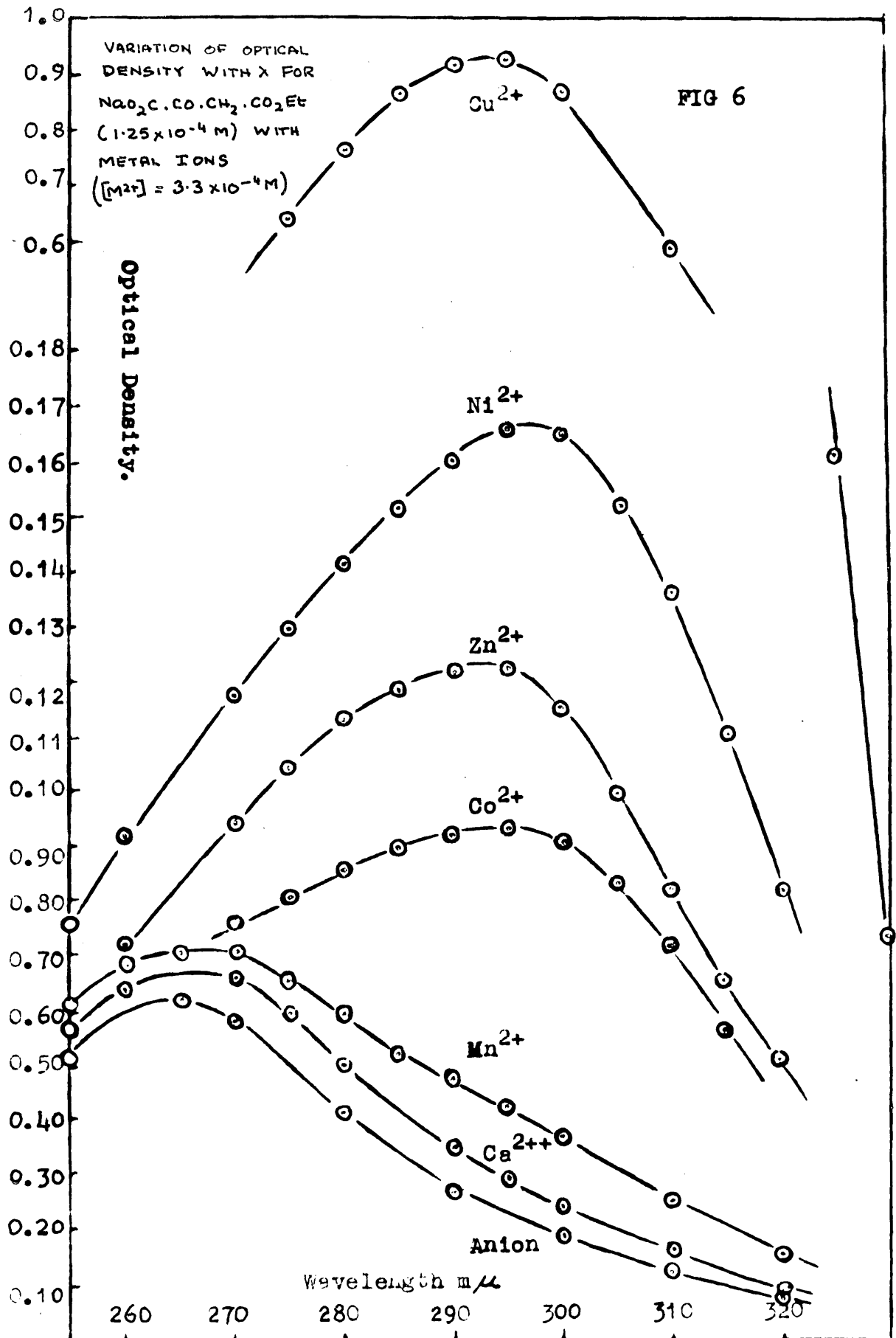


FIG 5

Ultra-violet absorption of  
 $\text{Cu}[\text{EtO}_2\text{C}\cdot\text{CO}^-:\text{CH}\cdot\text{CO}_2\text{Et}]_2$  in  $\text{CHCl}_3$





$\text{Cu} \left[ \text{EtO}_2\text{C}(\text{CO}^-):\text{CH}.\text{CO}_2\text{Et} \right]_2$  (in chloroform;  $\lambda_{\text{max}} = 295 \text{ m}\mu$ ,  $\epsilon = 2 \times 10^4$ ). The enolic peak of the oxaloacetate (III) at  $260 \text{ m}\mu$  and the shift of  $\lambda_{\text{max}}$  to  $295 \text{ m}\mu$  on chelation of the oxaloacetate with  $\text{Cu}^{2+}$ ,  $\text{Ni}^{2+}$ ,  $\text{Zn}^{2+}$  and  $\text{Co}^{2+}$  ions in aqueous solution is illustrated in Fig. 6. Enolic oxaloacetate complexes are expected to have  $\lambda_{\text{max}} = 295 \text{ m}\mu$  ( $\epsilon \sim 2 \times 10^4$ ), a value independent of solvent or the nature of the transition metal ion.

#### Speed of formation of chelates

Addition of metal ions to oxaloacetic acid under certain conditions produces a rise of optical density with time, Fig 7, which has been attributed<sup>3,8</sup> to the slow formation of the enolic complex B. The speed of formation of the chelate compounds of ethyl oxaloacetate (III), which cannot be decarboxylated, has now been measured under comparable conditions and has been shown to be very fast. The optical density first measured 45 seconds after addition of metal ion changed very little with ~~MAXX~~ time. (Table 7). The formation of a strongly absorbing intermediate on decarboxylation must therefore play a part in determining the changes in absorption spectra of metal oxaloacetates. The copper compounds are formed at a measurable rate at high pH, but for the other metal ions chelation appears to be complete within a fraction of a minute at pH's less than 6.

Fig. 7

Variation of optical density with time ( $\lambda = 290 \text{ m}\mu$ )  
for  $\text{HO}_2\text{C}\cdot\text{CO}\cdot\text{CH}_2\cdot\text{CO}_2\text{H}$ .  $[\text{I}] = 1.25 \times 10^{-4} \text{ M.}$ ,  
 $[\text{Zn}^{2+}] = 3.36 \times 10^{-4} \text{ M.}$ ,  $[\text{Acetate}] = 0.01 \text{ M.}$   
(1)  $\text{pH} = 5.30$  (2)  $\text{pH} = 5.66$  (3)  $\text{pH} = 5.94$ .

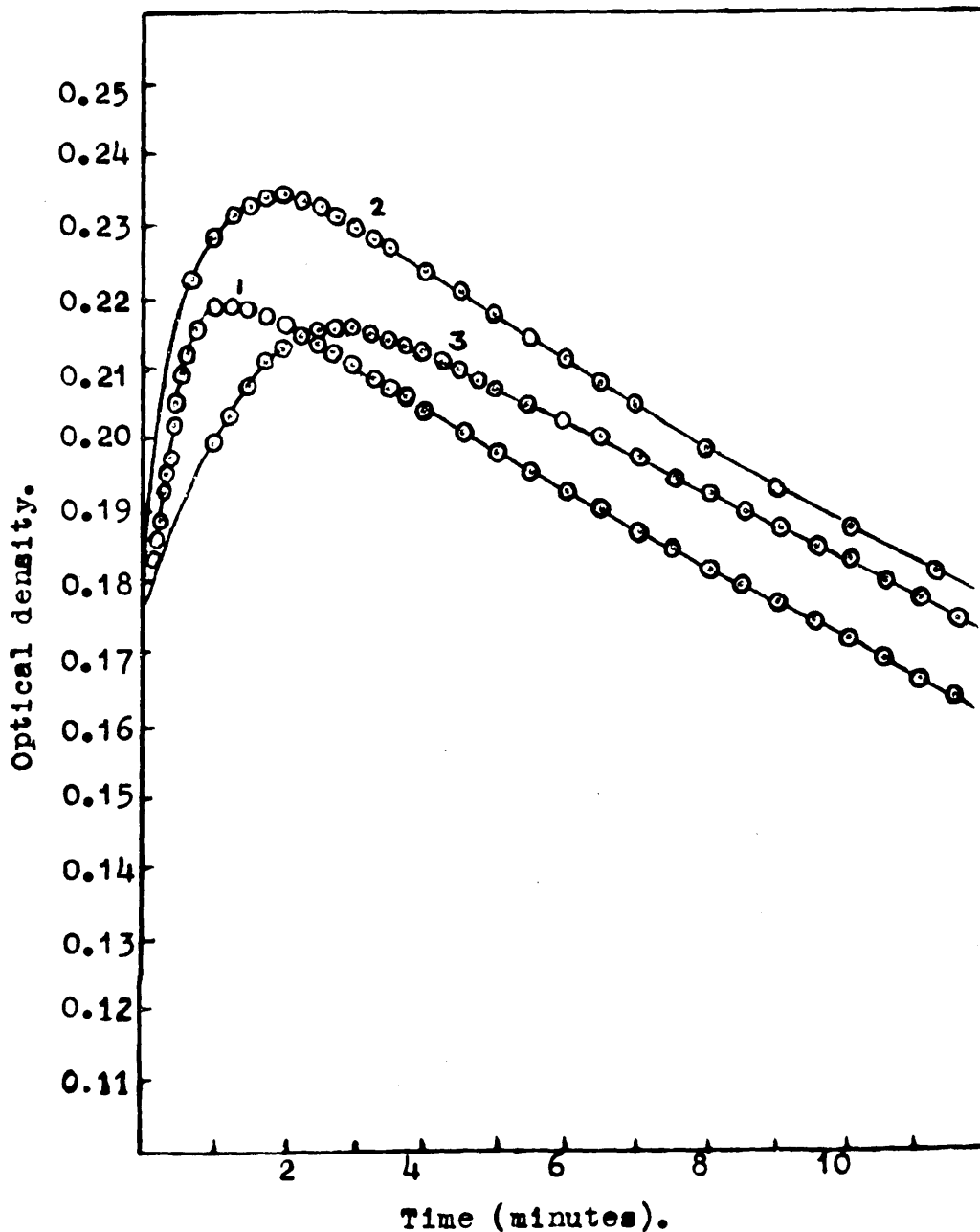


Table 7 Speed of formation of ethyl oxaloacetate chelates

$[\text{III}] = 1.20 \times 10^{-4} \text{M. pH} = 5.34.$

$[\text{III}] = 1.14 \times 10^{-4} \text{M. } [\text{Zn}^{2+}] = 3.20 \times 10^{-4} \text{M. } [\text{Cu}^{2+}] = 3.23 \times 10^{-4} \text{M.}$

PH	Time (secs.)	O.D. <sup>a</sup>	pH	Time (secs.)	O.D. <sup>a</sup>	Time (secs.)	O.D. <sup>a</sup>	Time (secs.)	O.D.
5.0	45	0.0725 <sup>b</sup>	6.5	60	0.463	45	1.10	120	1.325
5.5	45	0.122 <sup>b</sup>	,,	90	0.474	60	1.160	150	1.342
6.0	45	0.207 <sup>b</sup>	,,	120	0.477	75	1.236	180	1.349
6.5	45	0.457	,,	480	0.480	90	1.274	240	1.350
			,,	600	0.480			300	1.350

<sup>a</sup>At 295 m $\mu$ .    <sup>b</sup>Steady value

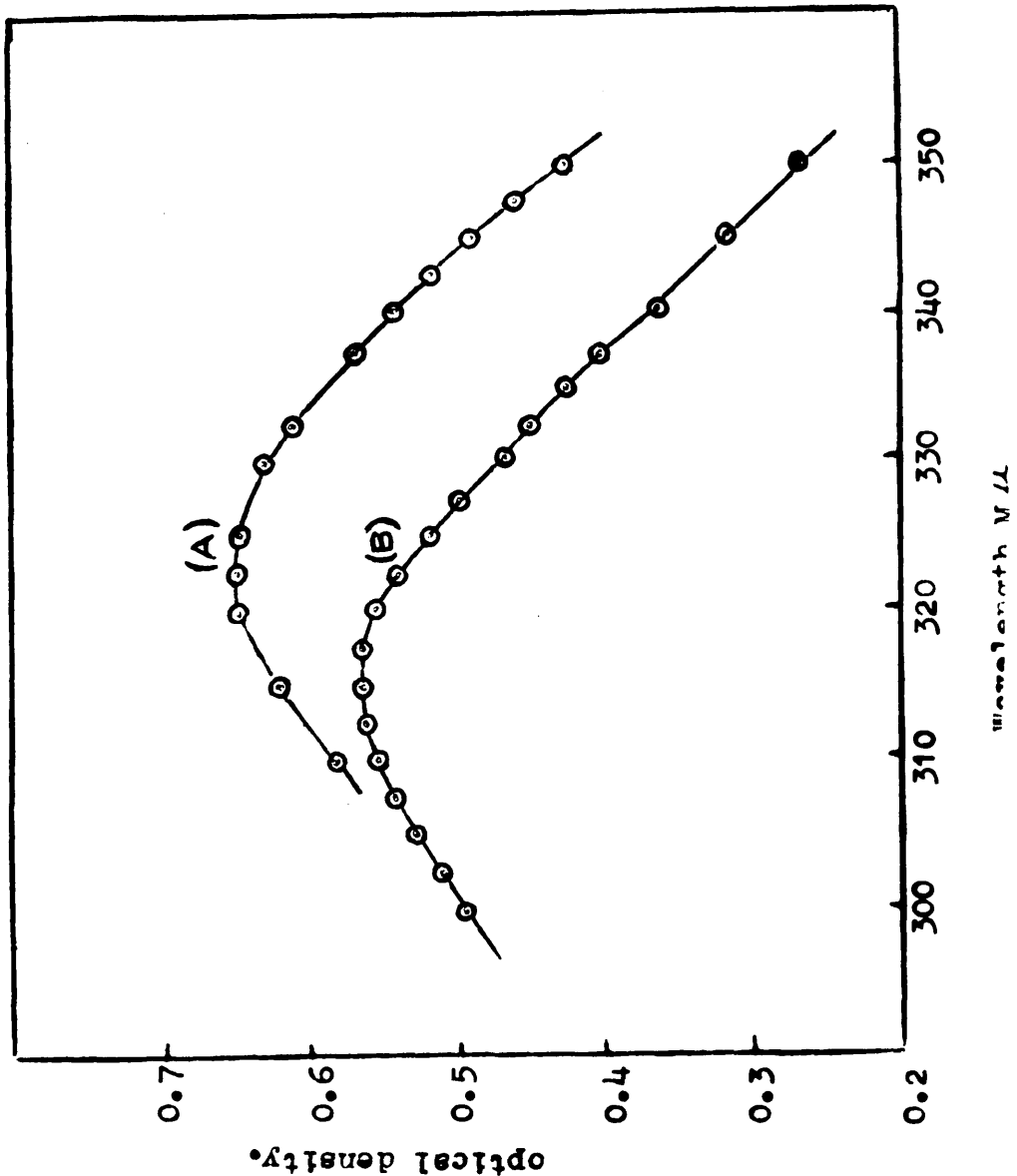
### Keto-enol equilibria

Previous studies<sup>28-29</sup> of the enol content of oxaloacetic acid in aqueous solution have been conflicting. By use of a value of 8,800 for  $\epsilon$  max of the enol, NOSSAL'S<sup>8</sup> spectrophotometric data can be interpreted in terms of about 3% of enol at pH 2 increasing to 9% at pH 5.5. At this pH the acid is almost entirely in the form of the dianion. The enol content as indicated by the optical density at 260 m $\mu$  remains constant as the pH is increased, until an enolate ion is formed with the loss of a third proton at a much higher pH.

The enol content of oxaloacetic acid and its anions

Fig.8

Decarboxylation of dimethyloxaloacetic acid at pH 13. Curve A shows the  $\alpha$ -keto acid peak at 1.3 hrs. of dimethyloxaloacetic acid. Curve B shows the  $\alpha$ -keto acid peak of its decomposition product dimethylpyruvic acid at 15 hrs. Soln.  $1.66 \times 10^{-2}$  M. Temperature  $25^{\circ}$ . 1 cm. cells.



has been studied by comparing the extinction coefficients at 260 m $\mu$  of acids (I) and (II) at different values of pH. The values  $\epsilon$ (I) = 420,  $\epsilon$ (II) = 22, and  $\epsilon$ (enol) = 8,800 indicate an enol  $[\text{HO}_2\text{C.C(OH):CH.CO}_2\text{H}]$  content of 4-5 % in undissociated oxaloacetic acid (in perchloric acid). At pH 6,  $\epsilon$ (I) = 850,  $\epsilon$ (II) = 92 and  $\epsilon$ enol = 8,800 indicate 9 % of enol  $[\text{O}_2\text{C.C(OH):CH.CO}_2^-]$  for the dianion of oxaloacetic acid.

In the above pH range optical densities changed with time owing to decarboxylation and values were extrapolated to zero time. At pH 13 complete enolisation to the trianion  $\text{O}_2\text{C.CO}^-:\text{CH.CO}_2^-$  is indicated by the stability of the solution. No evolution of carbon dioxide or change of optical density with time was detected with acid (I), in contrast to acid (II) which continues to decompose at this pH, Fig.8. The extinction coefficient of the enolate ion ( $\epsilon_{260} = 3,200$ ) is lower than that of the enols.

Keto-enol equilibria in the metal oxaloacetates were investigated by measurements of optical densities at 295 m $\mu$  ( $\lambda$  max for the enolic chelate compounds). The total concentration of chelate compound was calculated from the measured association constants and the initial concentrations, and the approximate proportions of ketonic and enolic forms, A and B, were estimated by using the values  $\epsilon_{295}(\text{A}) = 70$  and  $\epsilon_{295}(\text{B}) = 20,000$ .

The proportion of enolic complex increases with pH for ethyl oxaloacetate (III), since the formation of the



enolic complex must involve the displacement of a proton (eqn 15). The variation with pH is illustrated in Table 9. Under the conditions of these experiments the monoester is almost completely chelated. At low pH's and sufficiently high concentration of zinc ion the optical density corresponds to a concentration of ketonic chelate ( $\epsilon = 70$ ) equal to the initial concentration of the ester (III).

Table 8 Keto-enol equilibria for zinc and copper ethyl oxaloacetate

$10^4[\text{III}]$	1.25	1.10	$10^4[\text{III}]$	1.25	1.25	1.25	1.25
$10^4[\text{Zn}^{2+}]$	333	3.04	$10^4[\text{Cu}^{2+}]$	333	333	333	3.33
pH	2.75	6.50	pH	2.24	2.54	4.34	5.34
O.D. at 295 $m\mu$	0.009	0.48	O.D. at 295 $m\mu$	0.20	0.51	1.13	1.36
% Enolic Complex	0	22	% Enolic Complex	8	20	45	55

With oxaloacetic acid the position of the keto-enol equilibrium between A and B should be independent of the pH. The loss of a proton from the enol B to give the complex B' should occur at high pH, but the enol content of the metal oxaloacetates does not appear to increase below pH 6 or 6.5. With the known association constants and extinction coefficients, NOSSAL'S<sup>8</sup> spectrophotometric data on copper oxaloacetate can be interpreted. In the pH range 4-6 the optical densities extrapolated to zero time indicate a constant proportion (c.a. 40 %) of enolic complex. Experiments

on copper oxaloacetate ( $[I] = 1.25 \times 10^{-4}M.$ ,  $[Cu^{2+}] = 10^{-1}M.$ ) at pH 2 and 3 gave extrapolated values of the optical density between 0.9 and 1.0. The optical density falls very rapidly with time owing to decarboxylation. These values appear to indicate that the same proportion of enolic copper complex is maintained over the pH range 2-6.

Experiments with high concentrations of zinc ion at pH 2-3 indicate 15-20 % of enol. This content appears to be maintained up to pH 6.5. Fig.7 shows the optical density time curves for several experiments in the pH range 5-6.5; the rise is due to the formation of a strongly absorbing enolic pyruvate intermediate. The initial optical density appears to be independent of pH and with the known association constant and extinction coefficient gives a proportion of enolic zinc complex of about 15 %.

Fig.9 shows the optical density-time curves for a typical set of experiments with the series of transition metal ions; the rise is again attributed to formation of an enolic pyruvate intermediate on decarboxylation. The results of these experiments are collected in Table 9. Optical densities are values extrapolated to 30 seconds after addition of metal ion. Owing to uncertainties in the extrapolation of optical densities, in the association constants, and in the various extinction coefficients, the proportions of enolic complex given are approximate.

Fig. 9

Variation of optical density with time ( $\lambda = 295 \text{ m}\mu$ ) for  $\text{HO}_2\text{C}\cdot\text{CO}\cdot\text{CH}_2\cdot\text{CO}_2\text{H}$   
 $[\text{I}] = 1.25 \times 10^{-4} \text{ M.}, [\text{M}^{2+}] = 3.3 \times 10^{-4} \text{ M.}, \text{pH} = 6.35.$

Optical Density

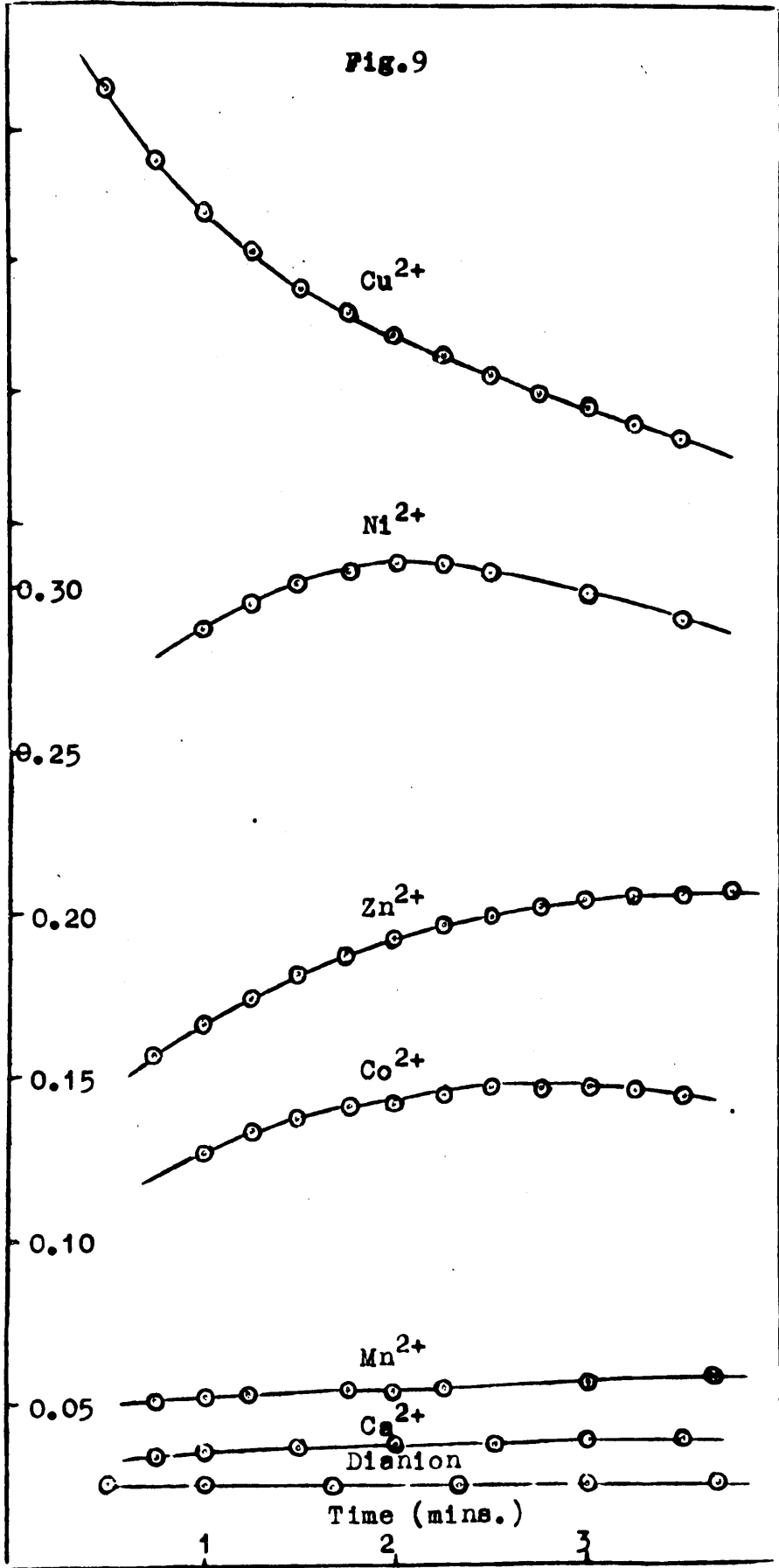


Table 9 Keto-enol equilibria for metal oxaloacetates

Oxaloacetate dianion; initial pH = 6.35

$$[I] = 1.25 \times 10^{-4} M. [M^{2+}] = 3.33 \times 10^{-4} M.$$

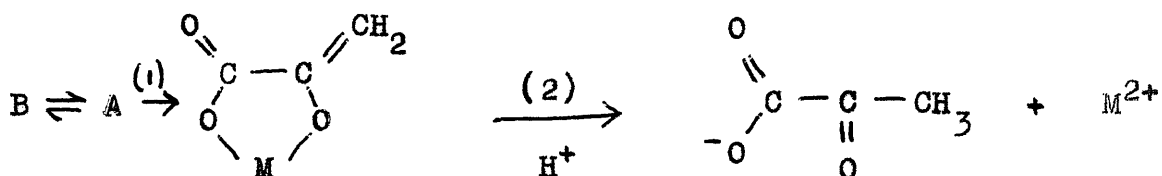
	Dianion	Ca <sup>2+</sup>	Mn <sup>2+</sup>	Co <sup>2+</sup>	Zn <sup>2+</sup>	Ni <sup>2+</sup>	Cu <sup>2+</sup>
10 <sup>4</sup> [MA]	-	0.14	0.24	0.37	0.43	0.58	1.25
O.D. at 295 m $\mu$	0.025	0.035	0.050	0.12	0.15	0.27	1.0
O.D. (B)	-	0.013	0.03	0.10	0.13	0.25	1.0
% Enolic Complex	-	5	6	13	15	22	40

Pyruvate chelate compounds

The spectra of freshly prepared aqueous solutions of pyruvic acid and of metal pyruvates show no evidence of enolic species. Pyruvic acid and its anion give keto acid peaks at 325 m $\mu$  ( $\epsilon = 5$ ) and 318 m $\mu$  ( $\epsilon = 22$ ). Copper pyruvate shows no absorption maximum and appears to be almost entirely ketonic ( $\epsilon_{295} = 200$ ).

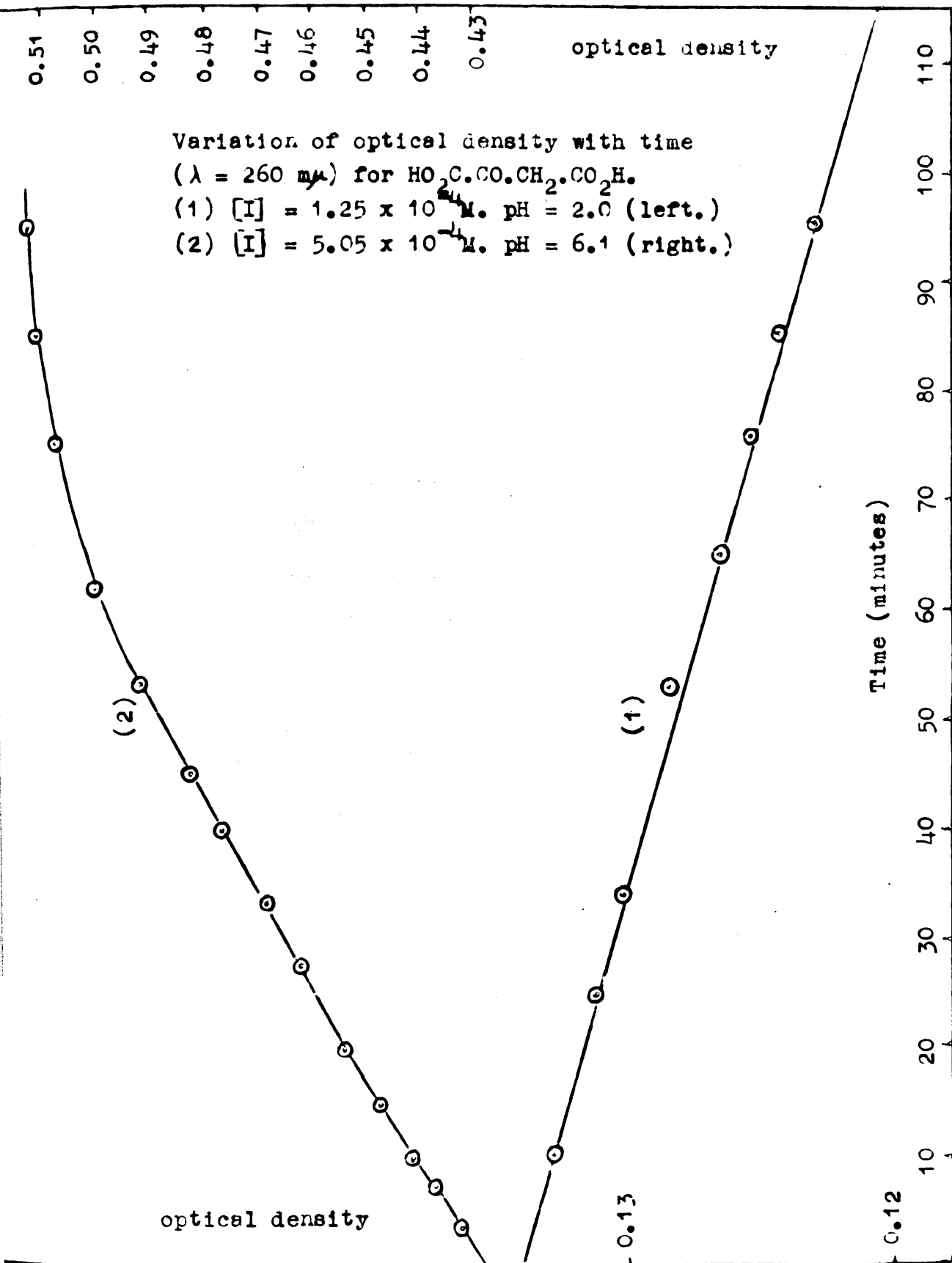
Enolic pyruvate intermediate

A comparison of the optical density-time curves for the metal chelate compounds of ethyl oxaloacetate, which are not decarboxylated, Table 7, and for the metal oxaloacetates Figs. 7 and 9, show that the rise in optical density with time for the oxaloacetates (other than the copper complex) must be due to formation of a strongly absorbing species on decarboxylation. This is believed to be an enolic pyruvate intermediate, which subsequently ketonises.



The variation of optical density with wavelength suggests that the enolic pyruvate has an absorption maximum at a somewhat lower wavelength than B and an extinction coefficient of several thousand. The disappearance of A and B on decarboxylation leads to a decrease in optical density, and a maximum will only be observed if ketonisation (2) is sufficiently slow to allow build up of the intermediate. It is found that the time of maximum optical density decreases with decrease of pH and at a low pH there is no maximum. The behaviour at two values of pH is illustrated for the unchelated acid in Fig. 10. At low pH the rate of fall of optical density (corrected for pyruvic acid) with time

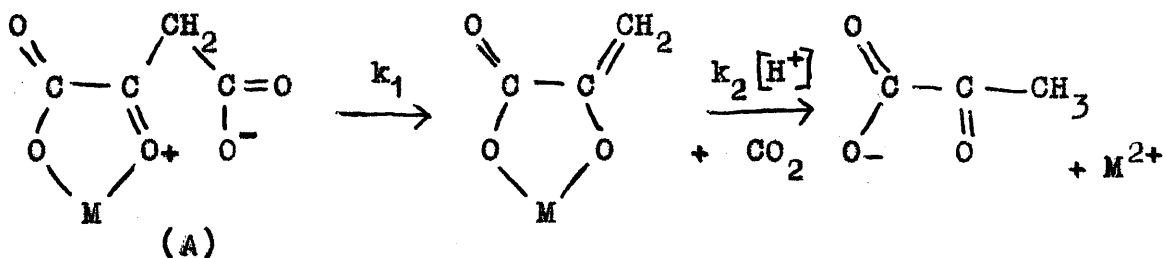
Fig.10



( $k = 1.11 \times 10^{-3} \text{ min}^{-1}$ ) corresponds to the manometric rate of decarboxylation ( $k = 1.15 \times 10^{-3} \text{ min}^{-1}$ ) at lower pH's ( $k = 1.11 \times 10^{-3} \text{ min}^{-1}$ ) corresponds to the manometric rate of decarboxylation. ( $k = 1.15 \times 10^{-3} \text{ min}^{-1}$ ). At higher pH's production of the enolic intermediate.

Dimethyl oxaloacetic acid cannot enolise, decarboxylation leads directly to the enolic dimethylpyruvate intermediate. This is illustrated in Fig.11. This enol has an absorption maximum at  $240 \text{ m}\mu$ , and appears to have an extinction coefficient of  $\sim 8,000$ . The rate of ketonisation is a function of pH and buffer concentration.

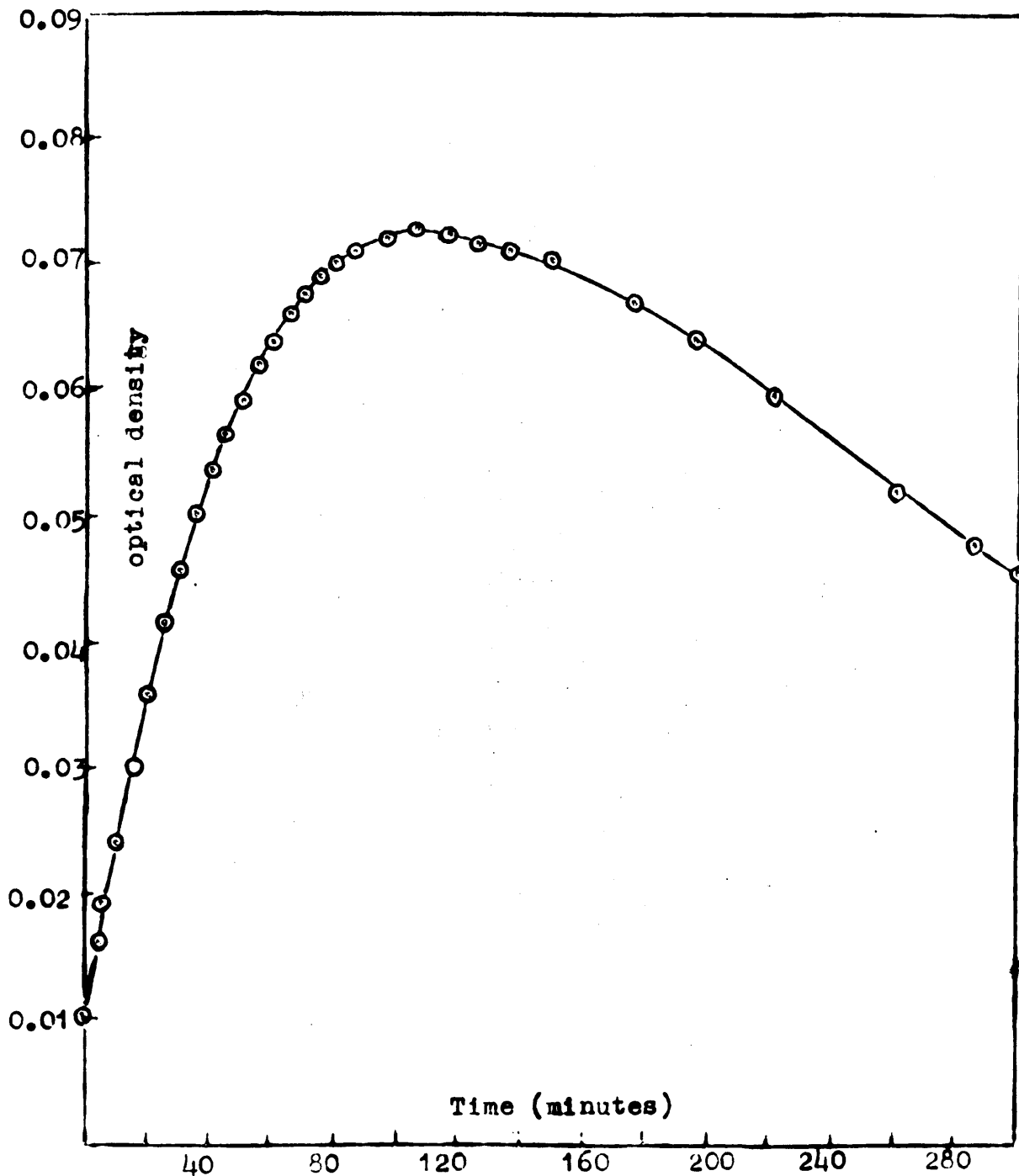
The metal ion catalysed decarboxylation of oxaloacetic acid has been shown to follow the scheme given in equation (1). Spectrophotometric measurements using ethyl oxaloacetate have shown that chelation is a very fast process and that the formation of the chelates A and B is not a rate controlling step. Writing equation (1) in terms of rate controlling steps only, we have



This is a first order reaction followed by a second order reaction. At constant hydrogen ion concentration this can be represented by the scheme (i.e. as two consecutive first

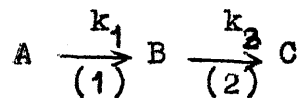
Fig.11

Enolic intermediate in the decarboxylation of dimethyl  
 oxaloacetic acid. pH = 4.68.  $[II] = 1.25 \times 10^{-4} M$ .  
 $(\lambda = 260 m\mu)$ .  $[HAc] = 0.1M$ .  $I = 0.10M$ .  $25^{\circ}$ .





order reactions.).



where  $k_3 = k_2 [H^+]$ , the differential equations are

$$d[A]/dt = -k_1 [A]$$

$$d[B]/dt = k_1 [A] - k_3 [B]$$

$$d[C]/dt = k_3 [B]$$

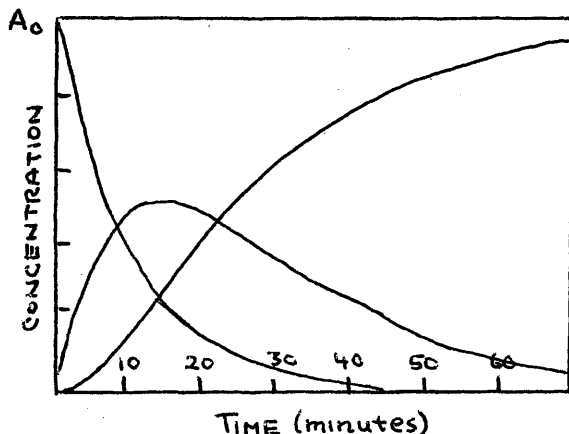
These may be integrated,<sup>30</sup>

$$[A] = [A_0] e^{-k_1 t}$$

$$[B] = [A_0] k_1 / (k_3 - k_1) [e^{-k_1 t} - e^{-k_3 t}]$$

$$[C] = [A_0] \left[ 1 + 1/(k_1 - k_3) (k_3 e^{-k_1 t} - k_1 e^{-k_3 t}) \right]$$

The figure is a plot of the concentrations A, B and C as a function of time for a typical case where  $k_1 = 0.10 \text{ min}^{-1}$  and  $k_3 = 0.05 \text{ min}^{-1}$ .



The concentration of the intermediate B passes through a maximum, then decays. The time of the maximum is given by the expression,

$$t_{\max} = \frac{\log_e(k_3/k_1)}{k_3 - k_1}$$

and the maximum concentration of the intermediate ( $[B]_{\max}$ ) by

$$\log [B]_{\max} = \log [A_0] + \frac{k_2}{k_1 - k_2} \log \frac{k_3}{k_1}$$

where  $A_0$  is the initial concentration of A, and  $k_1$  and  $k_3$  are the specific rate constants for reactions 1 and 2.

The Table below illustrates the manner in which  $t_{\max}$  and  $[B]_{\max}$  vary with different values of  $k_3$ .

Table 10 Maximum times and maximum concentrations of intermediate B for various values of  $k_3$

$$k_1 = 0.10 \text{ min.}^{-1} \quad A_0 = 1.0$$

$k_3$ (min. <sup>-1</sup> )	0.01	0.05	0.30	1.00
$t_{\max}$ (mins.)	25.59	13.86	5.49	2.56
$[B]_{\max}$	0.7743	0.500	0.1942	0.0774

As  $k_3$  becomes larger, the maximum times and the maximum concentrations of the intermediate decrease.

It should thus be possible to explain the optical-density time curves for the enolic intermediate in terms of equations of this type. In this case the second step involves hydrogen ion. At constant hydrogen ion concentration, substituting  $k_3 = k_2 [H^+]$  the equations become

$$t_{\max} = \frac{\log_e k_2 [H^+] / k_1}{k_2 [H^+] - k_1} \quad (2)$$

$$B_{\max} = \log A_0 + \frac{k_2 [H^+]}{k_1 - k_2 [H^+]} \log \frac{k_2 [H^+]}{k_1} \quad (3)$$

From the table it can be seen that  $t_{\max}$  and  $[B]_{\max}$  vary with  $k_3$  in a similar manner, thus the ratios of  $t_{\max}$  are 1: 2.14:5.14:10, while the  $[B]_{\max}$  ratios are 1:2.50:6.46:10.

A large number of runs was carried out with oxaloacetic acid and  $Zn^{2+}$  ions in acetate buffers. Table 11 shows a typical set carried out at both 270 and 290  $m\mu$  and at two different  $Zn^{2+}$  concentrations.

Little difference in the values of the maximum optical densities is noted, there is however considerable variation in the maximum times. The maximum times suggest that the optical densities of the intermediate at pH's 5.30, 5.66

Table 11 Maximum times and maximum optical densities of the enolic intermediate.

$I = 0.01$   $f_1$  (Davies) 0.903. Oxaloacetic acid  $1.25 \times 10^{-4} M$

$$290 \text{ m}\mu [\text{Zn}^{2+}] = 3.36 \times 10^{-4} M.$$

pH	NaAc	HAc	t max	o.d. max
5.30	0.01	0.0026	1.20	0.218
5.66	0.01	0.0010	2.0	0.234
5.94	0.01	0.0006	2.75	0.215

$$290 \text{ m}\mu [\text{Zn}^{2+}] = 6.73 \times 10^{-4} M.$$

pH	NaAc	HAc	t max	O.D. max
5.30	0.01	0.0026	1.20	0.345
5.66	0.01	0.0010	1.60	0.356
5.94	0.01	0.0006	2.0	0.333

$$270 \text{ m}\mu [\text{Zn}^{2+}] = 3.36 \times 10^{-4} M$$

pH	NaAc	HAc	t max	O.D. max
5.30	0.01	0.0026	1.25	0.219 (0.198)
5.66	0.01	0.0010	1.75	0.197 (0.203)
5.94	0.01	0.0006	2.50	0.208 (0.197)

$$270 \text{ m}\mu [\text{Zn}^{2+}] = 6.73 \times 10^{-4} M$$

pH	NaAc	HAc	t max	O.D. max
5.30	0.01	0.0026	1.0	0.242 (0.246)
5.66	0.01	0.0010	1.75	0.263 (0.268)
5.94	0.01	0.0006	2.0	0.242 (0.245)

and 5.94 should be roughly in the ratio 1:1.5:2, little variation is actually observed, because of interference by enolic zinc oxaloacetate. At a zinc concentration of  $3.36 \times 10^{-4}$  M., about 60% of the oxaloacetic acid will be complexed. If  $\epsilon$  enolic is  $2 \times 10^4$ , and the percentage of enolic complex is approximately 14; the initial optical density due to the enolic zinc complex will be around 0.2.

Fig. 12 shows a plot of the changes of optical density with time for the enolic intermediate and the enolic complex B; the half life of decarboxylation is around three minutes (the half life of ZnA at  $37^\circ$  is 23 seconds<sup>\*</sup>). The optical density observed, equal to that of the enolic intermediate and the enolic complex (the sum of curves A and B) does not vary much from run to run even though the concentration of the intermediate is in the ratio 1: 1.5:2. The maximum times observed are probably slightly lower than the actual maxima for the intermediate.

Above pH 5.3, practically all the oxaloacetate will be present as the dianion. The reaction scheme will be,

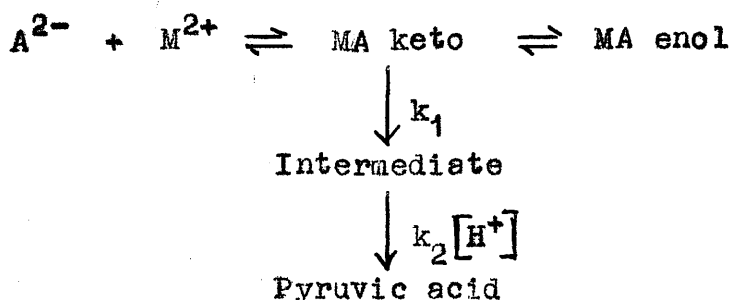
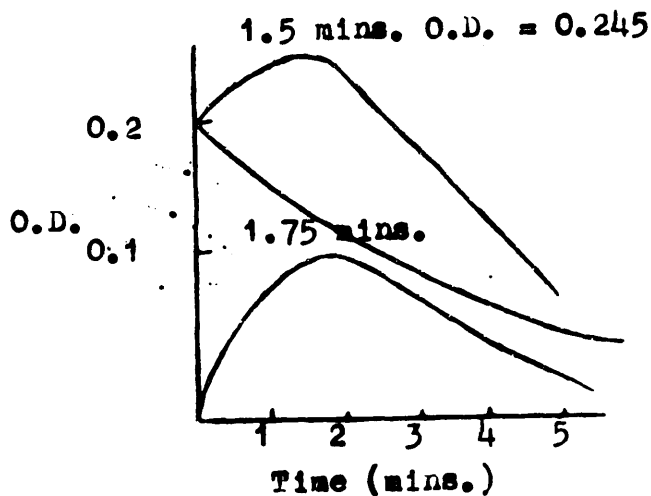
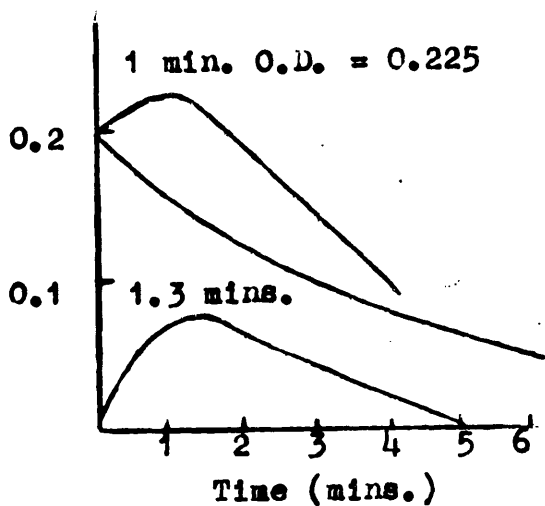
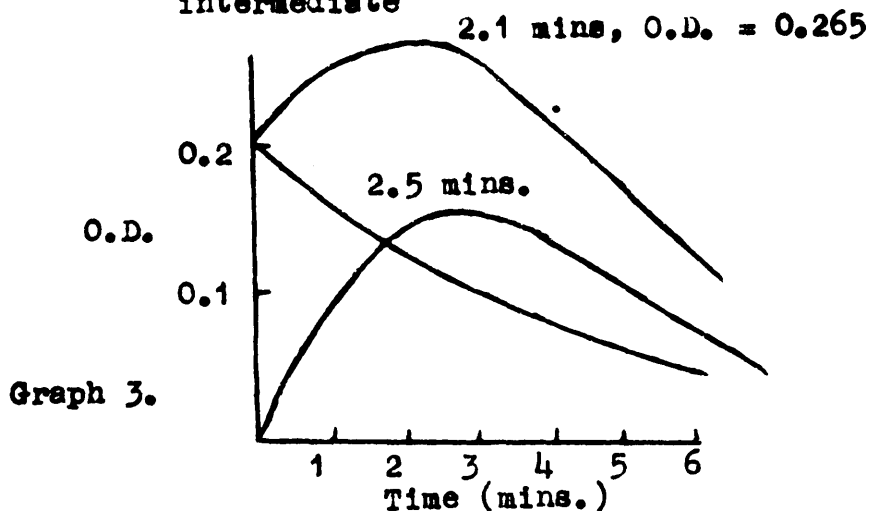


Fig.12

Plots of optical density-time curves, the enolic intermediate is in the ratio 1:1.5:2 for graphs 1, 2 and 3 respectively.

Curve B:- O.D./Time curve for the decarboxylation of enolic zinc oxaloacetate.

Curve A:- O.D./Time curve for the enolic pyruvate intermediate



Graph 1.

Graph 2.

Curve C:- Observed optical density-time curve (sum of curves A and B.)

If the total oxaloacetate =  $C_0 = [A^{2-}] + [MA]$

$$\begin{aligned} \text{then } -dC_0/dt &= k_0 [A^{2-}] + k_1 [MA] = k_x [C_0] \\ &= k_1 [MA] \quad (k_0 \ll k_1) \end{aligned}$$

Above pH 5.3  $A^{2-} + M^{2+} \rightleftharpoons MA$  ;  $K_{MA} = [MA] / [A^{2-}] [M^{2+}]$

$$[MA] = K [M^{2+}] [A^{2-}] \quad \text{and} \quad [A^{2-}] = [MA] / K [M^{2+}]$$

$$\begin{aligned} C_0 &= [MA] + [A^{2-}] = [MA] + [MA] / K [M^{2+}] \\ &= [MA] \left[ 1 + 1 / K [M^{2+}] \right] \end{aligned}$$

$$k_x [MA] \left[ 1 + 1 / K [M^{2+}] \right] = k_1 [MA]$$

$$k_x / k_1 = K [M^{2+}] / (1 + K [M^{2+}]) \quad (4)$$

$$\text{and } t_{\max} = ( \ln k_2 [H^+] - \ln k_x ) / ( k_2 [H^+] - k_x ) \quad (5)$$

Values of  $k_x$  and  $k_2$  were chosen to give reasonable agreement with the observed maximum times, for  $[Zn^{2+}] = 3.36 \times 10^{-4} M$ .

$k_x = 0.2$ ,  $k_2 = 4.5 \times 10^5$ , and for  $[Zn^{2+}] = 6.73 \times 10^{-4} M$ .

$k_x = 0.3$  and  $k_2 = 4.5 \times 10^5$ . The values are shown in Table 12.

Reasonable agreement is found between the observed maximum times and those calculated from equation (5).

Equation (4) gives a value for  $K$  the complexity constant of zinc oxaloacetate equal to approximately  $1.7 \times 10^3$  at  $I = 0.01$  agreeing very well with the value of  $1.7 \times 10^3$  at  $I = 0$  found from potentiometric data.  $k_1$  is found to be approximately 0.6.

Table 12 Observed and calculated maximum times.

$$[\text{Zn}^{2+}] = 3.36 \times 10^{-4} \text{ M. } k_x = 0.2$$

pH	$10^6 [\text{H}^+]$	Time obs.	Time calc.
5.30	5.55	$1.15 \pm 0.1$	1.10
5.66	2.43	$1.9 \pm 0.1$	1.90
5.94	1.27	$2.85 \pm 0.1$	2.85

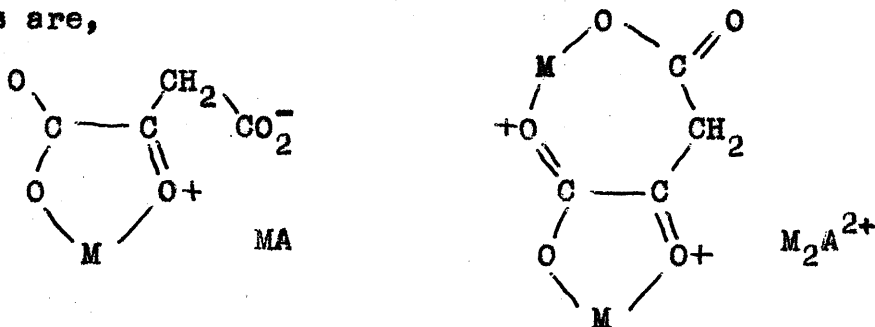
$$[\text{Zn}^{2+}] = 6.73 \times 10^{-4} \text{ M. } k_x = 0.3$$

pH	$10^6 [\text{H}^+]$	Time obs.	Time calc.
5.30	5.55	$1.1 \pm 0.1$	1.0
5.66	2.43	$1.6 \pm 0.1$	1.63
5.94	1.27	$2.2 \pm 0.1$	2.36

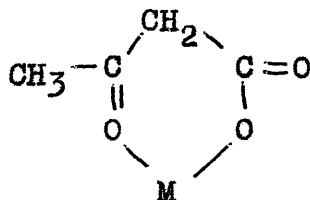


Inhibition

Potentiometric measurements by GELLES and SALAMA<sup>16</sup> on oxaloacetates have shown that in addition to the species MA there is also present a species  $M_2A^{2+}$ . The probable structures of these complexes are,



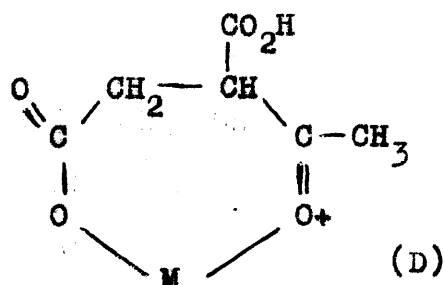
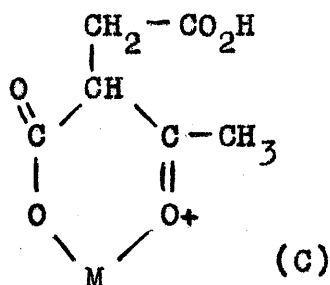
The complex  $M_2A^{2+}$  involves the formation of a low stability seven membered ring. Binding of the carboxyl group lost during decarboxylation, in the seven membered ring should inhibit decarboxylation in a similar manner to the acetoacetates.



Acetoacetate MA

<sup>31</sup>PEDERSEN has recently shown that a similar situation exists in acetosuccinic acid. The decarboxylation of this acid is subject to only very slight catalysis by metal ions. Two chelates are possible, the six membered ring structure (C) involving the unstable carboxyl group, which should inhibit decarboxylation, and a low stability seven membered ring

chelate (D) which should decarboxylate.



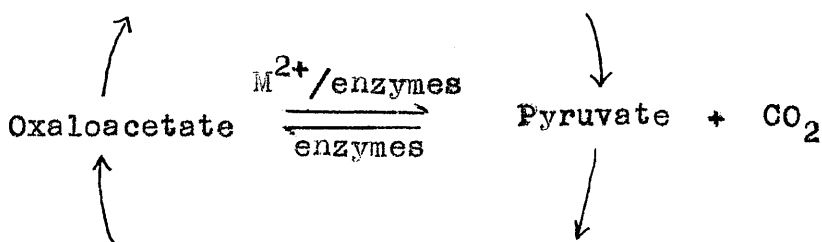
Only slight catalysis is observed since the chelate of high stability is inactive, while the active chelate is only present in small amounts.

It can be simply shown that for the oxaloacetates,

$$\frac{[M_2A^{2+}]}{[MA]} = K_{M_2A^{2+}} [M^{2+}]$$

and the concentration of  $M_2A^{2+}$  should increase proportionally with the metal ion concentration. Inhibition of decarboxylation at high copper ion concentration has been found, Table 13. SPECK has obtained similar results with  $Mn^{2+}$ ,  $Co^{2+}$ ,  $Cd^{2+}$ ,  $Zn^{2+}$  and  $Pb^{2+}$  in the enzymatic decarboxylation.

This appears to be one of the few examples of a catalyst also acting as an inhibitor and might be a very important reaction biochemically. The interconversion of oxaloacetic acid and pyruvic acid occurs in the KREBS cycle.<sup>32</sup>



When the oxaloacetate reaches a low level, the  $M^{2+}$  / Oxaloacetate ratio will be large and decarboxylation will slow down.

The concentration of oxaloacetate will then build up until the  $M^{2+}$  / Oxaloacetate ratio becomes small enough to allow rapid decarboxylation via the MA complex. The metal ion will act as a 'governor' on the system. Further work on this topic is being carried out in this laboratory by Mr R.G.COCHAN.

Table 13 Inhibition of catalysis at high copper ion concentrations at 25°.

Acetate buffer, I = 1.000. Oxaloacetic acid 0.02M. pH 5.0

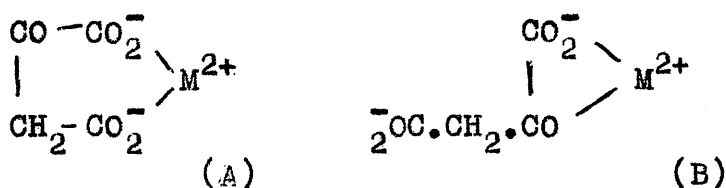
HAc	NaAc	KCl	CuCl <sub>2</sub>	$10^3 k^*$
0.163	0.40	0.51	0.03	20.0
0.163	0.40	0.42	0.06	6.4
0.163	0.40	0.33	0.09	3.6
0.163	0.40	0.24	0.12	2.7
0.163	0.40	0.50	0.15	2.17
0.163	0.40	-	0.21	1.36

Decarboxylation of metal oxaloacetates can also be inhibited by raising the pH. KREBS<sup>1</sup> carried out some rough manometric measurements which indicated that the rate went through a maximum around pH 4.0. Further experiments, Table 14 agree with this.

Table 14 pH inhibition of the copper ion catalysed decarboxylation of oxaloacetic acid at 27°

NaAc	HAc	pH	$10^3 k^*$
1.6	2.213	4.67	74
1.6	0.700	5.10	48.4
1.6	0.070	6.15	16.8

WILLIAMS<sup>6</sup> suggested that pH inhibition was due to the production of a dicarboxylate complex (A) which was stable, decarboxylation



occurring through (B). He suggested that (B) would be present at low pH, while (A) would predominate at high pH. This cannot, however, be the case, since the ratio  $[A]/[B]$  would not involve hydrogen ion and would not be pH dependent. It seems most likely that pH inhibition is due to the formation of the enolic complex which cannot decarboxylate. Further work on these lines is being continued in this laboratory by Mr. R. G. COGAN.

References.

1. Krebs, Biochem. J. 36, 303, 1942.
2. Krampitz and Werkman, Biochem. J. 35, 595, 1941.
3. Kornberg, Ochoa and Mehler, J. Biol. Chem. 174, 159, 1948.  
Speck, *ibid*, 178, 315, 1949.
4. Steinberger and Westheimer, J.A.C.S. 73, 429, 1951.
5. Pedersen, Acta Chem. Scand. 6, 243, 285, 1952.
6. Williams, Nature, 171, 304, 1953.
7. Williams, Biol. Rev. 28, 381, 1953.
8. Nossal, Austral. J. Exp. Biol. 27, 143, 313, 1949.
9. Rossi and Schinz, Helv. Chim. Acta 31, 473, 1948.
10. Wislicenus and Endres, Ann. 321, 381, 1902.
11. Hudson and Hauser, J.A.C.S. 63, 3156, 1941.
12. Steinberger and Westheimer J.A.C.S. 71, 4158, 1949.
13. Organic Syntheses, Coll. Vol. III, p.142.
14. Rasso and Bauer, J. prakt. chem. 80, 87, 1909.
15. Abromovitch, Shivers, Hudson and Hauser, J.A.C.S. 65, 986, 19
16. Gelles and Salema, J.C.S. 3684, 1958.
17. Rasmussen and Brattain, J.A.C.S. 71, 1073, 1949.
18. Lecompte, Diss. Faraday Soc. 9, 125, 1950.
19. Duval, Freymann and Lecompte, Bull. Soc. Chim. 19, 106, 1952.
20. Morgan, U.S. Atomic Energy Commission 1949. A.E.C.D. 12659, 16
21. Belford, Martell and Calvin, J. Inorg. and Nuclear Chem. 2, 11, 1956.
22. Bellamy and Branch, J.C.S. 4491, 1954.
23. Lecompte, Rev. Optique, 28, 353, 1949.
24. Duval, Lecompte and Douville, Ann. Physique 17, 5, 1942.
25. Mellor and Maley, Nature, 159, 370, 1948. 161, 436, 1950.
26. Irving and Williams, Nature, 162, 746, 1948.
27. Speakman, J.C.S. 855, 1940.
28. Meyer, Ber. 45, 2860, 1912.
29. Hantzsch, Ber. 48, 1407, 1915.
30. Frost and Pearson, "Kinetics and Mechanism". John Wiley and Sons. New York. 1953.
31. Pedersen, Acta Chem. Scand. 9, 1640, 1955.
32. Krebs and Johnson, Enzymologia 4, 148, 1937.

Abstract

The rate of decarboxylation of oxaloacetic acid catalyzed by aniline was studied. **Part 2** of the kinetic study is presented. The effect of the concentration of the catalyst on the rate of decarboxylation is discussed.

### The Aniline-catalysed Decarboxylation

of Oxaloacetic Acid

**Summary of Oxaloacetic Acid** is the most important of the dicarboxylic acids that play a role in the metabolism of the animal. It is a central intermediate in the Krebs cycle. It is formed in the liver from pyruvate and carbon dioxide. The decarboxylation of oxaloacetic acid is a reversible reaction. The rate of decarboxylation is increased by the presence of aniline. It is suggested that the rate of decarboxylation is increased by the formation of a hydrogen bonded intermediate. The rate of decarboxylation is increased by the presence of aniline. It is suggested that the rate of decarboxylation is increased by the formation of a hydrogen bonded intermediate.



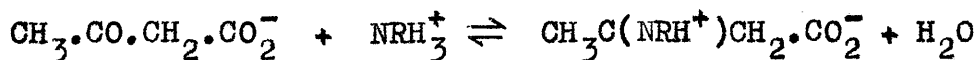
This hypothesis has been checked by IR and NMR measurements. IR measurements in dry solvents showed that a hydrogen bonded intermediate (A) may be present.

Part 2. The Aniline Catalysed Decarboxylation of Oxaloacetic Acid

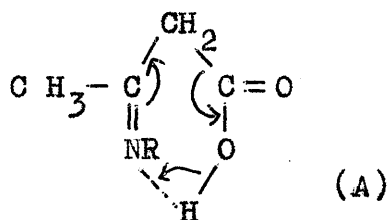
Introduction

The fact that primary and secondary, but not tertiary, amines catalyse the decarboxylation of oxaloacetic acid was first established by WOHL and OESTERLIN.<sup>1</sup> The effect of various amines and amino-acids on the decarboxylation has been studied by KANEKO<sup>2</sup> and BESSMAN and LAYNE.<sup>3</sup>

PEDERSEN had previously shown in the case of *dd*-dimethyl acetoacetic acid that this was an example of specific amine and not general base catalysis. He also found that the decarboxylation was not preceded by isomerisation of the keto-acid to the enol form and suggested that the reactive intermediate was formed by a fast reaction of the amine with the keto group.



This hypothesis has been discussed by WESTHEIMER.<sup>5</sup> JONES and WESTHEIMER<sup>6</sup> made measurements in mixed solvents which suggest that a hydrogen bonded intermediate (A) may be a more appropriate structure.



PEDERSEN<sup>7</sup> made the first quantitative study of the kinetics of decarboxylation of oxaloacetic acid, using ammonium, ethylammonium, and anilinium ions as catalysts. He found that all the amines had a greater catalytic effect on the divalent ion than on the univalent oxaloacetate ion, and that the anilinium ion was by far the most effective catalyst. He also found that in solutions containing hydrochloric acid, the anilinium ion catalysis could be represented by the equations,

$$k_0^* 10^3 = 0.176 + 1.19 [\text{AnH}^+] \quad (1)$$

$$k_1^* 10^3 = 6.47 + 404 [\text{AnH}^+] + 260 [\text{AnH}^+]^2 \quad (2)$$

$$k_2^* = 0.00181 + 38.4 [\text{AnH}^+] + 55 [\text{AnH}^+]^2 \quad (3)$$

The increase in  $k_0$  is so small that it is of uncertain significance.

However there is a serious discrepancy between these values and those obtained in acetate buffers. Values calculated from equations (2) and (3) are 64-93 % too high, and PEDERSEN<sup>7</sup> was forced to employ the equations,

$$k_1^* 10^3 = 6.47 + 4.4 \times 10^3 [\text{AnH}^+]$$

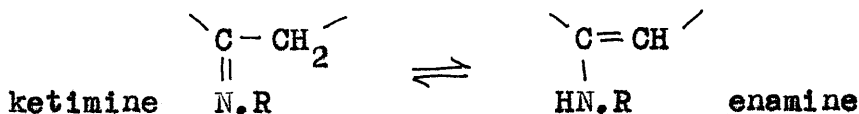
$$k_2^* 10^3 = 1.81 + (16.4 + 4.8 [\text{Ac}^-]) 10^3 [\text{AnH}^+]$$

to explain his experimental results. In all his calculations PEDERSEN<sup>7</sup> made the assumption that the amount of complex between the keto-acid and the amine was negligible; if this were not so it might explain the discrepancy. However PEDERSEN





(formation of the ketimine could only occur with a primary amine). Previous work has not shown (1) if (B) or (C) are indeed formed (2) whether (B) or (C) is the reactive intermediate (3) if they are formed slowly enough to be involved in rate-determining steps (4) what the strengths of their conjugate acids are / the fall in rate at about pH 4 observed by PEDERSEN<sup>7</sup> may be simply due to their dissociation (5) whether the proportion of compounds (B) and (C) varies with pH (6) whether different mechanisms apply in different solvents (7) and whether ketimine-enamine tautomerism of the type,



occurs or has any effect on the reaction.

Experimental Part 21) Materialsa) The ketimine  $\text{EtO}_2\text{C.C}(\text{:N}\emptyset).\text{CH}_2.\text{CO}_2\text{Et}$ 

3.12 gms. of the diester of oxaloacetic acid prepared as in Part 1, were refluxed for ten minutes with 1.56 gms. of pure aniline (mole/mole). A little absolute alcohol was used as solvent. On cooling in acetone-Drikold a yellow solid crystallised. This was filtered off and recrystallised three times from water-ethanol. Pale yellow needles m.p.  $47^\circ-48^\circ$ . Found, C, 63.66; H, 6.58; N, 5.49 %. Calculated for  $\text{C}_{14}\text{H}_{17}\text{O}_4\text{N}$ , C, 63.86; H, 6.46; N, 5.32 %.

The infra-red spectrum showed a very strong band at  $1600\text{ cm.}^{-1}$ , attributed to conjugated  $-\text{C}=\text{N}$ . PICKARD and POLLY<sup>8</sup> give for  $-\text{C}=\text{N}$ ,  $6.05 - 6.24\mu$  ( $1600-1650\text{ cm.}^{-1}$ ) and found no evidence for ene-amine tautomerism in a series of 15 ketimines studied.

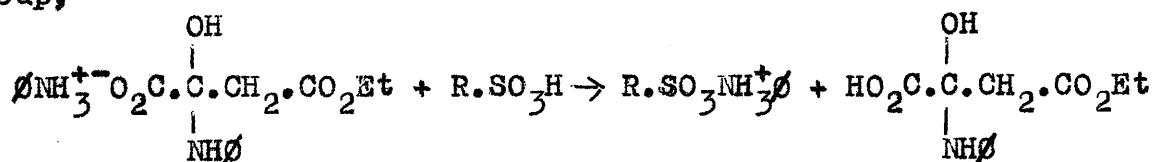
b) The ketimine hydrate  $\frac{1}{3}\text{NH}_3^+\text{O}_2\text{C.C}(\text{OH.NH}\emptyset).\text{CH}_2.\text{CO}_2\text{Et}$ 

1 gm. of the half ester of oxaloacetic acid,  $\text{HO}_2\text{C.CO.CH}_2.\text{CO}_2\text{Et}$ , prepared as described in Part 1, was dissolved in the minimum amount of water. 1.5 gms. of pure aniline (1 to 2.2 moles) were suspended in water and glacial acetic acid added until a homogeneous solution resulted. This was then added to the concentrated solution of the half ester. On scratching, the ketimine hydrate was precipitated as fine white crystals. Yield 1.7 gms. (80 %). The ketimine hydrate was recrystallised from

the minimum amount of warm water giving flat white plates, m.p.  $73^{\circ}$ - $74^{\circ}$ , which appeared to lose water at  $62^{\circ}$ - $63^{\circ}$ . Soluble in acetone, chloroform, ethanol, and benzene. Insoluble in  $100^{\circ}$ - $120^{\circ}$  petrol, slightly soluble in water.

Found, C, 62.34; H, 6.23; N, 8.12 %. Calculated for  $C_{18}H_{22}O_5N_2$ , C, 62.43; H, 6.36; N, 8.09 %.

Attempts to remove the second molecule of aniline by means of ion exchange resins (IR-120(H)) in the acid form, i.e. cross linked polystyrene with  $SO_3H$  as the functional group,



proved unsuccessful. On standing in a vacuum desiccator over  $P_2O_5$  the white ketimine hydrate turned bright yellow, indicating production of the ketimine; however, analysis showed that decomposition was also occurring under these conditions.

c) Methyl oxomalonate  $MeO_2C \cdot CO \cdot CO_2Me$

This was prepared essentially as described in Organic Syntheses,<sup>9</sup> by oxidising methyl malonate with  $N_2O_3$ . 30 cc. of methyl malonate gave 25 cc. of methyl oxomalonate as a yellow green oil b.p.  $106^{\circ}/40$  mm. D 1.2464. It absorbed atmospheric moisture rapidly to give the ketone hydrate  $MeO_2C \cdot C(OH)_2 \cdot CO_2Me$  m.p.  $81^{\circ}$  (from chloroform), and was kept in an evacuated

desiccator over silica gel. The material was purified by standing over  $P_2O_5$  overnight and vacuum distilling. This converted the hydrate to the keto compound.

d)  $MeO_2C.C(OH, NH\emptyset).CO_2Me$  <sup>10</sup>

2 cc. of anhydrous methyl oxomalonate (2.5 gms.) were pipetted rapidly into a 25 ml. flask protected by a silica gel guard tube. The solution was then chilled in acetone-Drikold. 1.5 gms. of pure aniline (slightly less than mole/mole quantities) were then dropped slowly into the chilled solution. A yellowish gum resulted. This was allowed to stand 1/4 hour at room temperature. A little sodium-dried ether was then added. On scratching with a glass rod, the material solidified as a pale yellow mass. It was then recrystallised from sodium-dried ether, giving white crystals m.p.  $100^{\circ}$ - $102^{\circ}$ . Yield 3.5 gms. (theoretical) Found C, 55.47; H, 5.34; N, 6.01 %. Calculated for  $C_{11}H_{13}O_5N$ , C, 55.24; H, 5.44; N, 5.86 %. Soluble in ethanol, methanol, insoluble in water.

e)  $MeO_2C(NH\emptyset)_2.CO_2Me$  <sup>10</sup>

2 ml. of anhydrous methyl oxomalonate (2.5 gms.) were pipetted rapidly into a 25 ml. flask protected by a silica gel guard tube. 3.2 gms. (mole/mole) of pure aniline dissolved in dry absolute ether were then added at room temperature, a yellow oil was obtained. On cooling and scratching in an acetone-Drikold freezing mixture, the material crystallised as a pale yellow solid. It was recrystallised from water-ethanol to give

colourless needles m.p.  $121^{\circ}$ - $123^{\circ}$ . Yield theoretical. Fairly soluble in cold ethanol, very soluble hot, insoluble in water.

#### Correlation of I.R. Spectra for OH and NH stretches

The infra-red spectrum of,

(e) shows a single band at  $3330\text{ cm.}^{-1}$  (NH stretch)

(d) shows two bands, one at  $3350\text{ cm.}^{-1}$  (NH stretch), and one at  $3460\text{ cm.}^{-1}$  (free OH).

(a) shows no bands in this region.

(b) shows two bands, one at  $3220\text{ cm.}^{-1}$  (NH stretch), which is a broad band, probably because of superposition by the second molecule of aniline, and one at  $3570\text{ cm.}^{-1}$  (free OH) (Nujol mull).

In chloroform, which gives yellow solutions indicating dehydration only one band occurs, at  $3320\text{ cm.}^{-1}$  (NH stretch in the second molecule of aniline (sharp band)). This gives further evidence for dehydration.

#### Preparation of Pure Dry Ethanol for Kinetic Work

Burrough's absolute alcohol was dried in the normal manner using magnesium turnings, purity 99.95%. Traces of organic bases were removed by redistillation from a little 2:4:6 trinitrobenzoic acid; this acid is not esterified by alcohols, consequently no water is introduced into the alcohol. The pure dry alcohol was kept in a dark glass Winchester protected by guard tubes and siphoned out as required Fig.1.

Pure Aniline

B.D.H. aniline was dried with sodium hydroxide pellets and distilled. The reasonably pure material was then vacuum distilled over zinc dust and kept in sealed ampoules under nitrogen. Aniline b.p.  $184.4^{\circ}/760$  mm.

Pure Dimethylaniline

Traces of primary and secondary amines were removed from a commercial sample by refluxing 52.5 ml. with 23 ml. of acetic anhydride for three hours, then distilling. The relatively pure dimethylaniline was then vacuum-distilled and kept in sealed ampoules under nitrogen. Ampoules of aniline and dimethyl-aniline were kept in the dark. B.p. dimethylaniline  $192.5^{\circ}/760$  mm. Ampoules of dimethylaniline remained water-clear almost indefinitely by this method.

## 2) Methods

### a) Potentiometric measurements

pH measurements were carried out using a Cambridge bench type pH meter and a commercial glass electrode. The apparatus was calibrated using B.D.H. phosphate buffer pH 6.99 at 25°, and B.D.H. phthalate buffer pH 4.01 at 25°. In cases where accurate temperature was required, potentiometric measurements were carried out in a double walled beaker through which water from a Circotherm unit was passed.

### b) Manometric measurements

A new manometric apparatus was developed (in conjunction with Mr. A. Wood) from the design of BELL and TROTMAN-DICKENSON.<sup>11</sup> This is much simpler to use and far less cumbersome than that of BRONSTED and KING.<sup>12</sup>

It is, however, unsuitable for use at temperatures above about 30°, as the grease is then too fluid and leaks develop.

The apparatus is illustrated diagrammatically in Fig.2. A small glass bucket containing 26.4 mgm. of oxaloacetic acid is suspended above 10 ml. of the appropriate solution by means of a magnetically operated plunger, consisting of a small piece of soft iron sealed in glass. This gives an initial concentration of oxaloacetic acid equal to 0.02 M. The solution is frozen in acetone-Drikold and the apparatus evacuated and sealed by means of a B.14 one way Quickfit



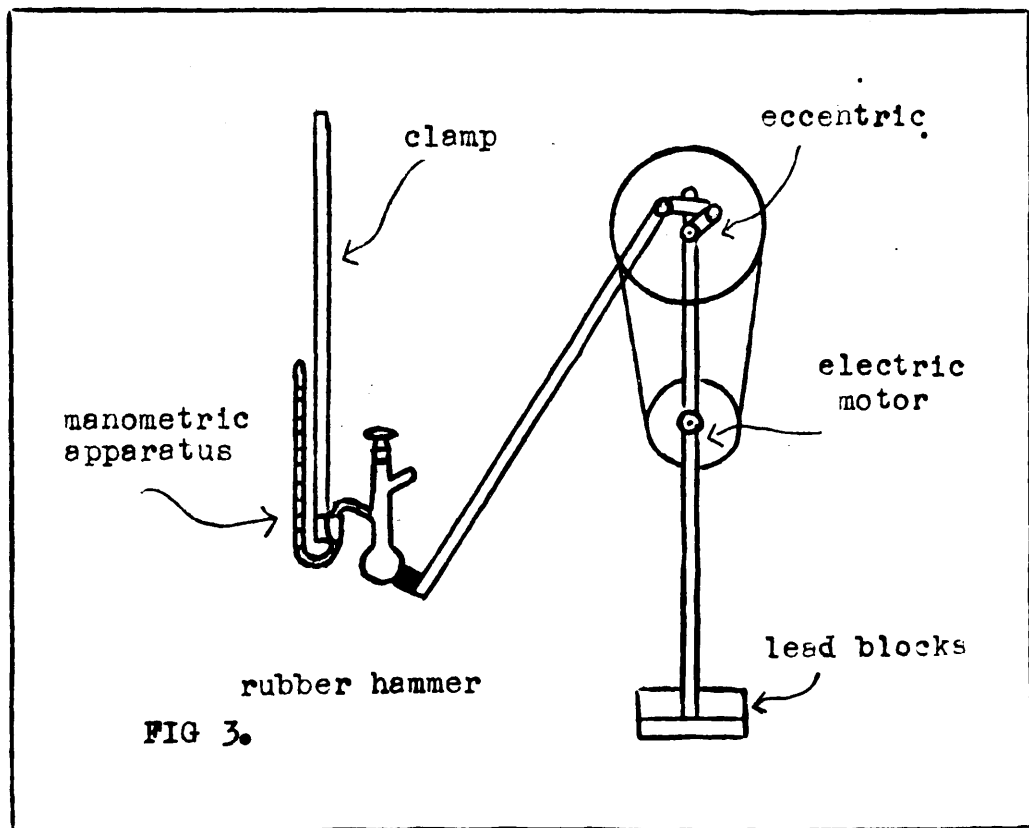
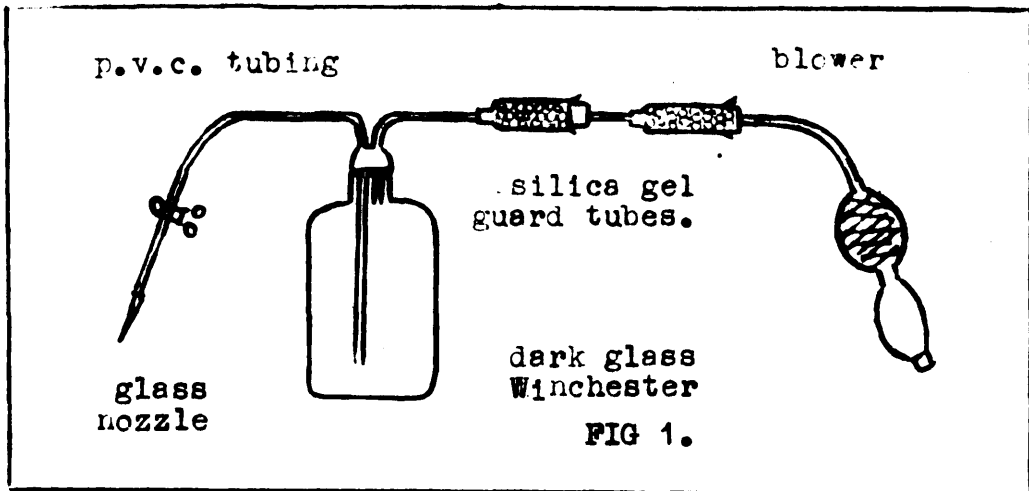
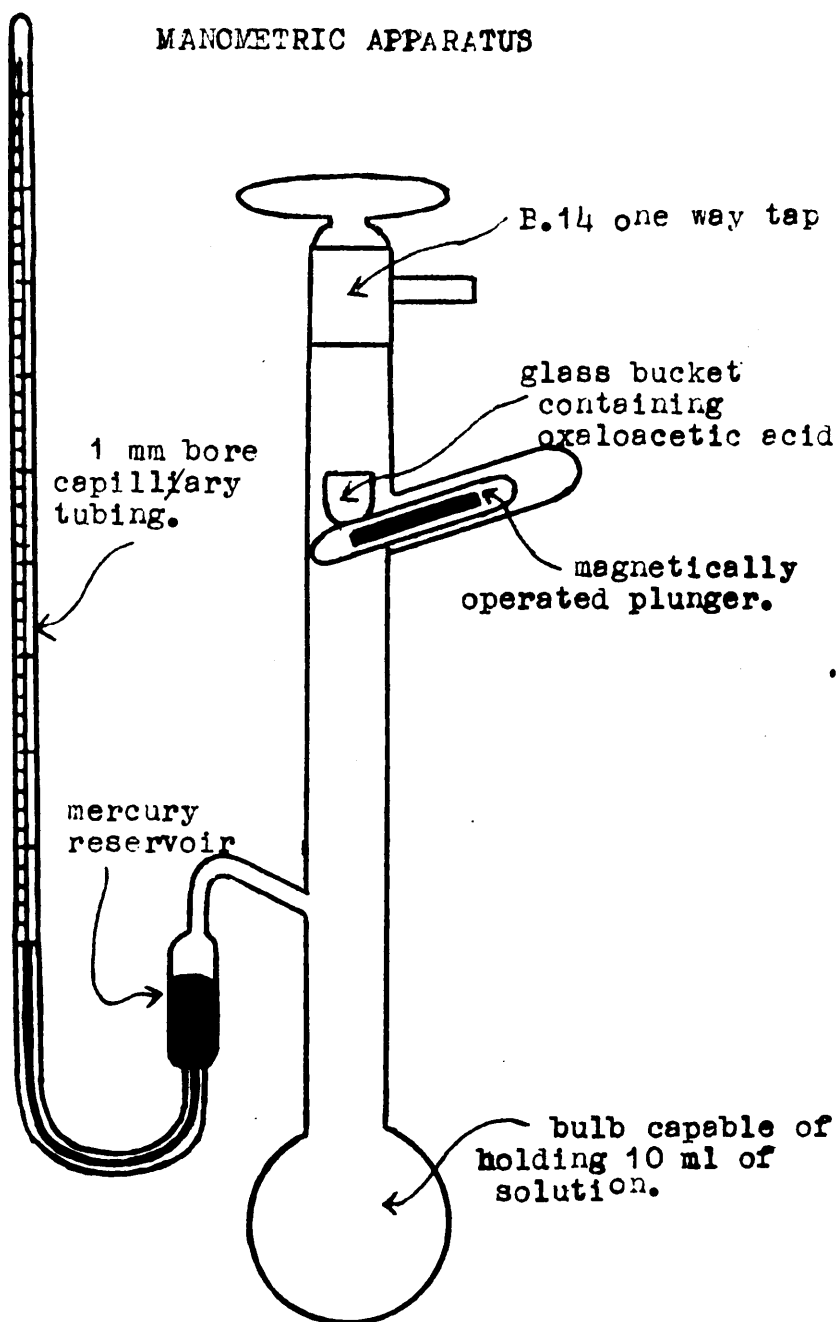


FIG 2.

MANOMETRIC APPARATUS



tap lubricated with Dow-Corning silicone grease. The reaction flask is allowed to attain room temperature and is then placed in a thermostat regulated at  $25.00^{\circ} \pm 0.02^{\circ}$  by means of a Circotherm unit. The reaction is initiated, after equilibration (10 minutes), by withdrawing the plunger into the side arm. Readings are taken through a window in the bath at  $1/4$  minute intervals.

#### Calibration of the Apparatus

It was found most convenient to calibrate the apparatus using sodium bicarbonate, since this avoided the tedium of waiting for infinity readings. 16.8 mgm. of bicarbonate are equivalent to 26.4 mgm. of oxaloacetic acid. A blank run was therefore carried out by the procedure previously noted, with 10 ml. of hydrochloric acid in the bulb. Very reproducible results could be obtained by this method, e.g. the changes for three calibrations were 9.42, 9.42, and 9.44 cm. The infinity reading for a run could thus be obtained by adding 9.42 cm. to the zero time reading. Checks were made on several oxaloacetate runs in the presence of amines; 100 %  $\text{CO}_2$  (calculated from bicarbonate) was liberated in every case showing that the reaction went to completion.

Similar calibrations were also carried out for runs in alcohol, with 10 ml. of alcohol and 0.05 ml. of concentrated hydrochloric acid in the bulb. The change in this case was 6.20 cm., i.e., only 66 % of that when water was used. This

reading remained steady for two days. Complete agreement with the  $\frac{f}{\lambda}$  infinity readings for the runs was obtained, thus for a series of runs the changes were 6.24, 6.10, 6.30, 6.25, 6.10, 6.25, 6.10, 6.18, 6.25 and 6.20 cm. (average 6.25 cm.). The tube was also standardised using dry alcohol saturated with dry carbon dioxide (cylinder). 10 ml. of the alcohol were taken and 0.05 ml. of concentrated hydrochloric acid added. It was necessary to pump out the tube three times as the excess carbon dioxide came out of solution. The bicarbonate change gave 6.11 cm. (steady for two days).

#### Cleaning of the Apparatus

The following cleaning procedure was always employed,

- a) A.R. Benzene to remove grease.
- b) Chromic acid (15 minutes).
- c) Washing with 2-litres of water.
- d) Washing with distilled water.
- e) A.R. Acetone to dry.

#### Agitation and Mixing

Timing was always begun on withdrawal of the plunger. In most cases half a minute was required for all the oxaloacetate to dissolve even under the most vigorous shaking conditions. Shaking of the apparatus during the run to prevent supersaturation of  $\text{CO}_2$  was carried out by an electrically-operated rubber hammer. This is illustrated diagrammatically in Fig.2. Very high shaking rates had to be employed in the fast runs (150 oscillations per minute) otherwise erroneous results

were obtained.

### Spectrophotometric Measurements

Were carried out using a Hilger Uvispek spectrophotometer (Series 308) fitted with a special silica prism capable of extending the range of the instrument in the extreme ultra-violet to 185  $m\mu$ . Spectra were obtained using 1 mm. quartz cells with solvent as blank unless otherwise stated. After each determination the solution-solvent cells were interchanged and the spectrum redetermined, the optical densities were then averaged. This was necessary since the cells were unbalanced in certain areas of the spectrum. The spectra were obtained in distilled water or Burroughs absolute alcohol, by diluting standard solutions.

Kinetic runs were carried out in standard stoppered 1 cm. quartz cells, capable of holding 3 ml. of solution. A Hilger water-jacket was used in conjunction with a Circotherm unit. Running the Circotherm at 25.0° thermostated the cells at 24.8°. Both aniline and ester solutions were initially thermostated at 25.0°. 2 ml. of the ester solution were pipetted into the absorption cell, followed by 1 ml. of the aniline solution. Timing was begun when approximately half the pipette had been drained. The mixture was rapidly shaken for 30 seconds to ensure homogeneity, readings begun at 45 seconds on the initially 'checked' instrument, and were repeated at 15 second intervals. Room temperature was raised to approximately 24.8° by means of electrical heaters.

'Analar' materials and Grade 'A' volumetric glassware were used throughout.

... ..  
... ..  
... ..



... .. since these cannot decompose to ... ..  
When sodium reacts with (1) in aqueous solution ... ..  
... .. is the sodium salt of the ... ..



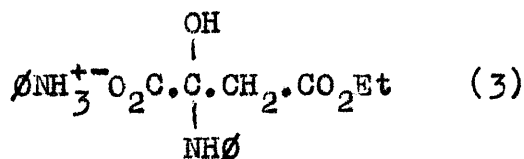
... ..  
This compound gives characteristic ... ..  
... .. dissolves in ethanol to give bright yellow ... ..  
... .. ultraviolet spectra in both solvents are ... ..  
... .. and ... .. the production of a new ... ..  
... .. absorption band in alcohol at ... .. the ... ..  
... .. yellow colour. This is attributed to ... ..

Results and Discussion      Part 2Nature of the Intermediates

The intermediates formed by the action of aniline on oxaloacetic acid are most easily studied by using its esters (1) and (2).



since these cannot decarboxylate in the presence of amines. When aniline reacts with (1) in aqueous solution, the product isolated is the aniline salt of the ketimine hydrate (3).



This compound gives colourless solutions in water, but dissolves in ethanol to give bright yellow solutions. Its ultra-violet spectra in both solvents are shown in Figs. 1 and 2. The production of a new high intensity ( $\epsilon = 15,200$ ) absorption band in alcohol at  $321 \text{ m}\mu$  is the cause of the yellow colour. This is attributed to dehydration of the ketimine hydrate producing the highly conjugated ketimine system (4).

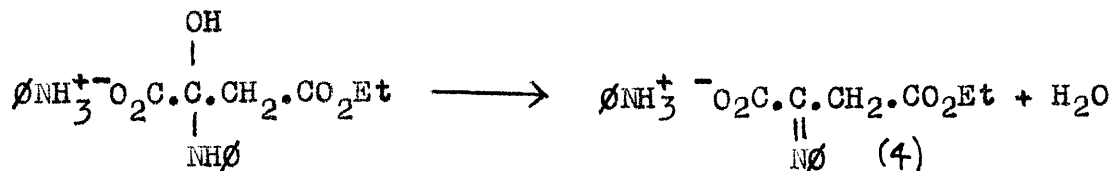


FIG 1

Ultra -Violet absorption spectra of the ketimine hydrate (3) in water. Solution  $1 \times 10^{-3} M$ , 1mm cells. Also the monoester (1).

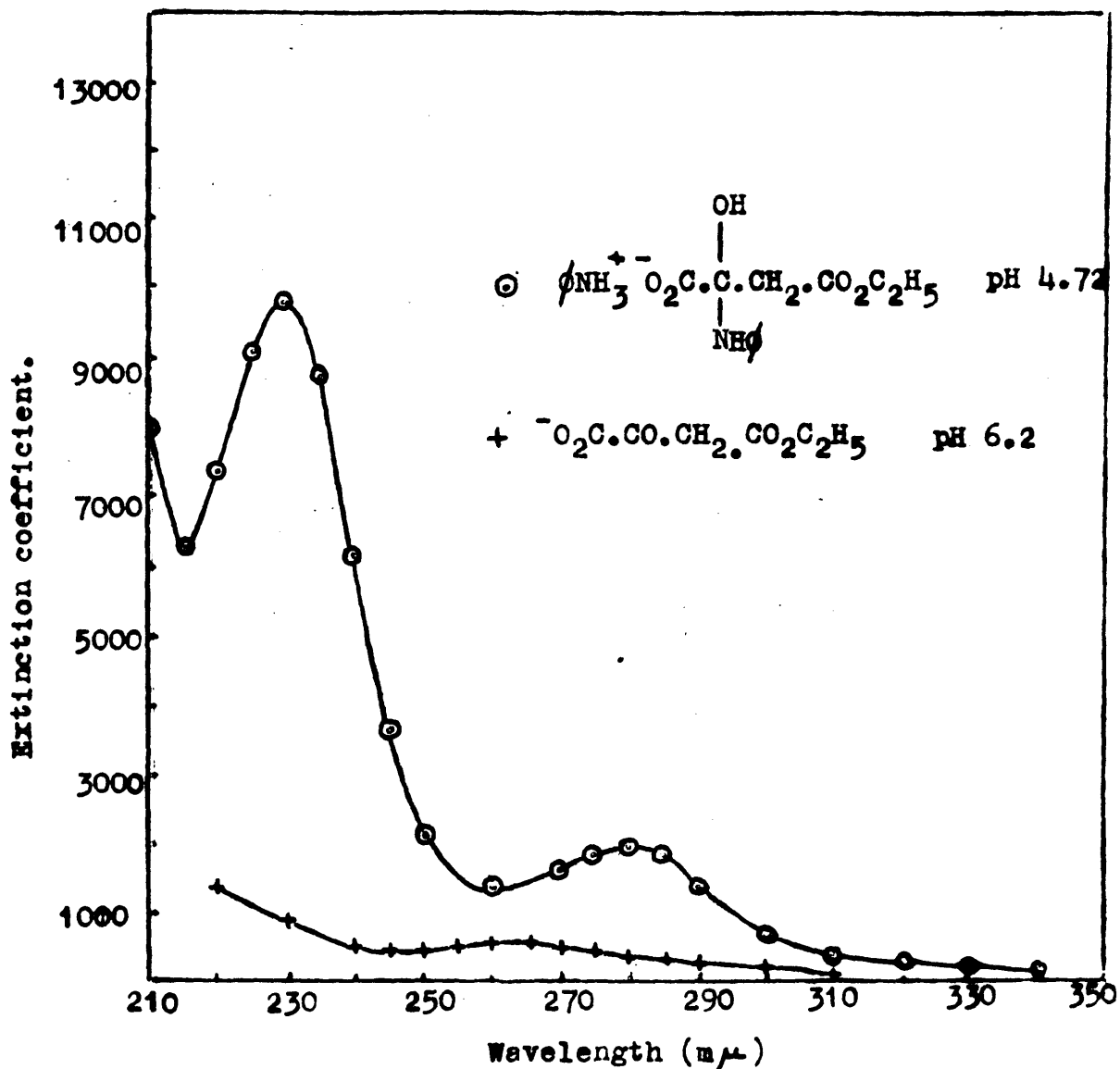
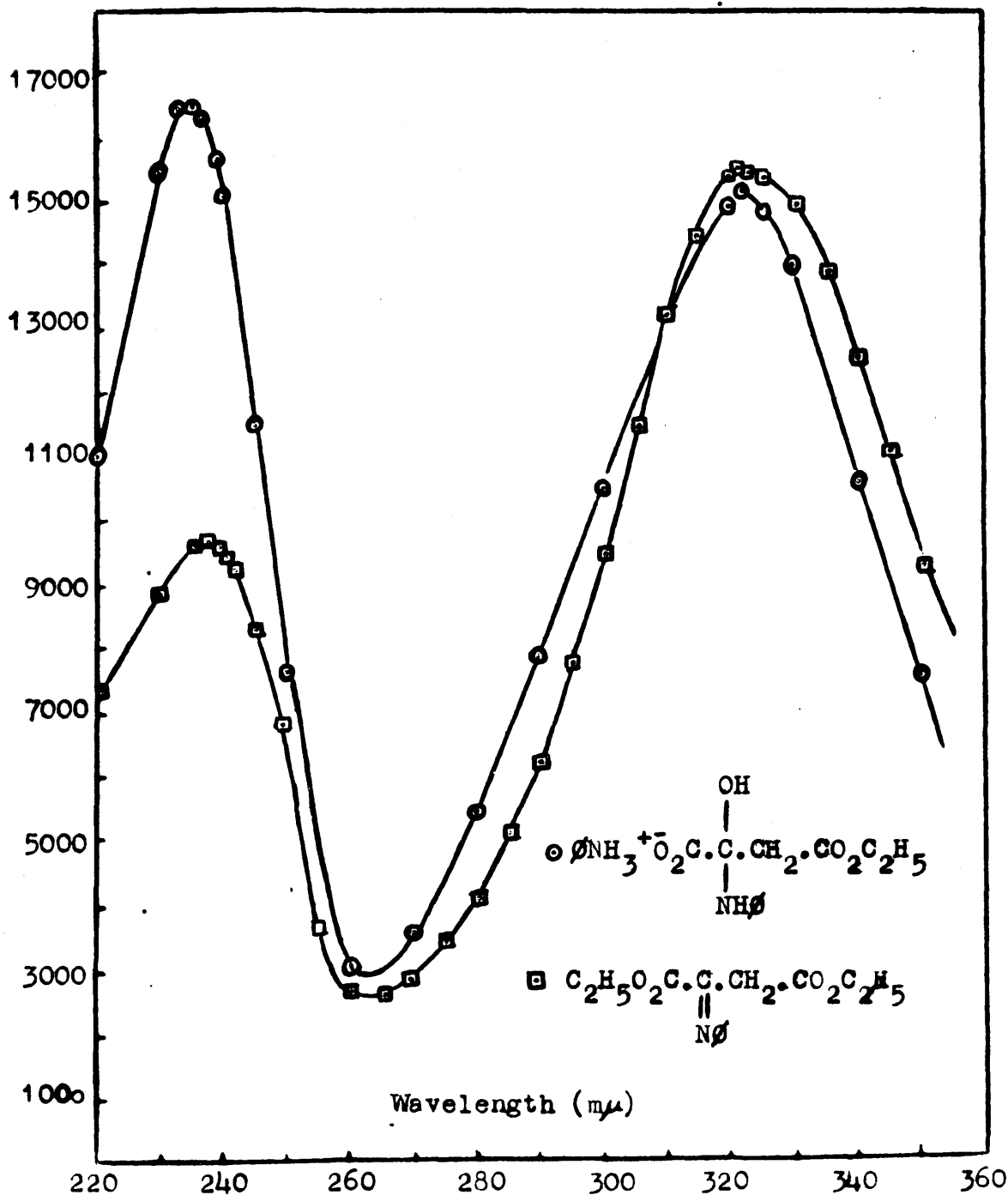


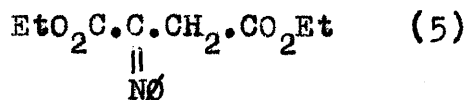


FIG 2.

Ultra-violet absorption spectra of the ketimine hydrate (3) and the ketimine (5) in absolute alcohol, showing the ketimine band at 321 m $\mu$ . Solution  $1 \times 10^{-3} M$ , 1mm cells.

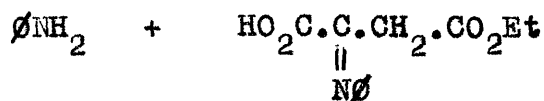


In agreement with this, when aniline reacts with the ester (2) in a non aqueous solvent such as alcohol, the product obtained is the ketimine (5).



In contrast to the ketimine (3) which is colourless, this is a pale yellow compound. It gives an identical band at 321  $m\mu$  ( $\epsilon = 15,400$ ) to (3) in ethanol, Fig2. Only very slight increases in the intensity of this band occur in solvents of even lower dielectric constant, such as diethyl ether.

The difference in intensity of the two spectra in the region of 230  $m\mu$  is due to the presence of a second molecule of aniline in (3). Aniline in ethanol, Fig.3, has an extinction coefficient of approximately 8,000, this agrees very well with the difference of approximately 7,000, in the extinction coefficients of (4) and (5) in ethanol at 235  $m\mu$ . This indicates that in ethanol (4) must be represented by,



there can be no proton transfer to produce the anilinium ion, since this shows no absorption at 235  $m\mu$ , Fig.3.

The spectrum of the ketimine hydrate (3) shown in

FIG 3

Ultra-violet absorption spectra of aniline and the anilinium ion.

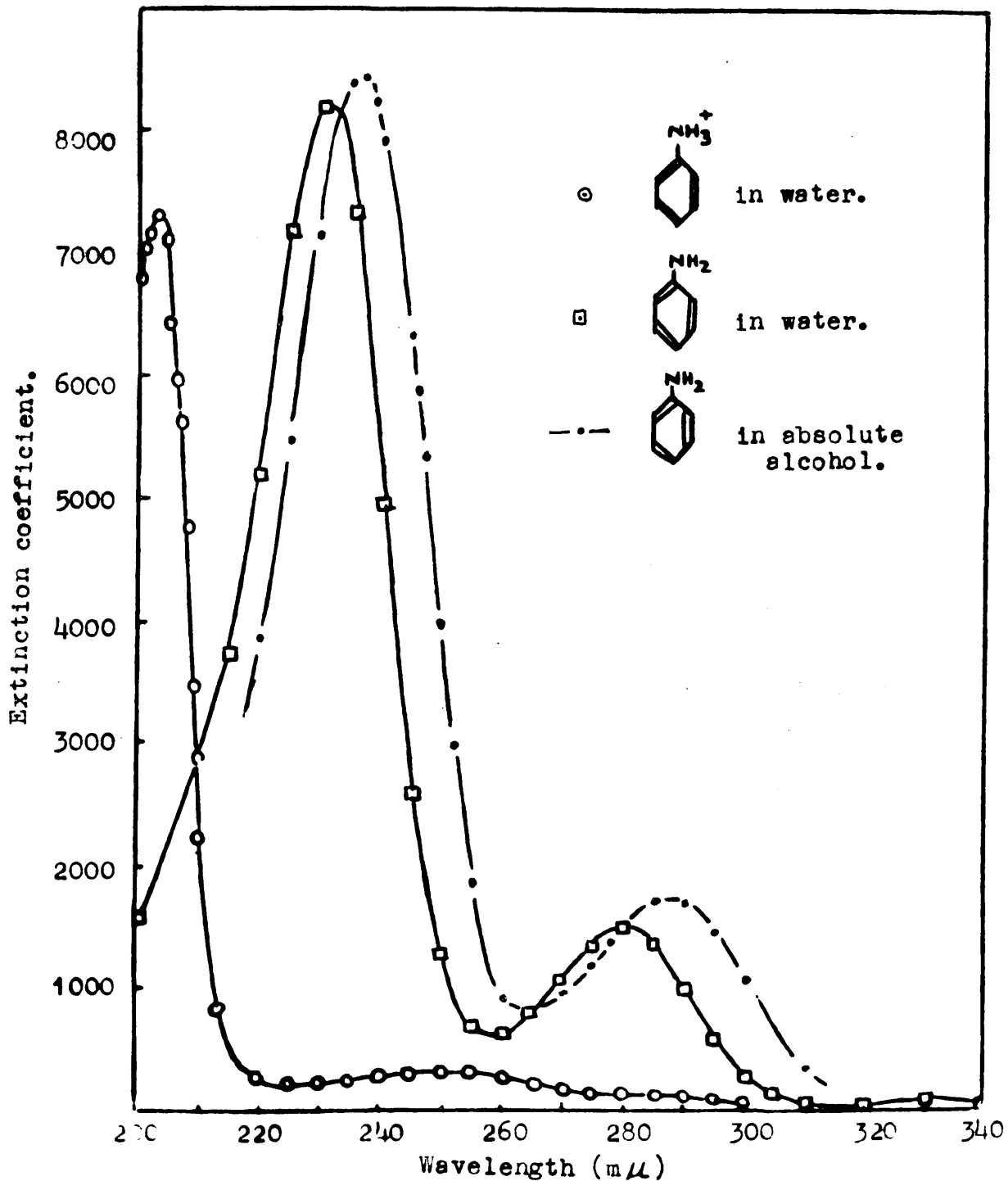
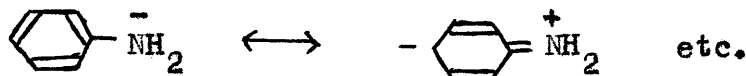
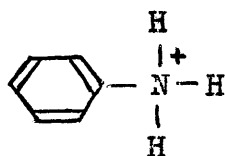


Fig.1, is a composite spectrum of four species, aniline (An), the anilinium ion ( $\text{AnH}^+$ ), the ketimine hydrate (K), and its conjugate acid ( $\text{KH}^+$ ). The spectrum of aniline in water shows two bands,<sup>13</sup> one of  $\epsilon = 8,200$  at  $230 \text{ m}\mu$  and a low intensity band at  $280 \text{ m}\mu$  ( $\epsilon = 1,450$ ) which is the characteristic benzenoid band.

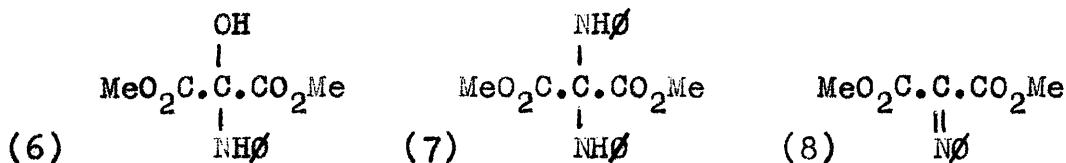
The high intensity band is due to various resonance forms involving the lone pair of electrons,<sup>14</sup>



These are destroyed in the anilinium ion since the lone pair is used to bind the proton and the band disappears.



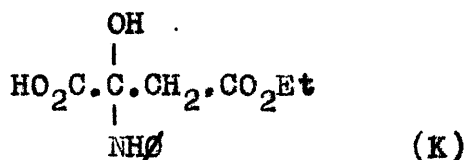
In order to make a more thorough study of the ketimine hydrate spectra, it was decided to synthesise the corresponding compounds derived from methyl keto malonate  $\text{CH}_3\text{O}_2\text{C}\cdot\text{C}\cdot\text{CO}_2\text{CH}_3$ ,<sup>10</sup> which should closely resemble oxaloacetate derivatives.



Both (6) and (7) are stable colourless compounds, however, (6) can react with excess aniline to give (7). (8) is a

bright yellow oil (ketimine), but is so reactive that it proved impossible to prepare it in a pure state.<sup>15</sup> Any compound with an easily dissociable hydrogen atom such as water, aniline or alcohol adds across the double bond with great ease, the first two giving (6) and (7) respectively. This is in marked contrast to most ketimines, the ketimine hydrate is usually very unstable losing water rapidly to give the ketimine.

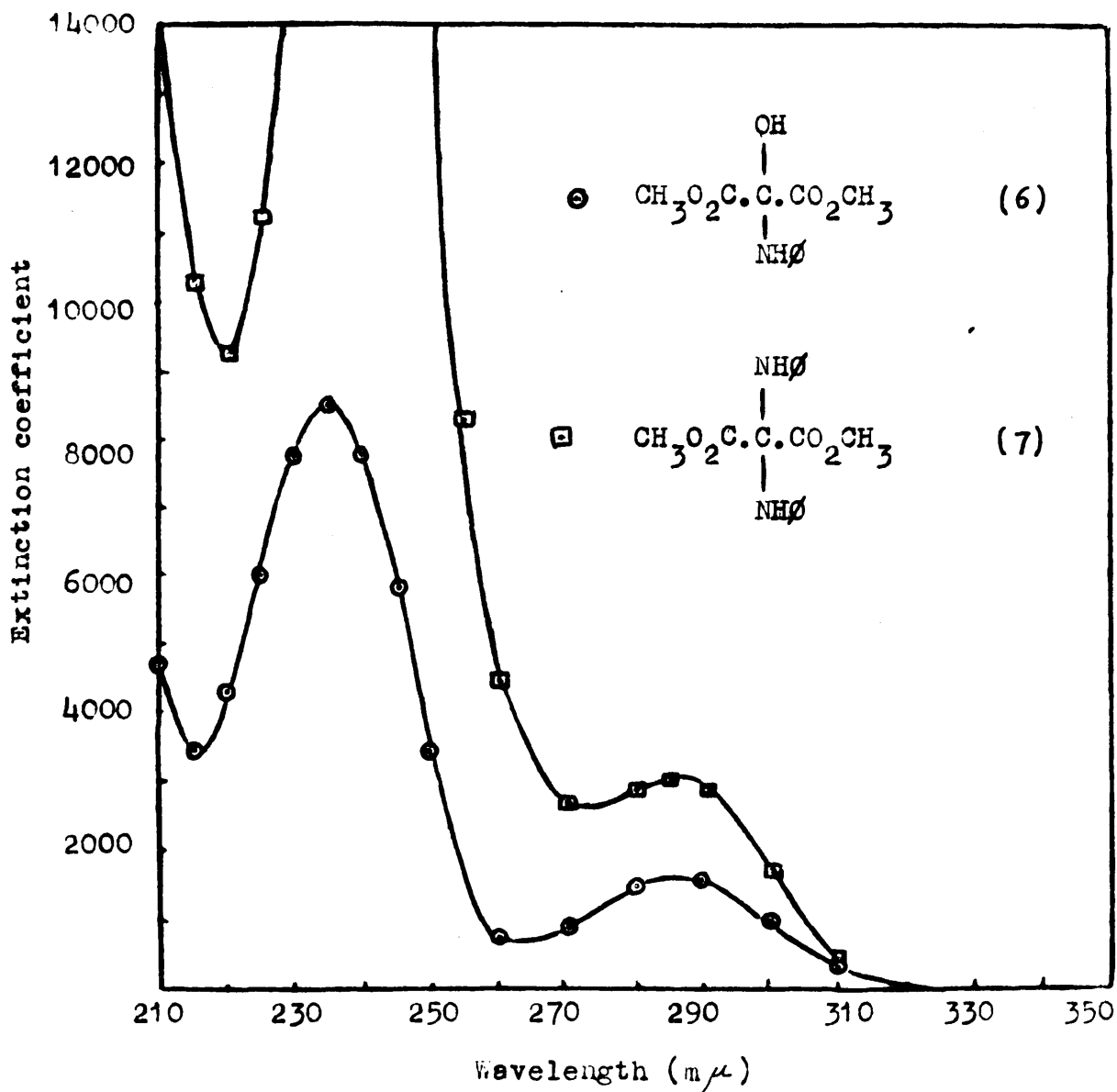
The ultra-violet absorption spectrum of (6), Fig.4, is almost identical to that of aniline, Fig.3. Thus (6) shows peaks at 235 m $\mu$  ( $\epsilon = 8,500$ ) and 285 m $\mu$  ( $\epsilon = 1,600$ ), compared to the aniline peaks at 235 m $\mu$  ( $\epsilon = 8,400$ ) and 285 m $\mu$  ( $\epsilon = 1,700$ ) in alcohol. The ultra-violet absorption properties of (6) depend solely on the  $\phi$ -NH- grouping; this can also be seen from the spectra of (1) and (3) in Fig.1. The monoester (1) has only very weak ultra-violet absorption and there can be no further conjugation on production of the hydrate. The ketimine hydrate (K) is expected to behave similarly,



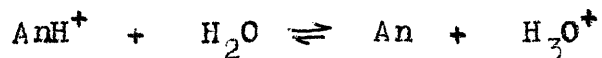
It is usually found that substituted anilines have very comparable basic strengths to aniline (e.g. aniline and dimethyl aniline).<sup>16-17</sup> It would, therefore, be expected that

FIG 4

Ultra-violet absorption spectra of (6) and (7) in absolute alcohol. The spectrum of (6) compares with that of (3), FIG 1. The band at 320  $m\mu$  is absent. Solutions  $1 \times 10^{-3}$  M. 1cm cells.



$pK_b$  for the ketimine hydrate (K) would be similar to that for aniline. Later potentiometric measurements show this to be the case. It would also be expected from previous reasoning that the conjugate acid ( $KH^+$ ) would show very weak ultra-violet absorption in the 230-300  $m\mu$  region. The ketimine hydrate should thus behave under different conditions of pH like two molecules of aniline. Fig. 5a, shows the spectra of the ketimine hydrate (3) in various buffer solutions, a band in the region of 230  $m\mu$  is present in each case. Table 1, shows a comparison between the intensity of this band and that shown by two molecules of aniline. A value of  $2.45 \times 10^{-5}$  was taken for the dissociation constant of the anilinium ion.



This compares with a value of  $2.33 \times 10^{-5}$  at  $25^\circ$  and  $I = 0.300$ , given by PEDERSEN.<sup>7</sup> This should be independent of ionic strength. However, slightly higher values have been found in dilute solutions.<sup>17</sup> Column 5 gives the optical density calculated for a  $1 \times 10^{-3}$  Molar solution of aniline in a 1mm cell at 230  $m\mu$  using the values  $\epsilon_{\text{aniline}} = 8,600$ ,  $\epsilon_{\text{anilinium ion}} = 0$ . The starred experiment was carried out at zero ionic strength. The agreement between the two final columns indicates that  $KH^+$  does have a similar dissociation constant to that of the anilinium ion and must have only very weak ultra-violet absorption

in the region of  $230 \text{ m}\mu$ .

Table 1 Absorption of the ketimine hydrate compared to that of aniline.

$I = 0.01$ ,  $f_1$  (Davies) = 0.903, Ketimine hydrate (3)  $1 \times 10^{-3} \text{ M}$ .

pH	$10^5\{H^+\}$	$10^5[\bar{H}^+]$	$10^3[An]$	Calc. O.D.	2 x Calc. O.D.	O.D. obs.
4.98	1.047	1.16	0.68	0.585	1.17	1.19
* 4.72	1.91	1.91	0.56	0.482	0.95	0.98
4.26	5.50	6.09	0.29	0.249	0.50	0.52
3.63	23.44	26.00	0.086	0.074	0.15	0.25

It is thus practically impossible to distinguish between aniline and the ketimine hydrate using the  $230 \text{ m}\mu$  peak, and no measure of the concentration of the ketimine hydrate under various conditions of pH can be made.

The absorption of (6) in the region of  $200 \text{ m}\mu$  was then investigated to see if any other high intensity absorption bands were present in this area. (6) shows an intense band, Fig. 5b, at  $205 \text{ m}\mu$  ( $\epsilon = 10,000$ ). The ketimine hydrate shows a similar band at  $203 \text{ m}\mu$ , Fig. 5a, illustrates its behavior <sup>$\mu$</sup>  with pH. Its conjugate acid  $KH^+$  is expected to show similar absorption to the anilinium ion in this region. Four species will absorb at  $205 \text{ m}\mu$ .  $AnH^+$ ,  $\epsilon = 7,000$ ;  $KH^+$ ,  $\epsilon = 7,000$ ;  $An$ ,  $\epsilon = 2,000$ . The value for K is unknown. A reasonable value can, however, be calculated, thus at pH 4.98, the optical density of a  $1 \times 10^{-3} \text{ M}$ . solution of (3)



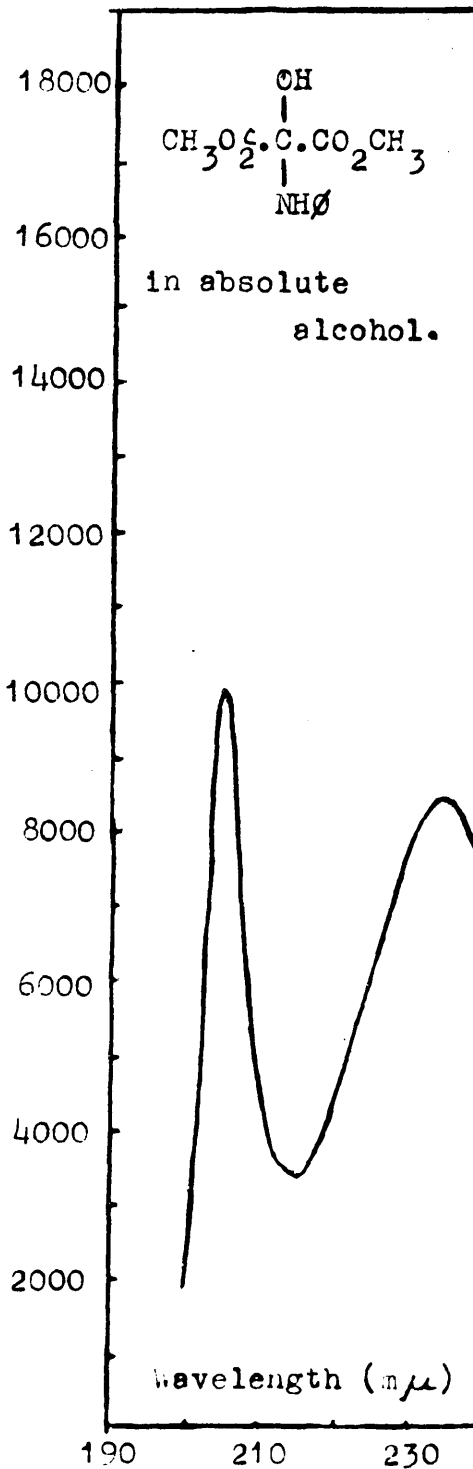
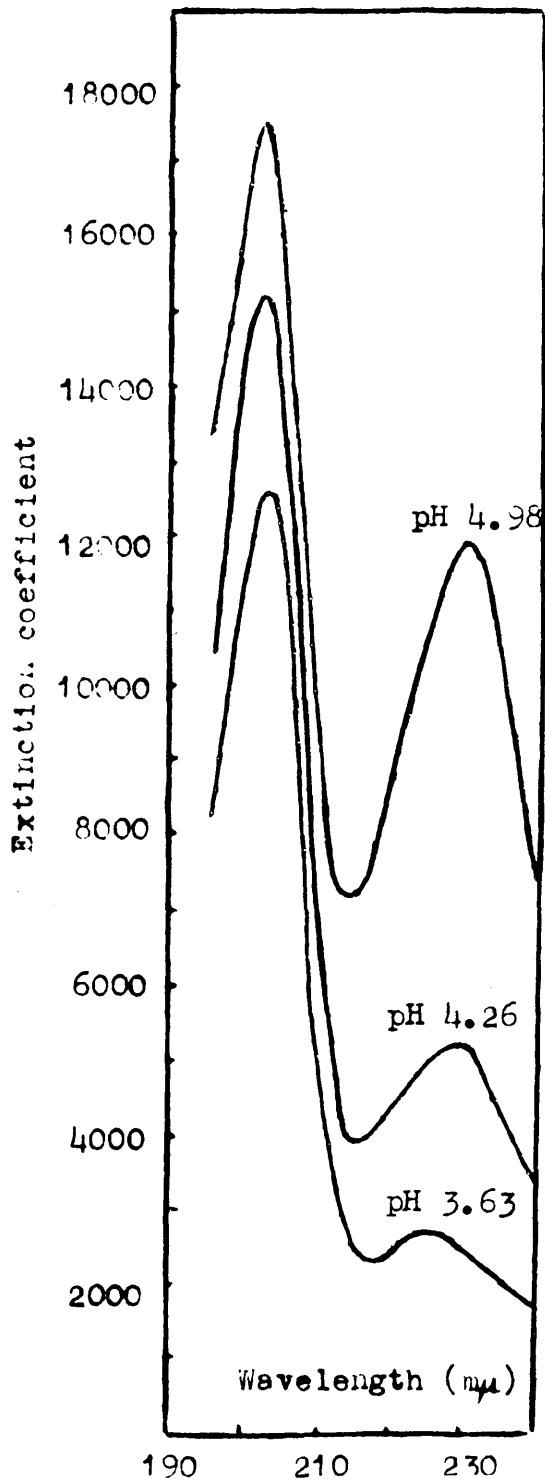
FIG 5

(a) Ultra-violet absorption spectra of the ketimine hydrate (3) in acetate buffers.

(b) Ultra-violet absorption spectrum of the ketimine hydrate (6) in absolute alcohol.

(a)

(b)



in a 1 mm. cell is 1.70 at 205  $m\mu$ , therefore,  $\xi(K) = 16,000$ . Table 2 shows observed and calculated optical densities at various pH's.

Table 2 Observed and calculated values of the optical density of the ketimine hydrate (3) at 205  $m\mu$ .

$I = 0.01$ ,  $f_1$  (Davies) = 0.903. 1 mm cells. Solution  $1 \times 10^{-3}$  M.

pH	$10^5 \{H^+\}$	$10^5 [H^+]$	$10^3 [An]$ or $[K]$	$10^3 [KH^+]$ or $[AnH^+]$	O.D. calc.	O.D. obs.
4.98	1.047	1.16	0.68	0.32	1.7	1.7
4.72	1.91	1.91	0.56	0.44	1.63	1.65
4.26	5.50	6.09	0.29	0.71	1.52	1.50
3.63	23.44	26.0	0.09	0.91	1.35	1.25
2.12	759.0	841.0	-	1.00	1.40	1.36

The agreement is very good considering the assumptions involved. It would be expected that  $\xi(K)$  could be easily obtained from measurements at high pH, since only two species would be present (An) and (K). The extinction coefficient observed at 205  $m\mu$  and pH 11.80 is around 15,700 giving a value of  $\xi(K) = 13,700$  ( $\xi(A) = 2,000$  at 205  $m\mu$ ). However, at this pH an intense new band appears in the spectrum at 273  $m\mu$ ,  $\xi = 17,800$ . Fig.6 shows the variation in intensity of this band with pH. The appearance of this band around pH 7.5 indicates that the species formed probably plays an important part in the inhibition of decarboxylation at high pH's, since around pH 12, no

FIG 6

New band appearing in the ultra-violet absorption spectrum of the ketimine hydrate (3) in alkaline solution (band at 273 m $\mu$ )

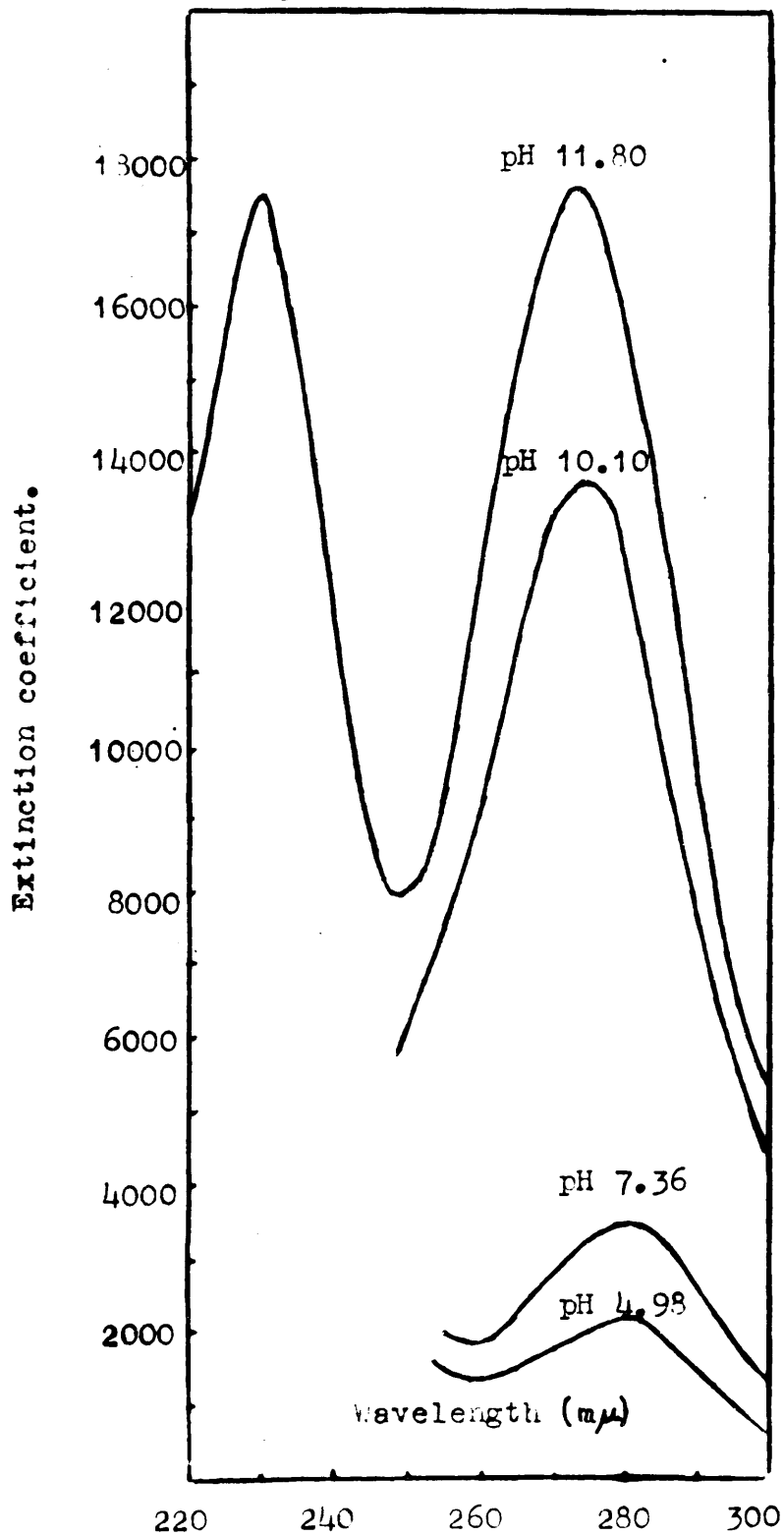


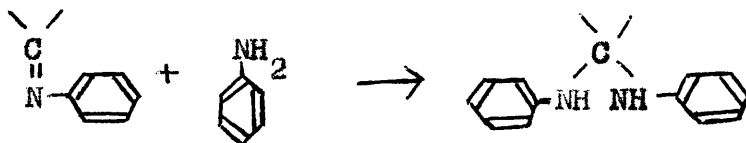


**Table 3 Final optical densities of mixtures of ester (1) and aniline at various aniline concentrations.**

Wavelength 420  $m\mu$ , 1 cm. cells.

(A) $[\text{HO}_2\text{C} \cdot \text{CO} \cdot \text{CH}_2 \cdot \text{CO}_2\text{Et}] = 0.02\text{M.}$		(B) $[\text{O}^-\text{NH}_3^+ \text{O}_2\text{C} \cdot \text{C}(\text{OH}, \text{NH}\emptyset) \cdot \text{CH}_2\text{CO}_2\text{Et}] = 0.02\text{M.}$		
[Aniline]	Final Optical Density	[Aniline]	Optical Density	%Dianiline Derivative
0.02	1.12	-	1.12	-
0.04	0.992	0.02	0.993	11.3
0.06	0.950	0.04	0.954	14.8
0.10	0.860	0.08	0.861	23.1
0.01	0.60	-	-	-

In column (A), the final optical densities decrease with increasing aniline concentration, but agree perfectly with those obtained by the addition of a corresponding amount of aniline to the ketimine hydrate (column B.). This is attributed to the fact that in the presence of excess aniline an additional reaction can occur. <sup>10</sup>



As has been previously shown, the dianiline derivative of methyl ketomalonate (7) has no absorption in this region (420  $m\mu$ ), thus the final optical densities decrease.

The percentage of dianiline derivative has been calculated using a value of  $\epsilon (K^*)$  at  $420 \text{ m}\mu$  equal to 56. In agreement with this, dimethylaniline which cannot give such a reaction, has no effect on the final optical densities. 0.08 dimethyl aniline + 0.02 ketimine hydrate (3) gives an optical density of 1.09.

These experiments indicate that complete condensation between the keto acid and aniline takes place with the formation of the ketimine.

Comparison of the rate of formation of the ketimine ( $K^*$ ) and the rate of decarboxylation of oxaloacetic acid in alcohol.

Although complete condensation occurs between aniline and the ester (1) in alcohol, the reaction does not take place instantaneously. Fig. 7 shows the rate of formation of the ketimine ( $K^*$ ) at different aniline concentrations given by the optical density-time curves. The reaction is second order, this is illustrated by data at two aniline concentrations, Table 4.

Oxaloacetic acid decarboxylates in alcohol, since spectrophotometric measurements indicate that it is only 45 % enolised under such conditions, Fig. 8. Enolic oxaloacetic acid does not decarboxylate. Aniline rapidly catalyses the decarboxylation of oxaloacetic acid in alcohol. Manometric measurements of the rate at high aniline concentrations were made. These gave pseudo first order plots with

FIG 7

Rate of ketimine formation at various aniline concentrations.  $\Delta$  Aniline 0.02,  $\odot$  Aniline 0.10  
 $\square$  Aniline 0.01. Temperature  $25^{\circ}$ ,  $420\text{ m}\mu$   
 Ester (1) 0.02M.

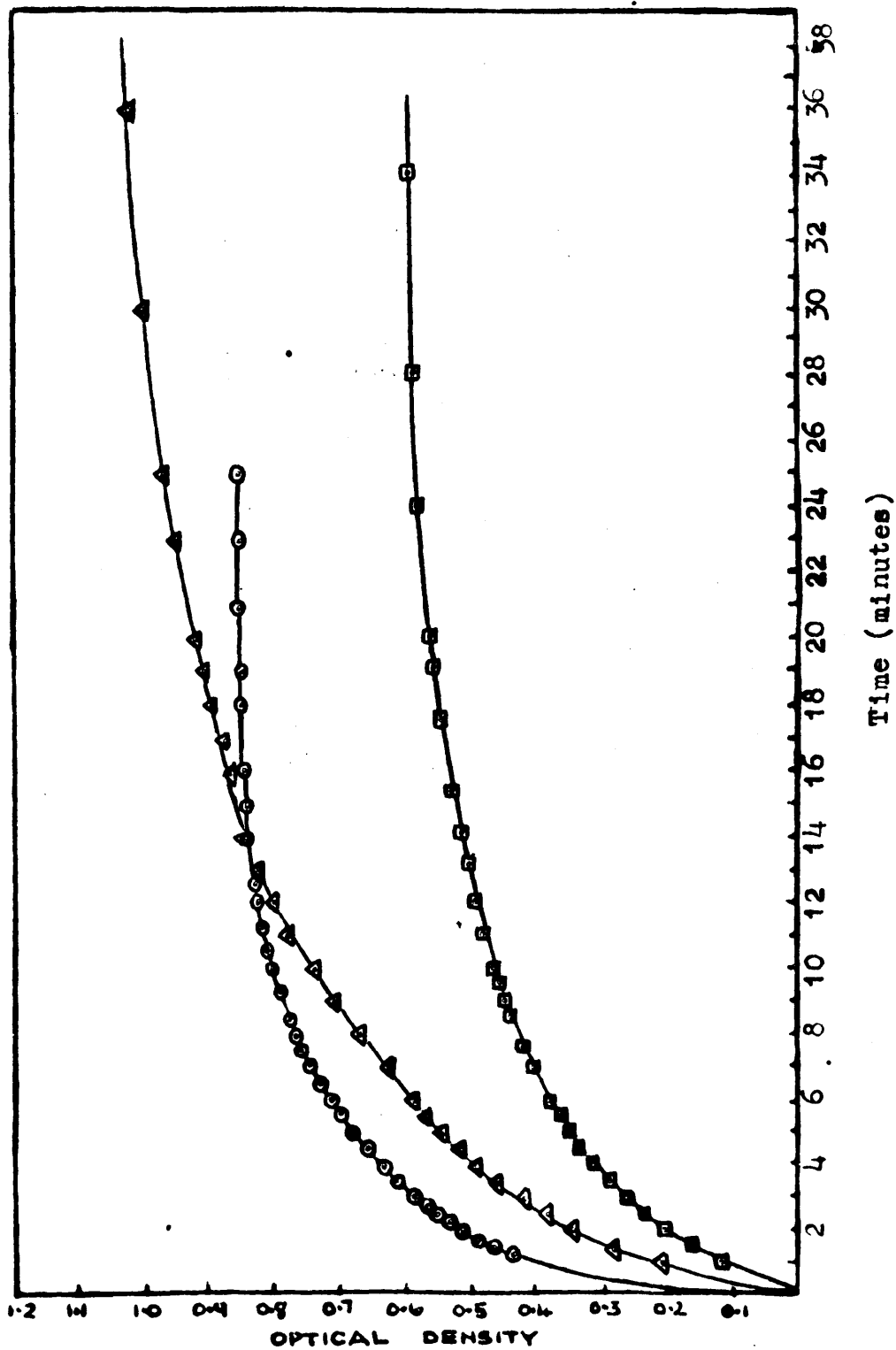


FIG 8

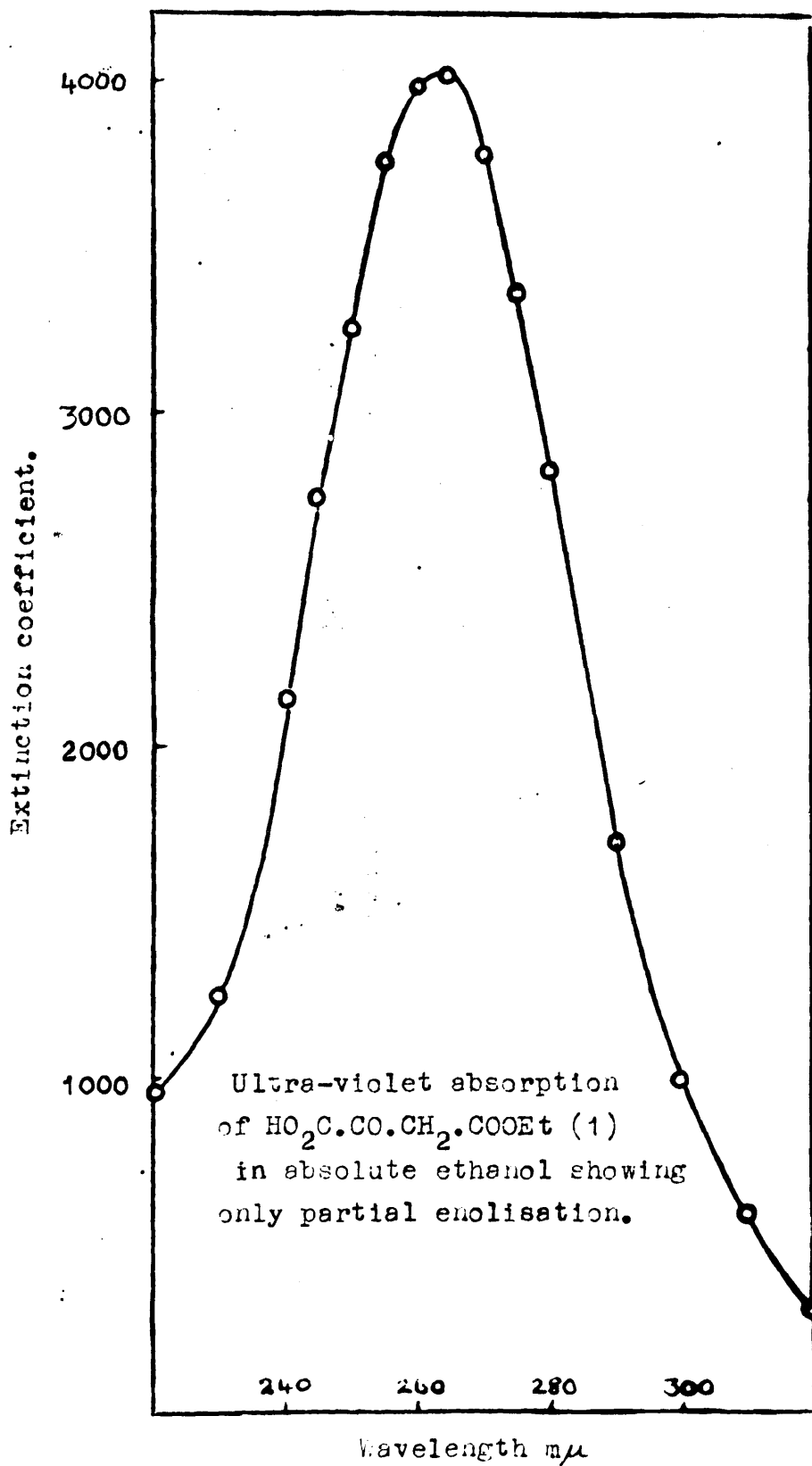




FIG 9

First order manometric plots for the aniline catalysed decarboxylation of oxaloacetic acid in absolute alcohol at 25°. Oxaloacetic acid 0.02 M. Figures in brackets, aniline concentrations.

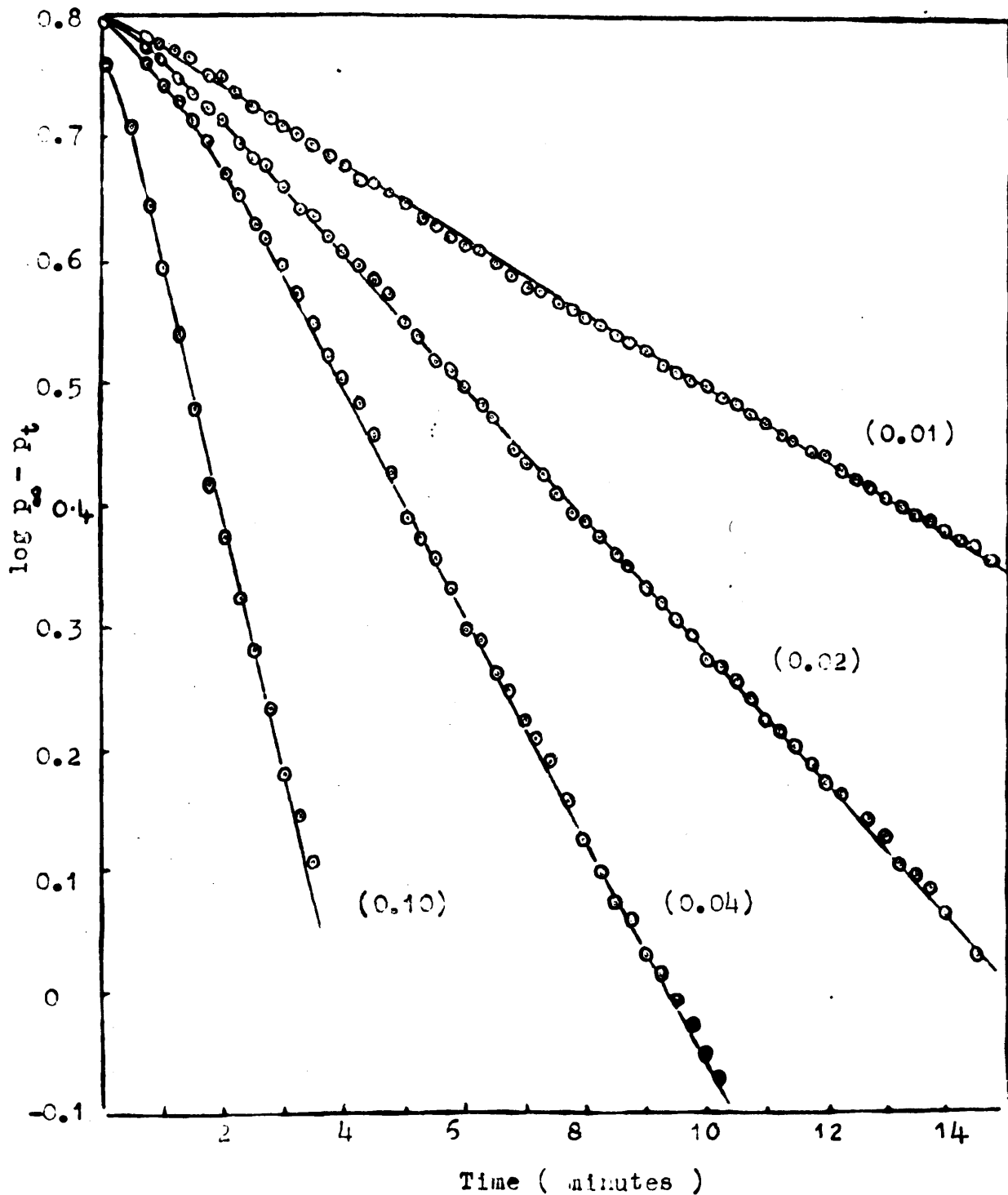


FIG 10

Rate of decarboxylation of oxaloacetic acid in alcohol at  $25^{\circ}$ , for various aniline concentrations. Oxaloacetic acid 0.02 M. The uncatalysed rate is given by  $k^{\circ} = 8.63 \times 10^{-5}$ .

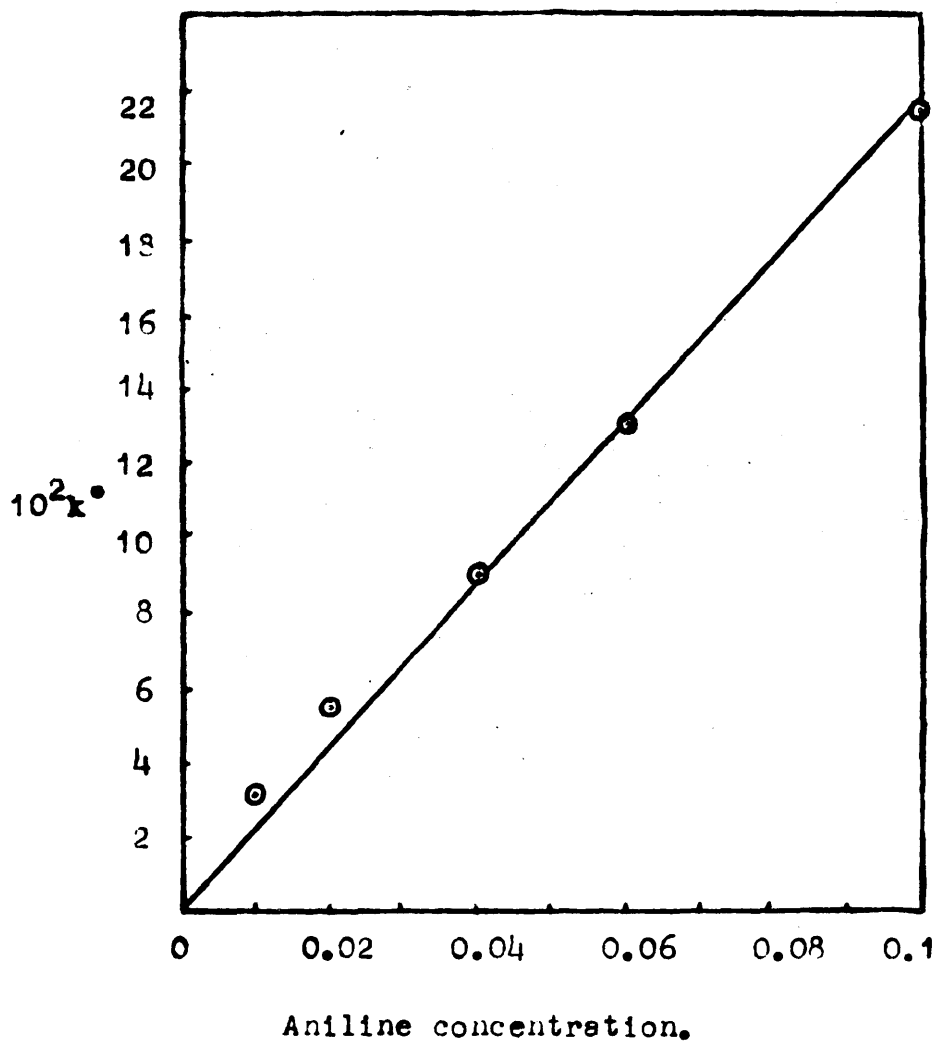


FIG 11

Comparison of the rate of decarboxylation of oxaloacetic acid and the rate of formation of the ketimine of ester (1) at 25°. Aniline 0.02 M. Oxaloacetic acid and ester (1) 0.02 M.

● Decarboxylation    □ Ketimine formation

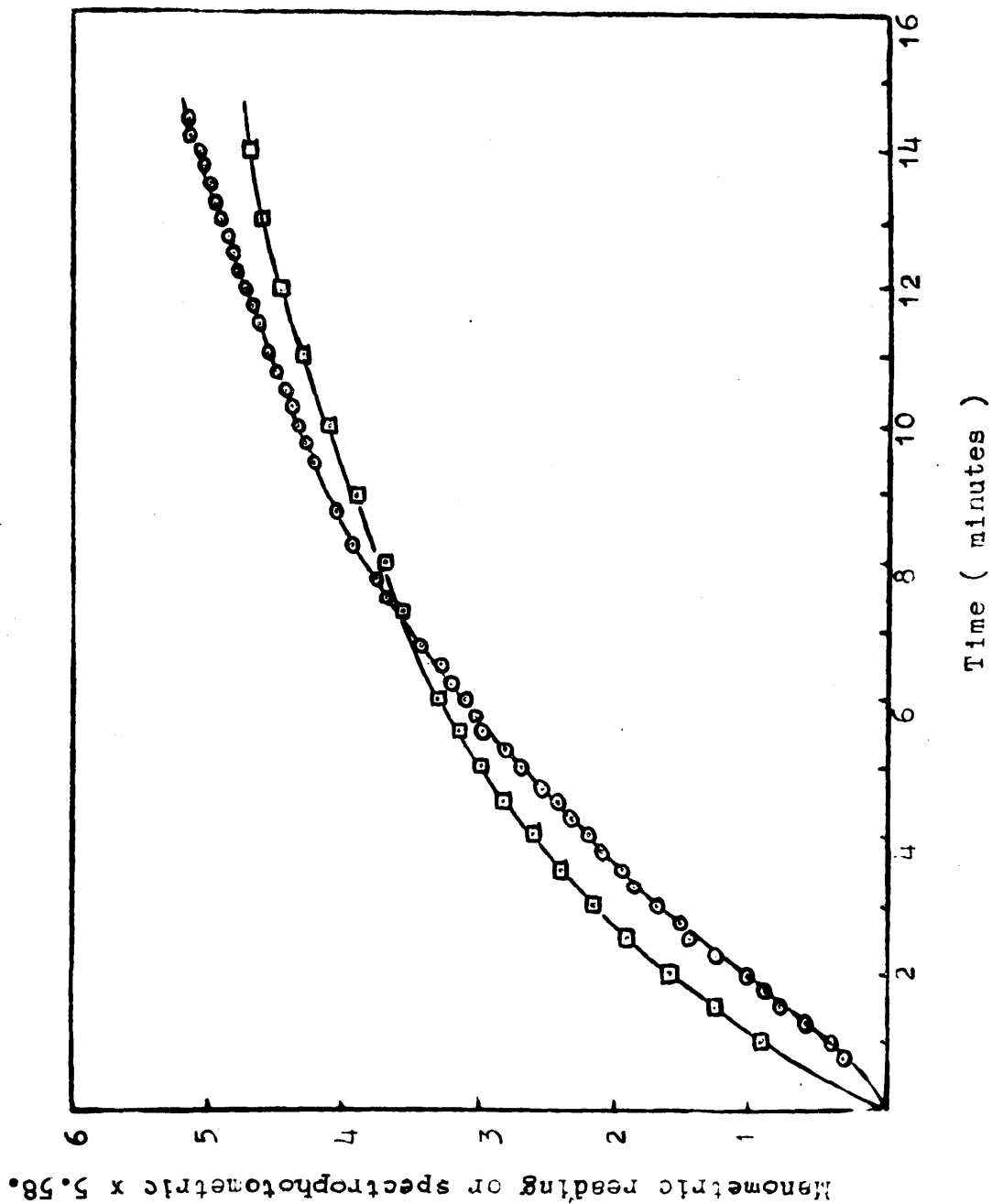


Table 4 Kinetic data on the rate of formation of the ketimine (K\*)  
in alcohol at 25°.

Run 1. Ester (1) = 0.02M. Aniline = 0.02M. 1 cm. cells. 420 m $\mu$

<u>Time (mins.)</u>	<u>Optical Density</u>	<u>[K]</u>	<u>[a - x]</u>	<u>k litres</u> <u>moles min<sup>-1</sup></u>
1	0.205	0.0037	0.0163	11.2
2	0.340	0.0061	0.0139	11.0
3	0.420	0.0075	0.0125	10.0
4	0.490	0.0088	0.0112	9.8
5	0.545	0.0097	0.0103	9.4
6	0.590	0.0105	0.0095	9.2
7	0.628	0.0112	0.0088	9.1
8	0.665	0.0119	0.0081	9.2
9	0.700	0.0125	0.0075	9.3
10	0.740	0.0132	0.0068	9.7
11	0.782	0.0140	0.0060	10.6
12	0.805	0.0144	0.0056	10.7
13	0.827	0.0147	0.0052	10.9
$\infty$	1.12			
			Average	10.01

Table 4 Kinetic data on the rate of formation of the ketimine (K\*)  
in alcohol at 25°.

Run 2. Ester (1) = 0.02M. Aniline = 0.01M. 1 cm. cells. 420 m $\mu$ .

<u>Time (mins.)</u>	<u>Optical Density</u>	<u>[x]</u>	<u>[b - x]</u>	<u>[a - x]</u>	<u>k litres</u> <u>moles min<sup>-1</sup></u>
1	0.120	0.0020	0.0180	0.0080	11.77
2	0.2050	0.0034	0.0166	0.0066	11.48
3	0.265	0.0044	0.0156	0.0056	11.08
4	0.312	0.0052	0.0148	0.0048	9.38
5	0.350	0.0058	0.0142	0.0042	10.55
6	0.381	0.0063	0.0137	0.0037	10.37
7	0.406	0.0067	0.0133	0.0033	10.14
8	0.440	0.0073	0.0127	0.0027	10.10
9	0.450	0.0075	0.0125	0.0025	10.08
10	0.466	0.0077	0.0123	0.0023	9.98
11	0.483	0.0080	0.0120	0.0020	10.07
12	0.496	0.0082	0.0118	0.0018	10.05
13	0.509	0.0085	0.0115	0.0015	10.14
$\infty$	0.602				
				Average	10.40

respect to oxaloacetic acid, Fig.9. The first order rate constants increased in an approximately linear manner with aniline concentration, Fig.10. Accurate kinetic information on the formation of the ketimine  $K^*$  of ester (1) is difficult to obtain, due to complications arising from the dianiline derivative. A direct comparison between the manometric and spectrophotometric data is most conveniently made by using the experimental half lives - i.e. a comparison of the times taken for half the ketimine to form and half the oxaloacetic acid to decarboxylate. These values are shown in Table 5. (It is expected that the rate of formation of the ketimine of ester (1) will be very similar to that for oxaloacetic acid).

Table 5 Comparison of the half lives of ketimine formation of ester (1) and of decarboxylation of oxaloacetic acid in alcohol at 25°.

<u>Aniline</u>	Oxaloacetic acid 0.02M.      Ester (1) 0.02M.	
	<u>Half life Decarboxylation (mins.)</u>	<u>Half life Ketimine formation (mins.)</u>
0.02	5.5	5.5
0.04	3.3	3.3 <sub>5</sub>
0.06	2.4	2.3
0.10	1.4	1.3

These values indicate that the rate of decarboxylation is equal to the rate of ketimine formation. The rate controlling step in alcohol is thus the formation of the ketimine, the actual decarboxylation being very fast. Fig.11, shows a comparison of optical density readings for ketimine formation of ester (1) and manometric decarboxylation readings for oxaloacetic acid. The initial slow rate of decarboxylation is probably due to mixing errors in the very fast reaction. As would be expected solutions of oxaloacetic acid and aniline show only very slight absorption at  $420\text{ m}\mu$  in alcohol.

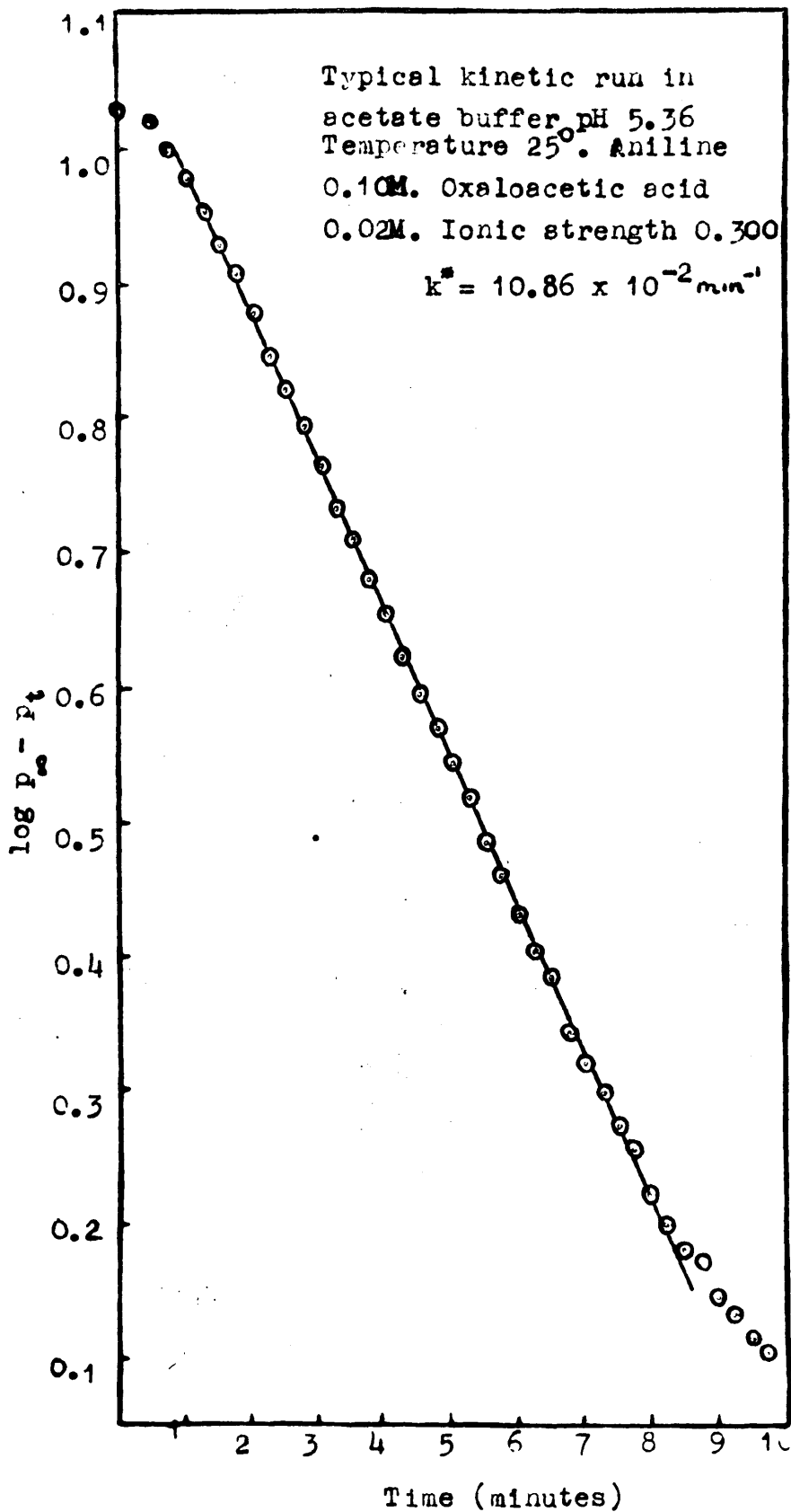
Decarboxylation in aqueous solution at  $25^{\circ}$ .

Measurements of the rate of decarboxylation of oxaloacetic acid in aqueous solution were made at a number of different pH's and aniline concentrations. Linear first order plots with respect to oxaloacetic acid were obtained in every case. Fig.12 shows a typical plot.

The rate increased linearly with aniline concentration and no evidence for a levelling in rate even at very high aniline concentrations could be found. Fig.13 illustrates data for a number of pH's and aniline concentrations. These experiments would appear to indicate that the reactive intermediates are present in only very small amounts.

Each set of kinetic experiments was carried out at a constant initial pH in an acetate buffer, The oxaloacetic

FIG 12





acid concentration being 0.02M. The rate constants were evaluated from first order infinity plots and are quoted in  $\text{min}^{-1}$  units using decadic logarithms.

The results obtained are shown in Table 6. Some experiments at low pH's were carried out in chloroacetate buffers. Experiments in both acetate and chloroacetate buffers at pH 3.6 indicated that in order to compare rates in acetate and chloroacetate buffers the <sup>rate constants in the</sup> latter must be multiplied by a factor of 1.40.

A pH-Rate profile was obtained by plotting the slope of the rate vs [aniline] curves against pH. The values shown on the rate axis are equivalent to the rate coefficients for an aniline concentration equal to 0.10 Molar. A maximum is observed around pH 4.0, Fig.14, the rate decreasing rapidly on either side of this value. An analysis of PEDERSEN'S<sup>7</sup> data shows a similar pH variation.

Fig.15, shows a plot of some of PEDERSEN'S<sup>7</sup> runs at an oxaloacetic acid concentration of 0.015M. and 37<sup>o</sup>, in both hydrochloric acid and acetate buffers.  $\alpha_1$  and  $\alpha_2$  are the degrees of dissociation of the mono and dianions of oxaloacetic acid calculated from equations (1) and (2).

$$\alpha_1 = k_1/f_1\{H^+\} / 1 + k_1/f_1\{H^+\} + k_1k_2\{H^+\}^2 \quad (1)$$

$$\alpha_2 = k_1k_2/f_2\{H^+\}^2 / 1 + k_1/f_1\{H^+\} + k_1k_2/f_2\{H^+\}^2$$

FIG 15

Rate of decarboxylation at various aniline concentrations  
 (An + AnH<sup>+</sup>). Oxaloacetic acid 0.02M. Temperature 25°.

Acetate buffer. + pH 3.94, ○ pH 4.40, □ pH 4.90.

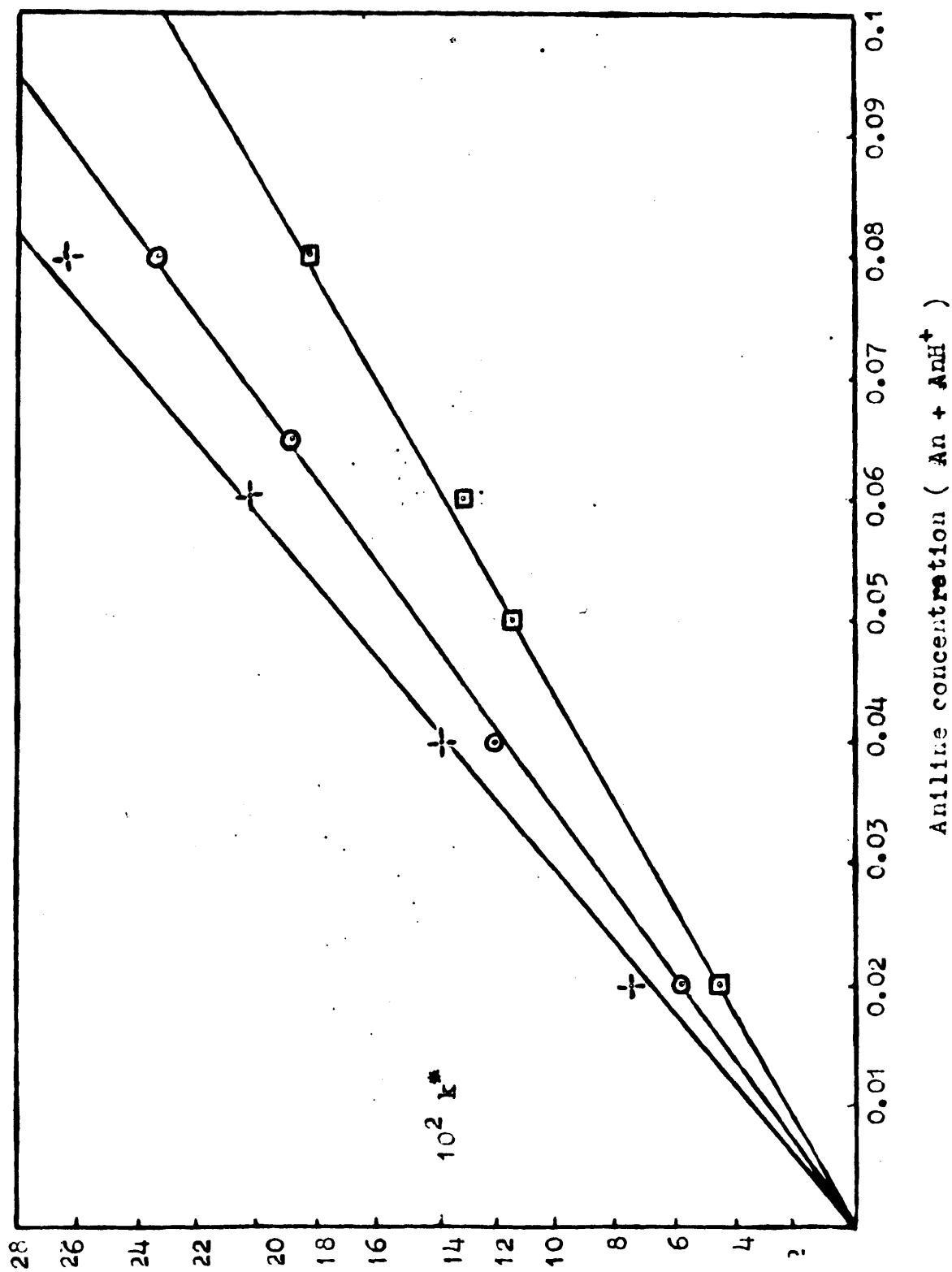


Table 6 Aniline catalysed decarboxylation of oxaloacetic acid at 25°.

a molar acetic acid, b molar sodium acetate, c molar aniline hydrochloride. Oxaloacetic acid 0.02M. I = 0.300

<u>a</u>	<u>b</u>	<u>c</u>	$10^2 k^* \text{min}^{-1}$	pH (measured)
0.1012	0.300	0.020	4.60	4.91
0.0884	0.300	0.050	11.60	4.89
0.0842	0.300	0.060	12.7	4.90
0.0750	0.300	0.080	18.30	4.90
0.0167	0.300	0.100	10.86	5.36
0.0500	0.300	0.100	7.00	5.58
0.400	0.300	0.020	5.7	4.42
0.400	0.300	0.040	12.0	4.40
0.400	0.300	0.060	18.8	4.40
0.400	0.300	0.080	22.4	4.41
1.140	0.300	0.020	8.0	3.94
1.140	0.300	0.040	13.8	3.94
1.140	0.300	0.060	20.2	3.94
1.140	0.300	0.080	26.0	3.94
1.950	0.300	0.020	7.01	3.76
1.950	0.300	0.040	13.98	3.76
1.950	0.300	0.060	18.80	3.76
1.950	0.300	0.080	27.0	3.76
2.000	0.300	0.020	6.40	3.60
2.000	0.300	0.040	12.60	3.60
2.000	0.300	0.060	18.50	3.60
2.000	0.300	0.080	24.00	3.60

FIG 14

pH-Rate profile calculated from data in table 6.

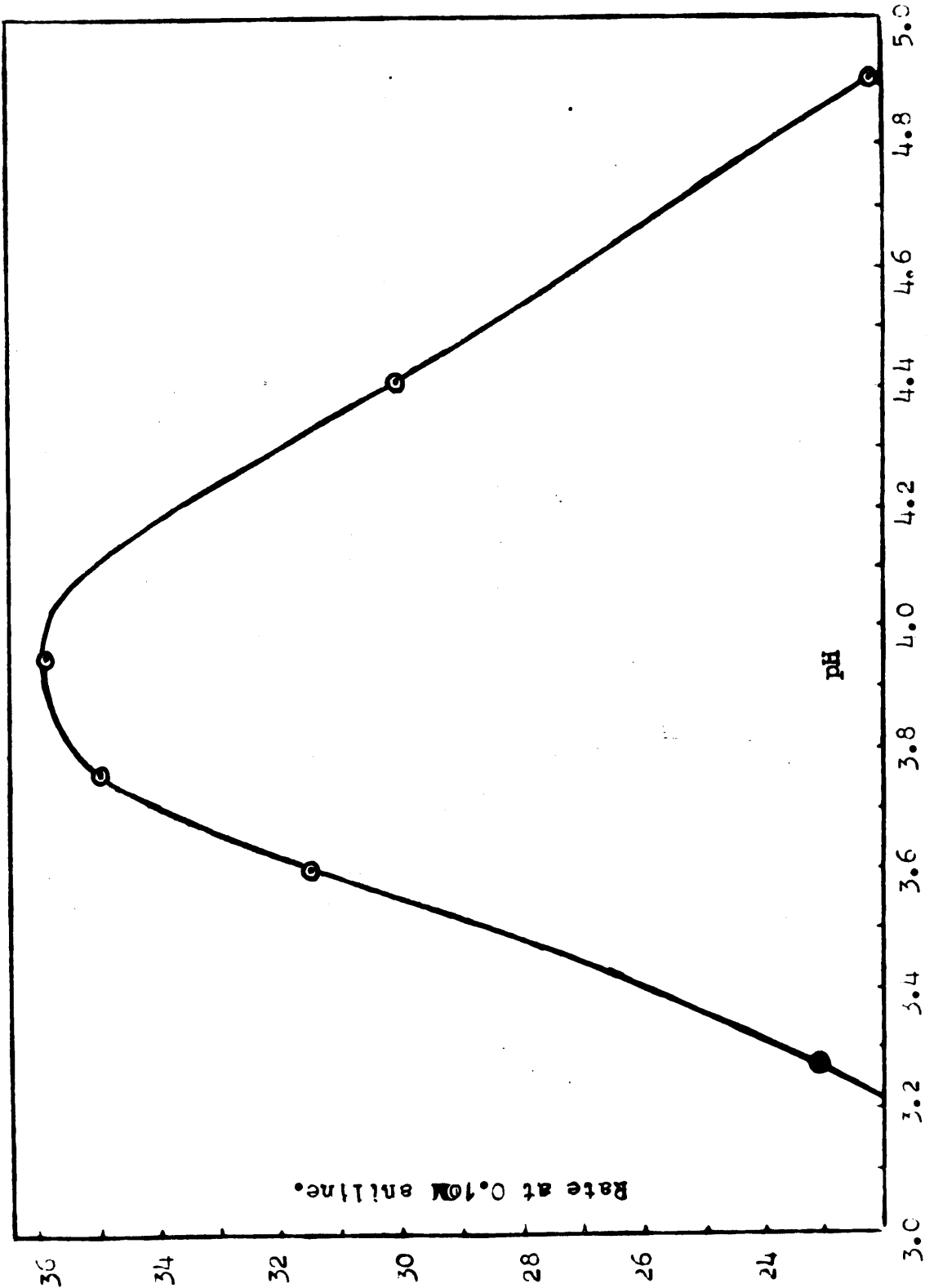


Table 6 Aniline catalysed decarboxylation of oxaloacetic acid at 25°.

Chloroacetate buffers: a molar chloroacetic acid,  
b molar sodium hydroxide, c molar aniline hydrochloride

<u>a</u>	<u>b</u>	<u>c</u>	$10^2 k^* \text{ min}^{-1}$	pH	$1.40 \times 10^2 k^* \text{ min}^{-1}$
0.200	0.196	0.040	9.0	3.60	12.60
0.200	0.180	0.040	6.6	3.28	9.24
0.200	0.170	0.040	5.8	3.10	8.12

$k_1$  and  $k_2$  are the thermodynamic ionisation constants of oxaloacetic acid. At 37° these have the values  $3.55 \times 10^{-3}$  and  $4.38 \times 10^{-5}$  respectively.  $\{H^+\}$  is the hydrogen ion activity and  $f_1$  and  $f_2$  the activity coefficients of univalent and bivalent ions obtained from the Davies equation.

Only very slight catalysis occurs at pH 1. Table 7 gives PEDERSEN'S<sup>7</sup> data at 37°, the rate increases linearly with aniline concentration. This effect is not due to general base catalysis since dimethylaniline, which has almost the same basic strength, does not catalyse the reaction, Table 8. Aniline can form a ketimine hydrate with oxaloacetic acid; this cannot occur with dimethylaniline. At higher pH's PEDERSEN<sup>7</sup> used only very low aniline concentrations; however, further experiments have shown that curve C, Fig.15, shows no levelling at aniline concentrations up to 0.08M.

PEDERSEN<sup>7</sup> attributed the pH variation of the catalysis to the decomposition of the mono and dianion complexes of

oxaloacetic acid and aniline. Complexes involving the undissociated acid having little effect except in very acid solutions.

**Table 7 Aniline catalysed decarboxylation of oxaloacetic acid at 37° after Pedersen.**

Oxaloacetic acid 0.015 M. I = 0.300

Aniline HCl	HCl	$10^3 k^* \text{ min}^{-1}$
-	0.100	0.568
0.01	0.100	0.926
0.02	0.100	1.272
0.05	0.100	2.314
0.10	0.100	4.205

**Table 8 Dimethylaniline catalysed decarboxylation of oxaloacetic acid at 25°.**

Oxaloacetic acid 0.02 M. I = 0.100

Dimethyl-aniline HCl	HCl	$10^3 k^* \text{ min}^{-1}$
-	0.100	0.096
0.020	0.100	0.099
0.093	0.100	0.098

In solutions containing hydrochloric acid, agreement with the experimental results could be obtained using the equations (at 37°).

$$10^3 k_0 = 0.176 + 1.19 [\text{AnH}^+]$$

$$10^3 k_1 = 6.47 + 404 [\bar{\text{AnH}}^+] + 260 [\bar{\text{AnH}}^+]^2$$

$$10^3 k_2 = 1.81 + 38,400 [\text{AnH}^+] + 55,000 [\text{AnH}^+]^2$$

where  $k_0$ ,  $k_1$  and  $k_2$  are the rate constants for the undissociated acid and its mono and dianions respectively.  $\text{AnH}^+$  is the anilinium ion. The catalytic effect of aniline on the dianion would appear to be enormous.

Unfortunately however, these equations do not apply in acetate buffers, the calculated rate constants being 64-93 % too high. In this case rate constants may be calculated using the equations,

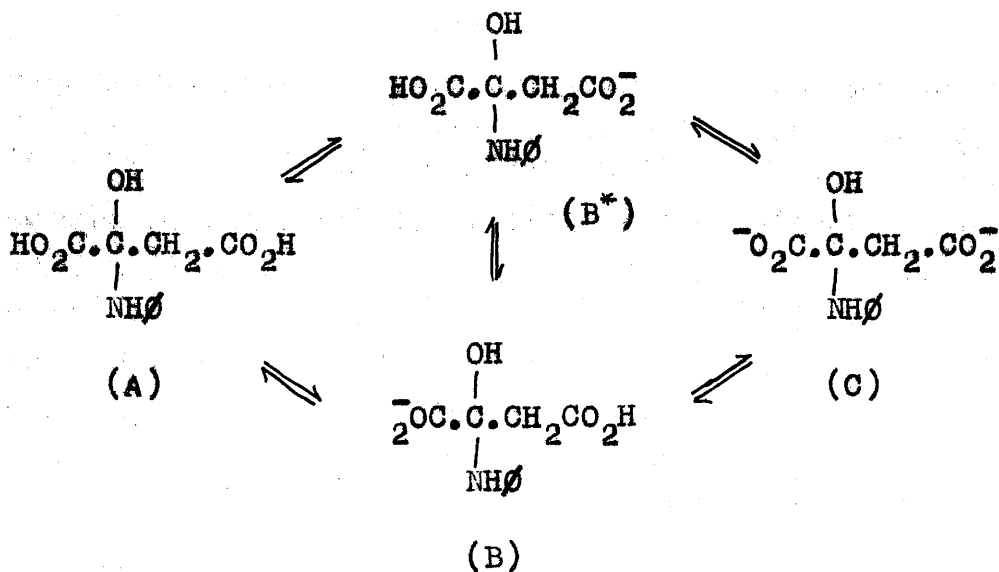
$$10^3 k_1 = 6.47 + 4.4 \times 10^3 [\bar{\text{AnH}}^+]$$

$$10^3 k_2 = 1.81 + (16.4 + 4.8 [\text{Ac}^-]) 10^3 [\bar{\text{AnH}}^+]$$

It is interesting that  $[\text{AnH}^+]^2$  terms are not required in acetate buffers. This is probably due to the fact that in acetate buffers the acid is highly ionised. The ketimine hydrate (3) was isolated in aqueous solution as its aniline salt, indicating that a secondary catalytic effect may occur by ionisation of the carboxyl groups by the aniline.

Alternatively however, the pH variation may be due to the pH dependence of the aniline-oxaloacetic acid equilibrium. Almost certainly the reactive intermediate in aqueous solution is a derivative of the ketimine hydrate (A) produced by an addition reaction of aniline and oxaloacetic

acid.



Presumably this type of addition reaction should not be pH dependent. The formation of the ketimine, involving the elimination of water would be pH dependent and it is well known that ketimines are hydrolysed in acid solution. Unfortunately it is not easy to measure the concentration of the reactive intermediates in solution at various pH's. The differences in rates of decarboxylation, arising from the carboxyl groups represented in the above scheme, have been demonstrated previously.<sup>23</sup> In the ketimine hydrates the proton ionisation equilibria at the nitrogen atom must also be considered.

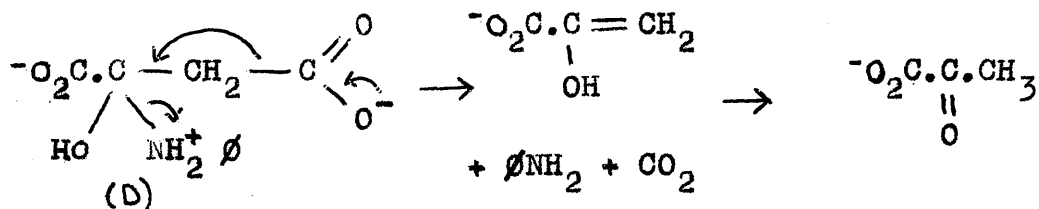
#### Potentiometric Measurements

Previous experiments using the half ester of oxaloacetic acid have shown that the intermediate in water is the

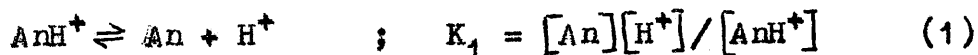


ketimine hydrate. In agreement with this, no yellow colourations expected from the ketimine were observed during the kinetic measurements.

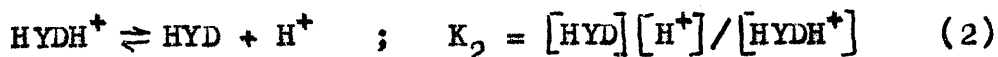
By analogy to metal ion catalysed decarboxylation, the reactive compound is the conjugate acid of the ketimine hydrate (D). A possible reaction scheme being,



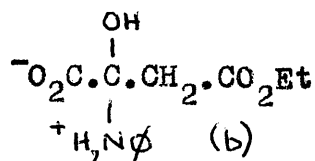
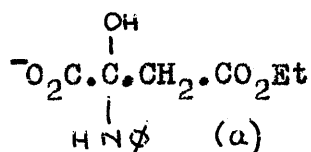
Spectrophotometric measurements on the anilinium salt of the ketimine hydrate (3) indicate that its conjugate acid has a similar dissociation constant to the anilinium ion. In aqueous solution the ionisation equilibria of the aniline salt can be represented by



PEDERSEN<sup>7</sup> gives a value for  $K_1$  at  $I = 0.300$  and  $25^\circ$  of  $2.33 \times 10^{-5}$ , and



where HYD and  $\text{HYDH}^+$  are the species (a) and (b) respectively.



The carboxyl group will be completely ionised, within the pH range (4-4.8) used for the calculations; since it must be at least as strong as in oxaloacetic acid ( $2.8 \times 10^{-3}$ ), this gives 1 % of unionised acid at pH 4.0 and  $I = 0.300$ .

In the presence of hydrochloric acid, we obtain the equations.

$$\text{Total hydrate} = [\text{HYD}] + [\text{HYDH}^+] = [\text{An}] + [\text{AnH}^+] \quad (3)$$

$$\begin{aligned} \text{Total acid} &= [\text{HYD}] + [\text{HYDH}^+] + [\text{HCl}] \quad (4) \\ &= [\text{HYDH}^+] + [\text{H}^+] + [\text{AnH}^+] \end{aligned}$$

$$\text{From (4) } [\text{HYD}] + [\text{HCl}] = [\text{H}^+] + [\text{AnH}^+] \quad (5)$$

From (1) and (3)  $[\text{An}]$  and  $[\text{AnH}^+]$  can be obtained, and hence from (5) and (3)  $[\text{HYD}]$  and  $[\text{HYDH}^+]$  and thus  $K_2 = [\text{HYD}][\text{H}^+]/[\text{HYDH}^+]$

Potentiometric titrations using hydrochloric acid were carried out at  $I = 0.300$  and  $24.8^\circ$  (comparable conditions to the kinetic runs). Table 9 shows a typical set of values for  $K_2$ . The hydrogen ion activity was obtained directly from the observed pH and converted to the hydrogen ion concentration using a value of  $f_1$ , the activity coefficient of a univalent ion, equal to 0.713, obtained at  $I = 0.300$  from the Davies equation,

$$-\log f_1 = 0.5 z_1^2 (I^{1/2} / 1 + I^{1/2} - 0.2I)$$

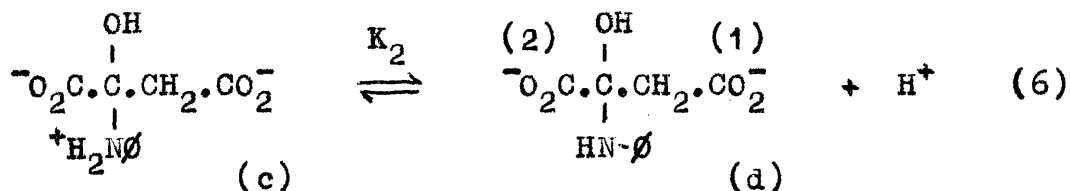
Table 9 Dissociation constant of the ketimine hydrate (3) at 24.8° and I = 0.300

$10^3$ Total Hydrate	$10^4$ [HCl]	pH	$10^5 \{H^+\}$	$10^5 [H^+]$	$10^3 [An]$	$10^3 [AnH^+]$	$10^3 [HYD]$	$10^3 [HYDH^+]$	$10^5 K_2$
2.66	-	4.77	1.70	2.38	1.32	1.34	1.36	1.30	2.49
2.66	4.79	4.62	2.40	3.37	1.09	1.57	1.12	1.54	2.45
2.66	6.38	4.59	2.57	3.60	1.05	1.61	1.01	1.65	2.20
2.65	7.97	4.53	2.95	4.14	0.95	1.70	0.94	1.71	2.28
2.65	9.55	4.48	3.31	4.64	0.89	1.76	0.85	1.80	2.19
2.64	11.10	4.43	3.72	5.22	0.81	1.83	0.78	1.86	2.19
2.64	12.70	4.36 <sub>5</sub>	4.32	6.06	0.73	1.19	0.70	1.94	2.19
2.64	14.30	4.31	4.90	6.87	0.67	1.97	0.61	2.03	2.07
2.64	15.90	4.25	5.62	7.88	0.60	2.06	0.55	2.09	2.07
2.64	17.40	4.19	6.46	9.06	0.54	2.10	0.45	2.19	2.0

An average value of  $2.21 \times 10^{-5}$  is obtained for the dissociation constant  $K_2$  at  $I = 0.300$ . As expected from spectrophotometric measurements this is almost identical to the value of  $2.33 \times 10^{-5}$  obtained for the dissociation constant of the anilinium ion at a similar ionic strength.<sup>7</sup> The slight drift in  $K_2$  is probably due to the presence of small amounts of impurities in the hydrate. Titration with sodium hydroxide Fig.16, suggests a purity of around 95 %, however, this may be due to the relative insolubility of the compound. The potentiometric titration with hydrochloric acid is shown in Fig.17. A very slight inflexion around one equivalent is noted. The potentiometric titrations were completely reproducible.

#### Correction of the pH-rate profile

Major discrepancies in the calculated rates of decarboxylation were found by PEDERSEN<sup>7</sup> between strongly acid solutions and those containing acetate buffers. It is expected that the dissociation constant of the ketimine hydrate of oxaloacetic acid will be similar to the value of  $2.21 \times 10^{-5}$  found for its half ester at  $25^\circ$  and  $I = 0.300$ . The reactive intermediate is almost certainly the compound (c). (d) will be much less reactive, due to the absence of a charge on the nitrogen atom.



Ionisation of the proton from (c) will begin to take place around pH 4 (i.e. at the maximum of the pH-rate profile) if  $K_2$  is  $2.21 \times 10^{-5}$ .

If (d) is relatively inactive, a corrected curve of rate vs pH can be obtained by dividing the rate coefficients at various pH's and 0.10 M. aniline by the percentage of (c) present, calculated from  $K_2 = 2.21 \times 10^{-5}$ . This is equivalent to calculating the rate constants if dissociation according to equation (6) did not take place. The values obtained are shown in Table 10 and are illustrated in Fig.18.

Table 10 Correction of the pH-rate profile for ionisation by (c).  $f_1$  0.713 I 0.300.

pH	$10^5 \{H^+\}$	$10^5 [H^+]$	$[HYD]/[HYDH^+]$	% HYDH <sup>+</sup>	$10^2 k$	$\frac{10^4 k}{\% HYDH^+}$
3.10	79.43	111.40	0.0198	98.0	20.3	20.7
3.30	50.12	70.29	0.0314	97.0	23.5	24.2
3.50	31.62	44.35	0.0498	95.3	29.0	30.4
3.60	25.12	35.23	0.0627	94.1	31.5	33.5
3.80	15.85	22.23	0.0994	91.0	35.4	38.9
3.95	11.20	15.74	0.140	87.7	36.0	41.0
4.20	6.31	8.85	0.25	80.0	33.7	42.1
4.40	3.98	5.58	0.40	71.4	30.0	44.0
4.80	1.59	2.23	0.99	50.3	23.5	46.7
4.90	1.26	1.77	1.25	44.5	22.2	49.9
5.36	0.44	0.62	3.56	21.9	10.9	49.8
5.58	0.26	0.36	6.14	14.0	7.0	50.0

FIG 16

Potentiometric titration of 0.0693 gms. of the ketimine hydrate (3), in 50 ml. of distilled water using N/5 sodium hydroxide.

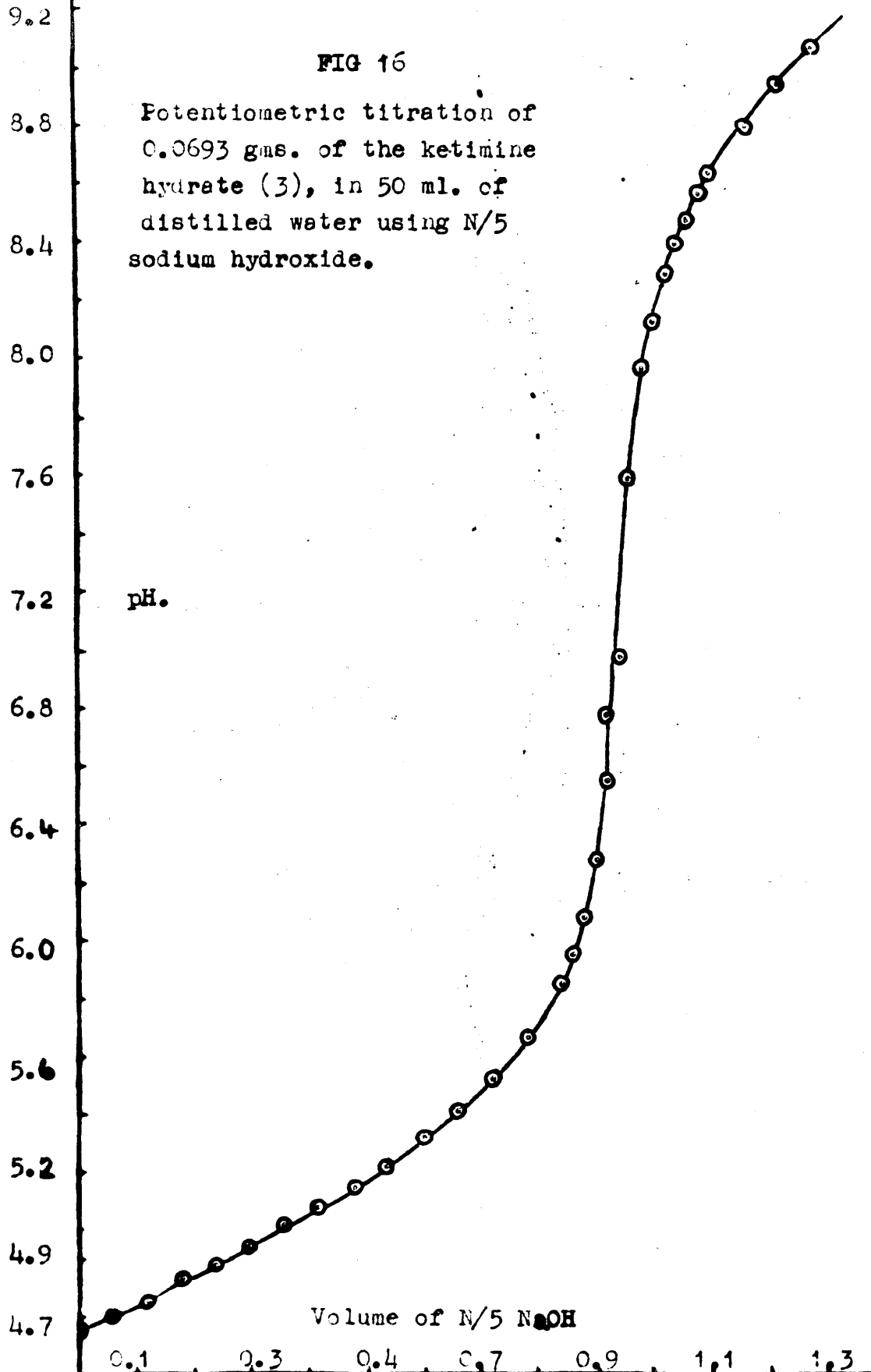


FIG 17

Potentiometric titration of 0.0695 gms. of the ketimine hydrate (3) in 75 ml. of 0.300 M. KCl at 24.8° with N/5 hydrochloric acid.

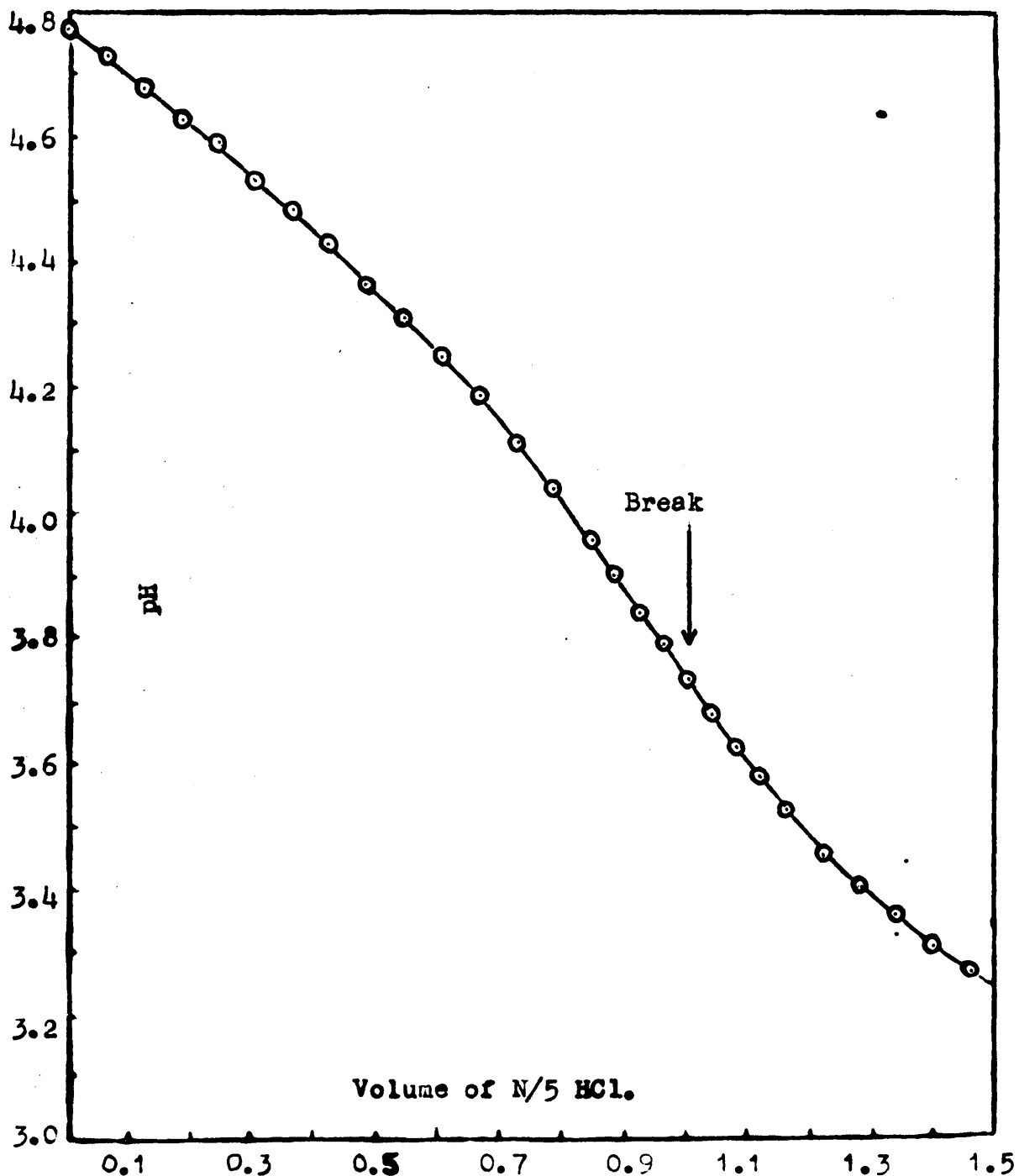
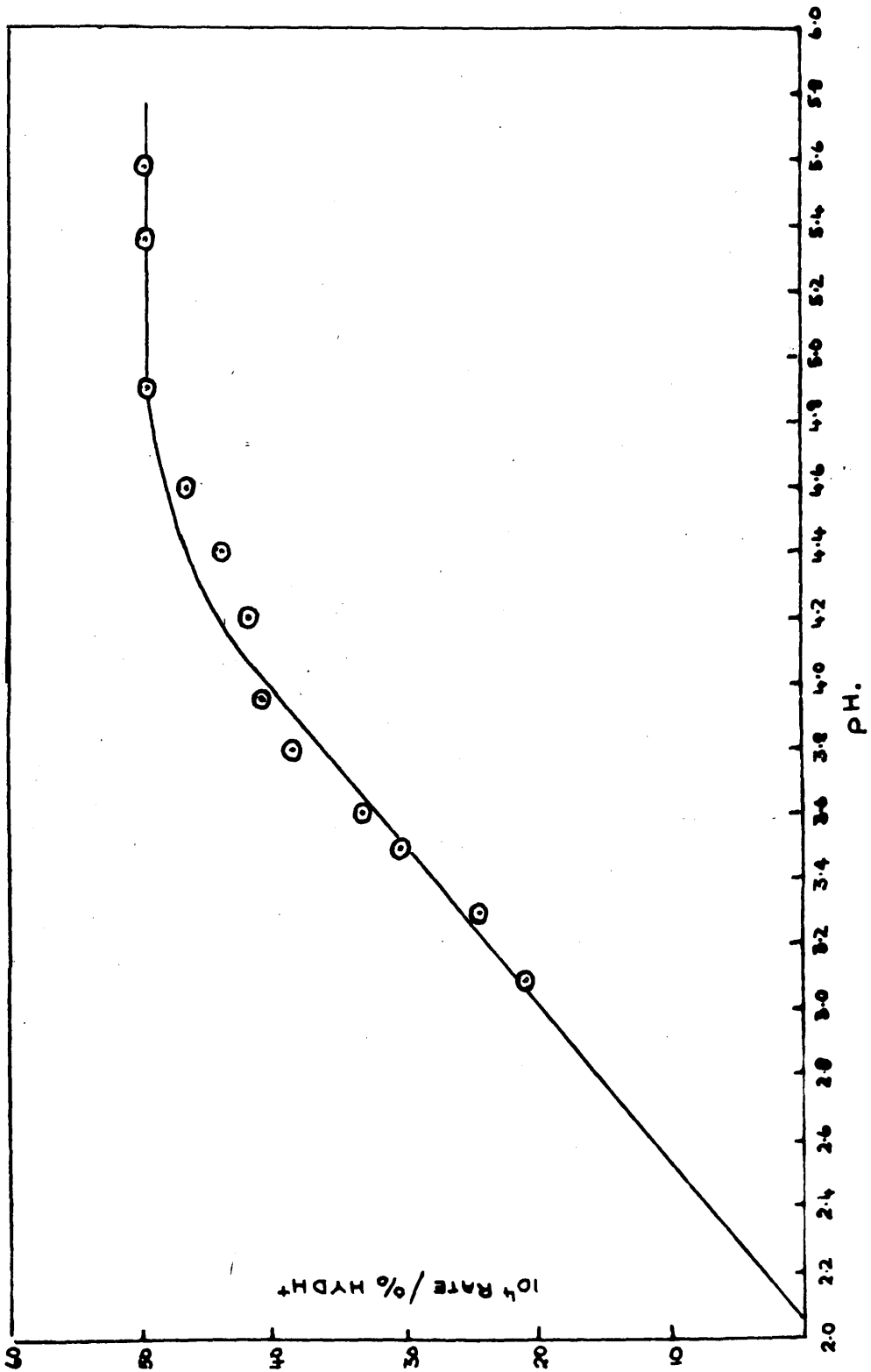


Fig.18

Correction of the pH-Rate profile.





(c) is represented by  $\text{HYDH}^+$  and (d) by  $\text{HYD}$ . In the pH range 4.9-5.6, the ratio  $\text{Rate}/\% \text{HYDH}^+$  is constant. In this area the ketimine hydrate should be present as the dianion since the carboxyl groups of the hydrate should be at least as acidic as those of oxaloacetic acid. The thermodynamic ionisation constants at  $25^\circ$  being  $k_1 = 2.79 \times 10^{-3}$  and  $k_2 = 4.27 \times 10^{-5}$ . This gives values of  $\alpha_1 = 0.08$  and  $\alpha_2 = 0.92$  at pH 5.0. The linear portion of the graph crosses the pH axis at around 2, where  $\alpha_1 = 0.003$  and  $\alpha_2 = 0.28$  i.e. where ionisation of carboxyl group (1) is just taking place. The dissociation constant of the half ester  $\text{HO}_2\text{C} \cdot \text{CO} \cdot \text{CH}_2 \cdot \text{CO}_2\text{Et}$  is  $1.9 \times 10^{-3}$  (Part 1) similar to the first dissociation constant of oxaloacetic acid indicating that carboxyl group (2) is by far the stronger.

The kinetically active species is thus almost certainly (D), the complexes of the undissociated acid and the monoanion B being relatively stable. The fall in reactivity in acetate buffers is due to ionisation according to equilibrium (6).

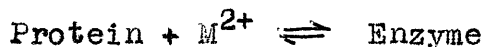
References

1. Wohl and Oesterlin, Ber. 34, 1139, 1901.
2. Kaneko, J. Biochem. (Japan) 28, 1, 1938.
3. Bessman and Layne, Arch. Biochem. 26, 25, 1950.
4. Pedersen, J.A.C.S. 51, 2098, 1929. 58, 240, 1936.  
60, 595, 1938. J. Phys. Chem. 38, 559, 1934.
5. Westheimer, Ann. N.Y. Acad. Sci. 401, 1940.
6. Westheimer and Jones, J.A.C.S. 63, 3283, 1941.
7. Pedersen, Acta Chem. Scand. 8, 710, 1954.
8. Pickard and Polly, J.A.C.S. 76, 5169, 1954.
9. Organic Syntheses, 10, 54, 1930.
10. Curtiss and Spencer, J.A.C.S. 31, 1056, 1909.
11. Bell and Trotman-Dickenson, J.C.S. 1288, 1949.
12. Bronsted and King, J.A.C.S. 47, 2523, 1925.
13. Doub and Vandenbelt, J.A.C.S. 69, 2714, 1947.  
ibid. 71, 2414, 1949.
14. Gillam and Stern, "Electronic Absorption Spectroscopy"  
Edward Arnold, London, 1954.
15. Curtiss and Spencer, J.A.C.S. 33, 985, 1911.
16. Davie and Addis J.C.S. 1622, 1937.
17. Beale, J.C.S. 4496, 1954.
18. Belford, Martell and Calvin, J. Inorg. and Nuclear Chem.  
2, 11, 1956.
19. Pedersen, Acta Chem. Scand. 6, 2859, 1952.
20. Westheimer and Cohen, J.A.C.S. 60, 90, 1938.
21. Speck and Florist, J.A.C.S. 79, 4659, 1957.
22. Ochoa, Physiological Reviews, 31, 56, 1951.
23. GELLES, J.C.S., 4736, 1956.

Enzymatic Decarboxylation.

The fact that a number of  $\beta$ -keto acids are catalytically decarboxylated by metal ion activated enzymes suggests that metal ion and amine catalysis bear some similarity to enzymatic catalysis.

A number of enzymes are known to catalyse the decarboxylation of oxaloacetic acid.<sup>1-3</sup> In every case a divalent metal ion is required for activity. Thus MEHLER<sup>4</sup> partially purified the enzyme from *M. lysodeikticus*. The enzyme was quite inactive in the absence of metallic cations, but was activated by  $Mn^{2+}$ ,  $Mg^{2+}$ ,  $Cd^{2+}$ ,  $Co^{2+}$  and  $Ni^{2+}$ .  $Mn^{2+}$  was the most effective cation. Such catalysis appears to involve an equilibrium of the type,



It is interesting to note that no metal ion activation is required for the enzymatic decarboxylation of acetoacetic acid.<sup>5</sup> The decarboxylation of this acid is not catalysed by metal ions,<sup>6</sup> but is by amines.<sup>7</sup> This suggests that the fundamental catalytic activity of the enzyme is supplied by the metal ion, which is bound to both the protein and to the substrate.

The usual expression for an enzymatic reaction is



where E, is the enzyme, S the substrate and P the products.

In the last step the enzyme must release the products and so



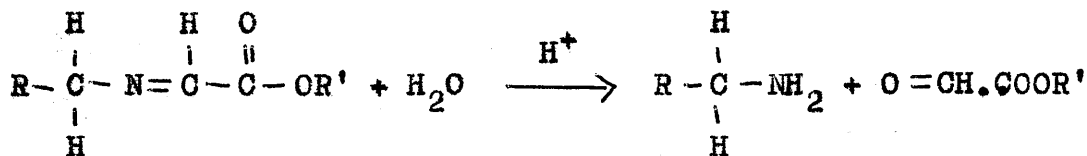
removing the protein from the substrate after decarboxylation has taken place by catalysing the hydrolysis of the ketimine bond . This would then allow the reaction to continue.

PFEIFFER<sup>9</sup> studied the copper and nickel chelates of ketimines formed from salicylaldehyde and esters of optically active  $\alpha$ -amino acids, which were shown to undergo rapid racemisation and oxidative deamination.

The racemisation and deamination are understandable in terms of the prototropic tautomerism of these ketimine systems ,

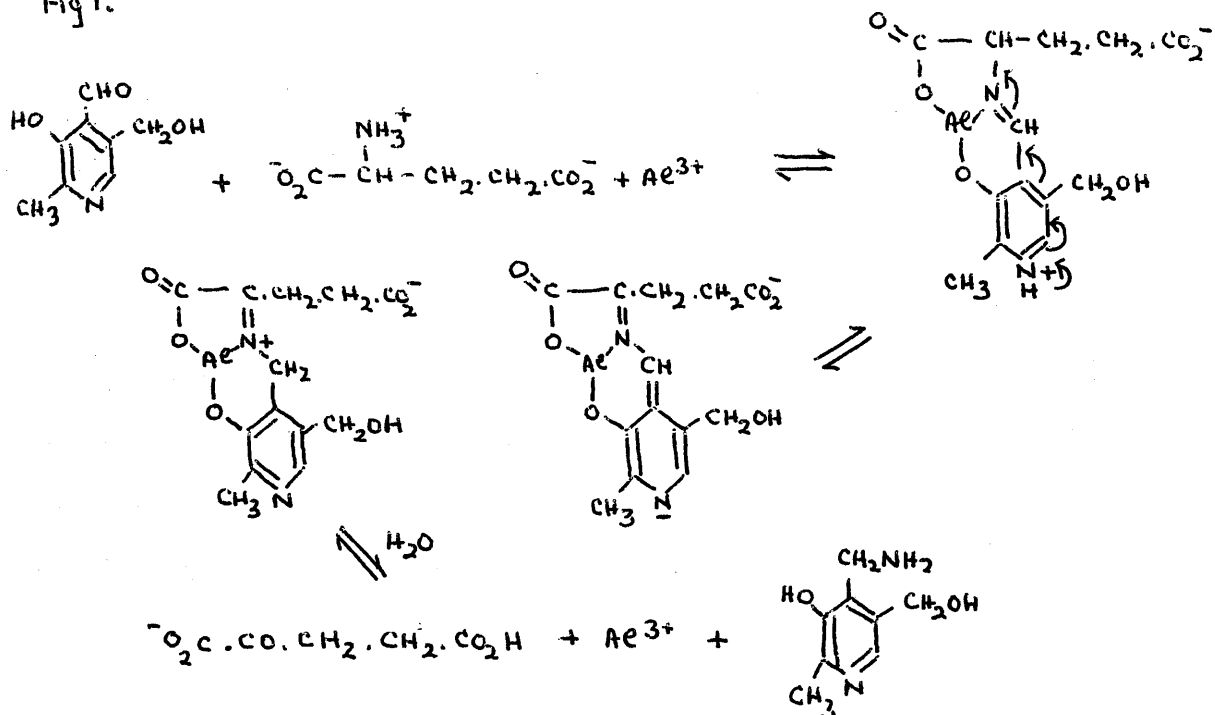


hydrolysis of the new tautomer will now lead to transamination.

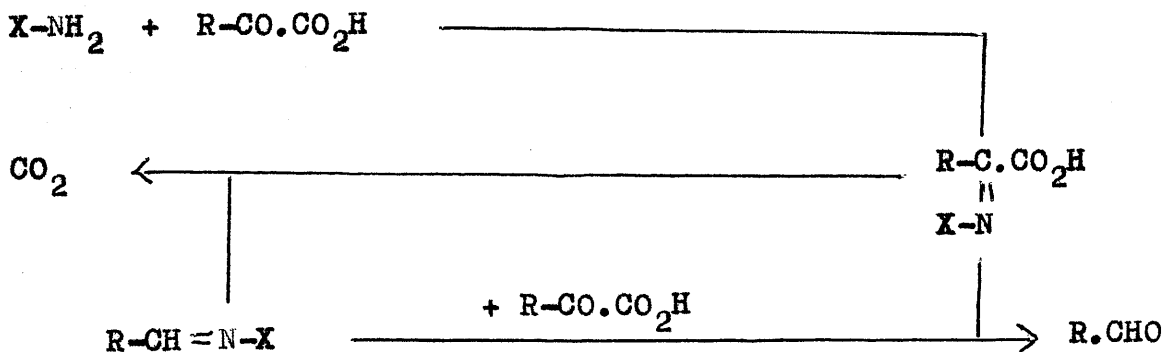


Both the tautomerism and the hydrolysis will be catalysed by metal ions. SNELL et al.<sup>10</sup> have shown how metal ions and ketimines may be involved in the pyridoxal (vitamin B<sub>6</sub>) catalysed decarboxylation and transamination of  $\alpha$ -amino acids. EICHHORN and DAWES,<sup>11</sup> and ROTHBERG and STEINBERG<sup>12</sup> have given confirmatory evidence as to the mechanism. The transamination of glutaric acid is illustrated in Fig.1.

Fig 1.

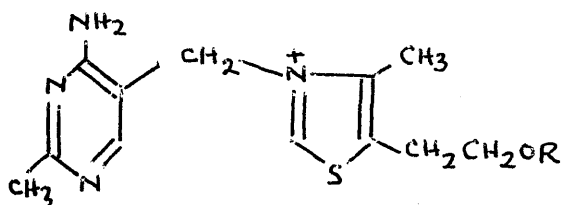


<sup>13</sup> LANGENBECK carried out extensive studies on carboxylase models and found that in non-aqueous media a number of amines were able to catalyse the decarboxylation of α-keto acids. He proposed the following scheme to explain the mechanism of action of the amines.



He predicted that when the prosthetic group of carboxylase were known it would be found to be an amine. His prediction was fulfilled when diphosphothiamine, which possesses a primary amino group was isolated.

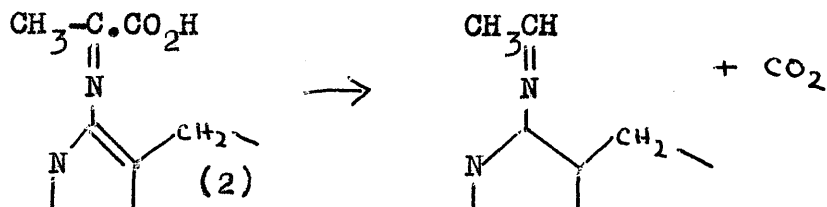
In recent years a great deal of effort has been directed to discovering the mechanism of the enzymatic decarboxylation of pyruvic acid. Thiamine (1a) in the form of its pyrophosphate cocarboxylase (1b) is the coenzyme for a number of important biochemical reactions, including the decarboxylation of pyruvic acid to acetaldehyde.



(1a) R = H

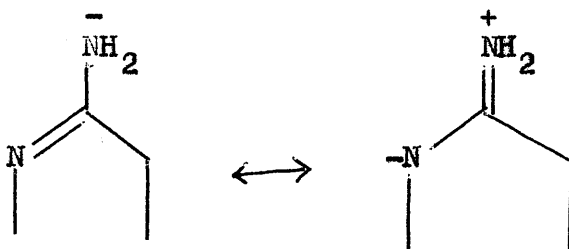
(1b) R =  $\text{P}(\text{O})\text{OP}(\text{O})\text{OH}$   
 $\text{P}(\text{O})\text{OP}(\text{O})\text{OH}$   
 OH OH

Several suggestions as to the possible role of thiamine in facilitating these reactions have been made. The early proposals of LANGENBECK<sup>13</sup> based on model systems using simple primary amine catalysts would involve condensation of the amino group of thiamine with the carbonyl of the keto acid to form a ketimine (2),



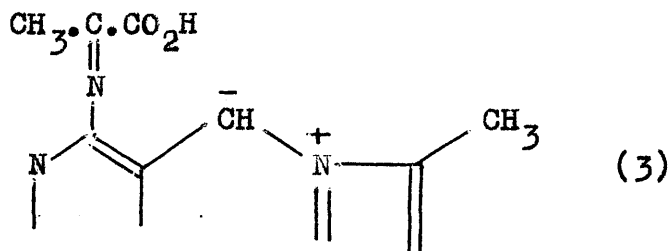
the latter compound hydrolysing to the free acid and

regenerating thiamine. However thiamine fails to react under conditions where other primary amines are active. Much evidence has accumulated to show that the amino group of diphosphothiamine is very unreactive. Thus STERN and MELNICK<sup>14</sup> found that it could not be acetylated with ketene and reacted only very sluggishly with nitrous acid. Presumably this is due to resonance contributions,



and the amino group would not be expected to form a ketimine directly. A minor objection to the LANGENBECK proposal is that it suggests no role for the thiazole ring of thiamine which is perhaps the most unusual feature of the molecule.

VALENTA and WIESNER<sup>15</sup> suggested that thiamine forms a ketimine with pyruvic acid as in LANGENBECK'S<sup>13</sup> scheme and that this tautomerises via an ylid of type (3).



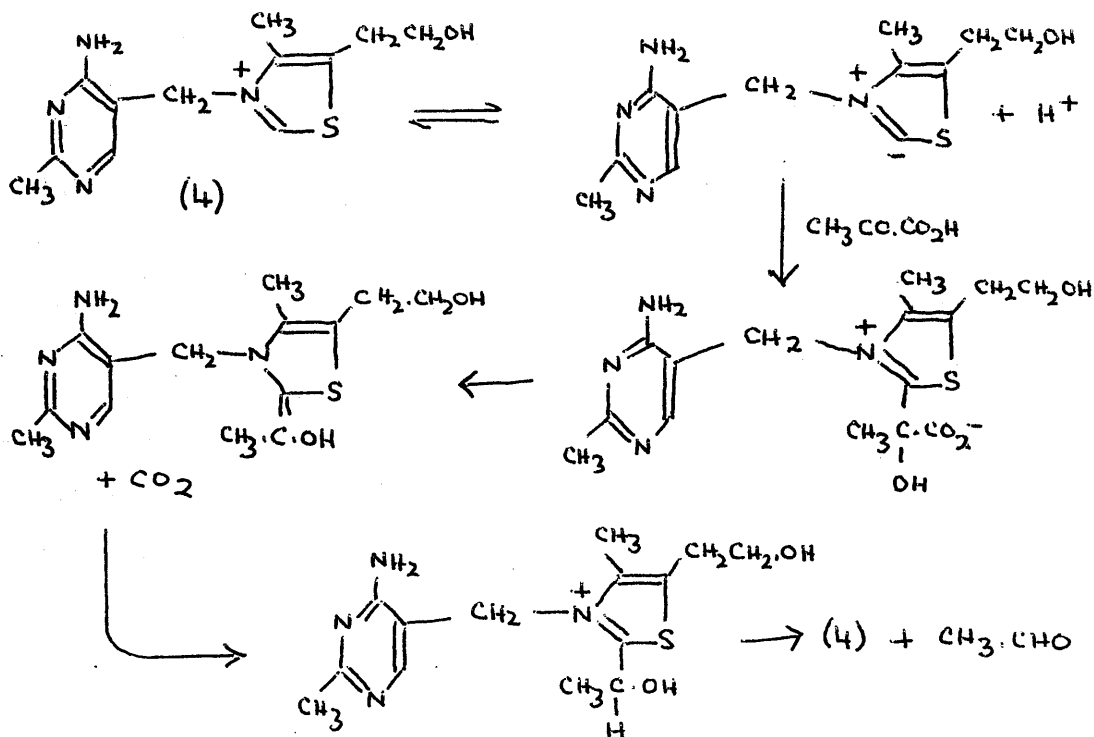
This mechanism also involves condensation of an unreactive amino group of thiamine, but does suggest a role for the thiazole portion of the molecule in helping to stabilise the



ylid. Moreover a very similar type of tautomerism is likely for many of LARGENBECK'S catalysts, such as the 3-amino oxindoles, although tautomerism cannot explain all of his cases (e.g. catalysis by aniline).

BRESLOW<sup>16</sup> first made the rather amazing observation that the hydrogen atom in the 2 position of the thiazole ring could ionise; this was demonstrated by deuterium exchange and has since been confirmed by WESTHEIMER.<sup>17</sup> BRESLOW<sup>16</sup> advanced the mechanism in Fig.2 for the thiamine catalysed decarboxylation of pyruvic acid.

Fig.2



the ylid (3) occurring in model systems involving thiamine. Recently DE TAR and WESTHEIMER<sup>18</sup> have studied the enzymatic decarboxylation of pyruvate by yeast carboxylase in the presence of tritiated water, and found that BRESLOW'S mechanism for the model thiamine catalysed decarboxylation also appears to occur in the enzymatic reaction.

These examples show the importance of model systems in the study of enzymatic catalysis, however, as in the case of pyruvic acid, care must be exercised in applying the results obtained from model systems to the enzymatic reaction.

18. DE TAR and WESTHEIMER, *J. Am. Chem. Soc.*, **71**, 4175, 1949.

References

1. Krampitz and Werkman, Biochem. J. 35, 595, 1949.
2. Evans, Vennesland and Slotin, J. Biol. Chem. 147, 771, 1943.
3. Plaut and Lardy, J. Biol. Chem. 180, 13, 1949.
4. Mehler, Kornberg, Grisolia and Ochoa, *ibid* 174 961, 1948.
5. Davies, Biochem. J. 37, 230, 1943.
6. Krebs, Biochem. J. 36, 303, 1942.
7. Edson, Biochem. J. 29, 2082, 1935.
8. Eichhorn and Trachtenberg J.A.C.S. 76 5183, 1954.
9. Pfeiffer, Offermann and Werner, J. prakt. chem. 159, 313, 1941
10. Metzler, Ikawa and Snell J.A.C.S. 76, 648, 1954.
11. Eichhorn and Dawes J.A.C.S. 76, 5663, 1954.
12. Rothberg and Steinberg J.A.C.S. 3274, 1957.
13. Langenbeck, Ergebn. d. Enzymforsch. 2, 314, 1933.
14. Stern and Melnick J. Biol. Chem. 131, 597, 1939
15. Valenta and Wiesner, Experientia, 12, 192, 1956.
16. Breslow. J.A.C.S. 80, 3719, 1958.
17. Westheimer, Fry and Ingram J.A.C.S. 79, 5225, 1957.
18. De Tar and Westheimer J.A.C.S. 81 , 175, 1959.